Synthesis of Functional Porous Poly(ethylene glycol) Microgels for Biotechnological Applications

Inaugural-Dissertation

to obtain the academic degree

Doctor rerum naturalium (Dr. rer. nat.)

submitted to the Department of Biology, Chemistry and Pharmacy

of Freie Universität Berlin

by

Muriel Behra

from Mulhouse, France

Berlin, March 2013

This thesis is based on research conducted between January 2010 and February 2013 at the Max Planck Institute of Colloids and Interfaces, Department of Biomolecular Systems and Free University of Berlin, Institute of Chemistry and Biochemistry, under the guidance of Dr. Laura Hartmann.

1st Reviewer: Dr. Laura Hartmann
2nd Reviewer: Prof. Dr. Rainer Haag

Date of submission: April 2nd, 2013
Date of defense: June 19th, 2013

Acknowledgements

preparation of the symposium with the Weizmann Institute of Science and all other events organized by the Ph.D. student representatives, as well as Stefanie Riedel and Judith Hoyer for their friendly assistance with administrative questions!

It was a great pleasure to work with my colleagues from the department of Biomolecular Systems, Interfaces and Biomaterials, especially my very good friends, Friederike, Claudia and Susann, who offered a warm and pleasant atmosphere, making the time very enjoyable at the institute, during the summer school in Italy, conferences, dinners and parties! I had a wonderful time!

Finally and most importantly, I would like to thank my family who always encouraged me. Thank you for your support in everything I do!

Table of Contents

Summary

Microgels are very attractive materials which have been employed for a wide range of applications and in particular for the detection, retrieval and elimination of bacteria. The current microgels however present some major limitations since they are most often not biocompatible and show low performance due to their restricted loading capacity. Therefore a novel platform of microgels based on functional porous PEG hydrogel microparticles is presented in this thesis and evaluated for both the removal of bacteria and potential delivery of drugs. These microgels are based on a biocompatible PEG scaffold which reduces unspecific interactions and allows for surface functionalization. In addition, they feature internal pores of a few tens of nanometers allowing for a more efficient loading of drugs and nanoparticles as well as larger pores of a few microns on the surface of the particles for the binding of a higher number of bacteria.

Such porous PEG microgels are prepared by a hard templating method based on porous $CaCO_3$ microparticles. This strategy allows for an exact inverse replication of $CaCO_3$ microparticles into PEG microgels and provides the expected porosity. These microgels are thereafter functionalized via benzophenone-based radical surface chemistry and amide bond formation. Mannose ligands are thereby introduced for bacteria targeting and cationic amines are incorporated for the loading of model drugs and nanoparticles via electrostatic interactions.

For the retrieval of bacteria, these microgels are then made magnetic by loading with superparamagnetic nanoparticles. The resulting magnetic, porous, sugar-functionalized (MaPoS) PEG microgels are able to selectively bind strains of bacteria *E. coli* via carbohydrate-protein interactions and remove them by simply using a magnet. Compared to the standard microparticles, these microgels allow for the binding of two to three times more bacteria and higher yields of removal at high concentrations of bacteria. For the potential delivery of drugs, the porous PEG microgels are made pH-sensitive by functionalization with ammonium-carbamate moieties via the reaction of CO_2 with amines. The resulting microgels are able to switch their charge from negative at pH 10 to positive at pH 5 and therefore can be loaded with both cationic and anionic model drugs under these conditions and release them at pH values between 5 and 7.4 via electrostatic interactions. Compared to PEG microgels purely functionalized with carboxylate or ammonium groups, the PEG-ammonium-carbamate microgels lead to a release up to eight times more efficient under physiological pH conditions.

Overall, the presented functional porous PEG microgels show great potential for the treatment of bacteria but also for a wider range of biotechnological and biomedical applications, such as the bioseparation of cells, detection of viruses, purification of proteins or catalysis.

Zusammenfassung

Mikrogele gehören zu einer sehr interessanten Klasse von Materialien, die in vielen verschiedenen Bereichen der Wissenschaft und Technologie ihre Anwendung finden, insbesondere für die Detektion, Isolierung und Eliminierung von Bakterien. Die Anwendung etablierter Mikrogel-Systeme ist allerdings eingeschränkt, weil die meisten dieser Systeme häufig eine geringe oder keine Biokompatibilität aufweisen und ihre Beladungskapazität begrenzt ist. Im Rahmen dieser Doktorarbeit wurden daher neuartige Mikrogele untersucht, welche aus porösen PEG-Hydrogelen bestehen. Diese sind sowohl für die Isolierung von Bakterien als auch für weitere potenzielle Anwendungen im Bereich des Drug Delivery interessant. Das PEG-Grundgerüst dieser Mikrogele erlaubt eine einfache chemische Funktionalisierung und vermeidet unspezifische Wechselwirkung mit dem Zielobjekt. Außerdem verfügen diese PEG-Mikrogele im Inneren über Nanometer kleine Poren, die für eine effiziente Beladung mit kleinen Wirkstoffmolekülen geeignet sind, und auf der Partikeloberfläche über wesentlich größere (Mikrometer) Poren, die eine erhöhte Anbindung etwa von Bakterien erlauben.

Zur Herstellung dieser porösen PEG Mikrogele werden poröse $CaCO_3$ Mikropartikeln als harte Template genutzt, wodurch eine exakte inverse Kopie der $CaCO_3$ Mikrostruktur samt ihrer Porosität auf dem PEG-Gel abgebildet werden kann. Eine Funktionalisierung der PEG Mikrogele mit Mannose-Liganden oder Amingruppen kann anschließend mit Hilfe der Benzophenon-Radikal-Chemie unter Bildung von Amidbindungen realisiert werden. Die Mannose-Funktionalitäten werden für die Anbindung der Bakterien verwendet und die Amin-Funktionalitäten für die Beladung der Mikrogele mit Modell-Wirkstoffmolekülen und/oder Nanopartikeln, die auf elektrostatischen Wechselwirkungen beruht.

Durch eingelagerte Eisenoxid-Nanopartikel werden die Mikrogele magnetisch, was eine einfache Isolierung/Entfernung der Bakterien ermöglicht. Die porösen, magnetischen und mit Zucker funktionalisierten PEG Mikrogele (MaPoS) sind in der Lage sehr selektiv bestimmte Stämme der E.Coli Bakterien zu binden. Mit Hilfe eines Magneten können die an die Mikrogele gebundenen Bakterien dann einfach gesammelt oder entfernt werden. Im Vergleich zu gängigen Mikropartikeln können die MaPoS Mikrogele die zwei- bis dreifache Menge an Bakterien binden und somit eine höhere Ausbeute realisieren. Mögliche Anwendungen im Bereich des Drug Delivery eröffnen sich durch die Umwandlung der Amingruppen mit CO_2 zu Ammonium-Carbamat Funktionalitäten, wodurch pH-sensitive PEG Mikrogele entstehen. Durch eine Änderung des pH-Wertes von pH 10 auf pH 5 kann die Oberflächenladung der pH-sensitiven Mikrogele von negativ auf positiv umgeschaltet werden, was somit eine Beladung sowohl negativ- als auch positiv-geladener Wirkstoffe ermöglicht. Eine Freisetzung wird dann zwischen pH 5 und 7.4 erreicht. Bei einem physiologischen pH ist die

Wirkstofffreisetzung dieser Carbamat-funktionalisierten PEG-Mikrogele ca. 8-mal höher als bei den gängigen Carboxy- oder Ammonium-funktionalisierten PEG-Mikrogelen.

Die im Rahmen dieser Doktorarbeit präsentierten funktionalisierten und porösen PEG Mikrogele stellen eine neue Plattform funktionaler Mikrogele dar und weisen ein großes Potenzial für verschiedenste Anwendungen im Bereich der Lebenswissenschaften, wie z.B. Biotechnologie und Biomedizin auf.

Publications:

1. <u>Behra, M.</u>; Schmidt, S.; Hartmann, J.; Volodkin, D. V.; Hartmann, L.
   Synthesis of Porous PEG Microgels Using $CaCO_3$ Microspheres as Hard Templates.
   Macromolocular Rapid Communications **2012**, 33, 1049-1054.

2. <u>Behra, M.</u>; Azzouz, N.; Schmidt, S.; Volodkin, D. V.; Mosca, S.; Chanana, M.; Seeberger, P. H.; Hartmann, L.
   Magnetic Porous Sugar-Functionalized PEG Microgels for Efficient Isolation and Removal of Bacteria from Solution.
   Biomacromolecules **2013**, DOI: 10.1021/bm400301v.

3. Pussak, D.; <u>Behra, M.</u>; Schmidt, S.; Hartmann, L.
   Synthesis and functionalization of poly(ethylene glycol) microparticles as soft colloidal probes for adhesion energy measurements.
   Soft Matter **2012**, 8, 1664-1672.

4. Schmidt, S.; <u>Behra, M.</u>; Uhlig, K.; Madaboosi, N.; Hartmann, L.; Duschl, C.; Volodkin, D.
   Mesoporous Protein Particles Through Colloidal $CaCO_3$ Templates.
   Advanced Functional Materials **2013**, 23, 116-123.

5. <u>Behra, M.</u>; Hartmann, L.
   Ammonium-carbamate functionalization for pH-sensitive loading and release of anionic and cationic molecules.
   Manuscript in preparation.

1. General Introduction

1.1. Microgels

Definitions and Properties of Microgels

Microparticles are small, solid particles within the size range of 100 nm to 100 µm. They can be found in nature *e.g.* in dust, sand or powdered sugar and can be manufactured from various natural and synthetic materials such as glass, metals and polymers. Synthetic microparticles offer a large diversity of chemical composition, size, morphology and rigidity. Usually monodisperse microparticles are preferred in order to obtain uniform and sharp physico-chemical properties as well as reliable and reproducible performance.[1] Due to their size, microparticles exhibit large specific surface areas. Such large surfaces are highly beneficial to obtain a higher capacity for specific adsorption or chemical reactions such as catalysis on microparticles. The surface of synthetic microparticles has therefore been modified with a great variety of functionalization and morphology. Thus, due to their versatility and large surface area, microparticles have found many applications *e.g.* as additives, pigments, UV-absorbers or catalysts.[1]

One particular class of microparticles encompasses microgels. Microgels are usually defined as microparticles composed of gel and capable of swelling.[2, 3] Gels are soft materials constituted of an insoluble 3D network resulting from the cross-linking of polymers. In particular, when the polymer network consists of hydrophilic polymers, the microgels are called hydrogels due to their ability to bind water in aqueous suspensions.
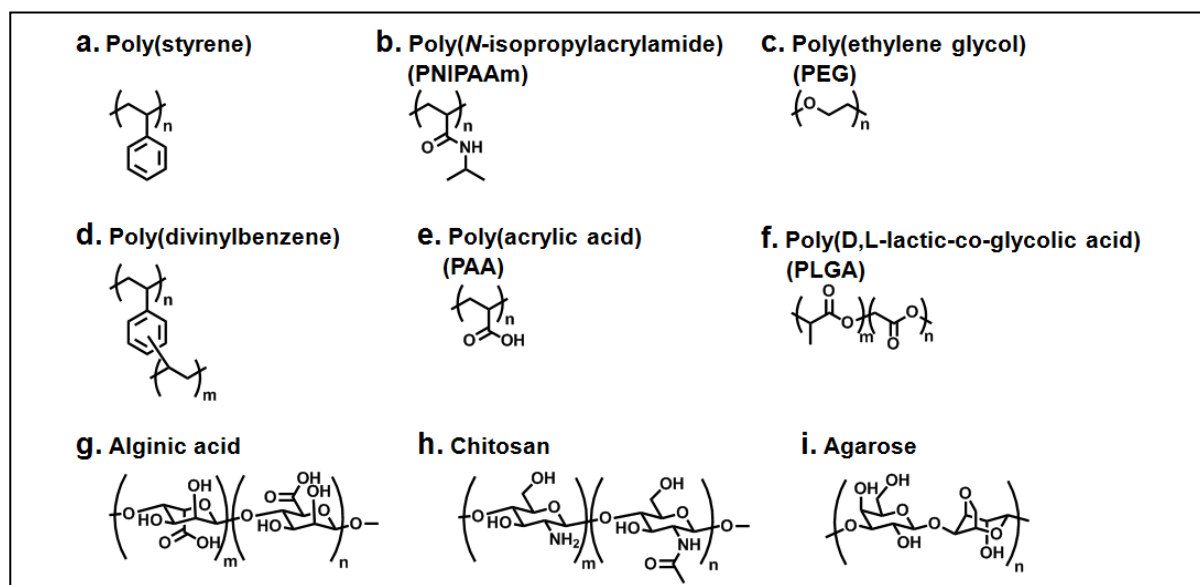
Scheme 1.1. Structural formulas of some polymers employed in microgels.

One of the most distinctive features of microgels lies in their stimuli-sensitivity. By definition, stimuli-sensitive systems are able to change their properties as a function of environmental conditions. Microgels are intrinsically stimuli-sensitive since they are able to undergo reversible volume transitions from swelling in good solvents to shrinkage in bad solvents (Scheme 1.2). A good solvent can be defined as a solvent in which polymer chains adopt an extended coil conformation in order to maximize the polymer-solvent interactions. Hydrogel microparticles therefore swell in water but collapse in organic solvents whereas microgels based on hydrophobic polymers such as polystyrene (Scheme 1.1) specifically swell in organic solvents. Depending on their chemical composition and functionalization, microgels may also be able to respond to other stimuli such as pH or temperature. For example, microgels of the pH-sensitive poly(acrylic acid) (PAA, Scheme 1.1) swell under basic pH conditions due to the electrostatic repulsion between deprotonated acidic groups. As another example, microgels of the thermosensitive poly(*N*-isopropylacrylamide) (PNIPAAm, Scheme 1.1) are swollen at room temperature but shrink above 32 °C due to the entropically-driven dehydration of the polymer. Because of these interesting properties, microgels based on PNIPAAm have been the most extensively studied in the two past decades. Generally, the extent of swelling can be controlled by the degree of cross-linking. Compared to stimuli-sensitive bulk materials, the small volume of microgels allows for faster response to stimuli.
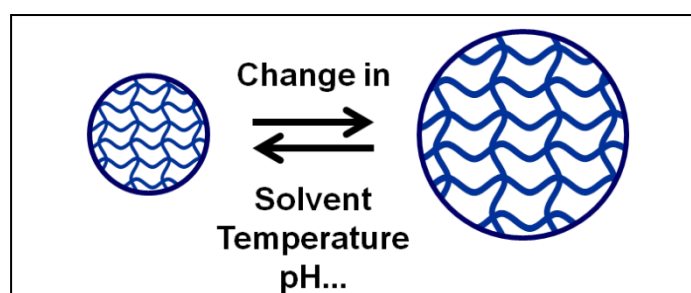
Scheme 1.2. *Intrinsic stimuli-sensitivity of microgels.*

Colloidal stability is another major attribute of microgels. In general, the large surface area of microparticles results in high surface energies. In order to reduce their energy, microparticles tend to aggregate. Aggregation however needs to be avoided in order to preserve the potential applications of microgels. The surface energy is determined by the contribution of three forces: electrostatic repulsive forces, Van der Waals attractive forces and steric repulsive forces. For microparticles, colloidal stability may be obtained by imparting a high surface charge in order to favor electrostatic repulsion between particles. For this, microparticles can be functionalized with acidic or basic groups. Microgels, however, are intrinsically stable due to steric repulsive interaction between the polymeric chains pointing out of the particles (so-called "hairy layer"). Aggregation of microgels is disfavored because the interactions between polymeric chains of two adjacent particles cause a locally increased

osmotic pressure which tends to push the particles apart. Moreover, the overlap between the polymer chains decreases their conformational freedom, which generates an unfavorable loss of entropy.[4]

In addition, microgels present many other attractive features.[5] As microparticles, they exhibit large specific surface areas and high surface reactivity. They are soft microparticles which are both viscous and elastic upon deformation ("viscoelasticity"). They can be made biodegradable in order to slowly dissolve in biological systems. Eventually, microgels are extremely versatile and can be easily synthesized featuring a great variety of chemical composition, surface chemistry, size and morphology. Moreover, very uniform microgels can be prepared with a polydispersity index smaller than 1.01. Eventually, microgels exhibiting sophisticated structures such as particles based on interpenetrated networks (IPN), hollow and core-shell microgels or Janus particles presenting distinct properties from one side to the other have been synthesized (Scheme 1.3).[6-8] Such microgels are for example able to achieve stimuli-sensitivity to both pH and temperature.
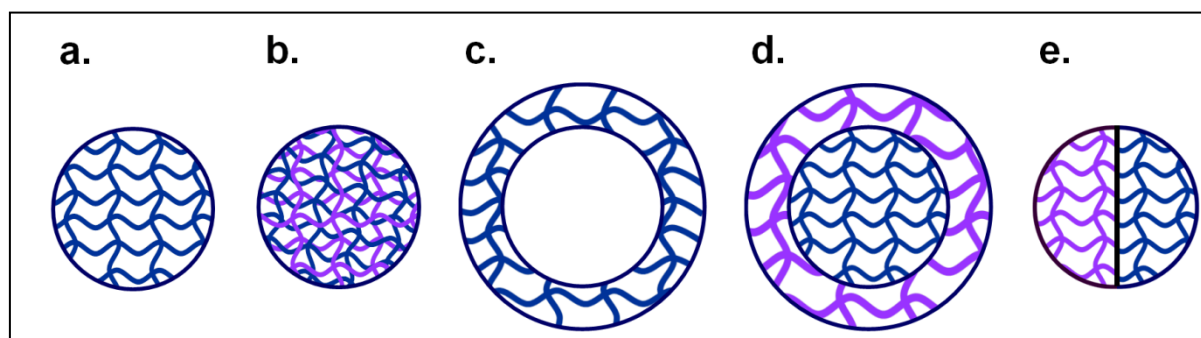
Scheme 1.3. *A few possible structures of microgels: a. classical 3D network from one polymer; b. interpenetrated network; c. hollow; d. core-shell; and e. Janus microgels.*

Applications of Microgels

Because of the plethora of attractive features, microgels are increasingly used in a wide range of applications.[3, 5, 9, 10] They are already industrially employed as additives to control the properties of the final composite materials. In particular, they have found extensive use in the coatings industry in order to improve the rheological properties and increase the viscosity of paints.[9, 10] Microgels have also been employed in enhanced oil recovery to absorb water and avoid water mixing with oil.[9] Due to their high surface areas and surface functionalization, microgels are also very useful in sensing and separation *e.g* via chromatography.[11] For the same reason, microgels have been applied as solid support to achieve a wide range of chemical reactions, such as catalysis, solid phase peptide and polymer synthesis as well as nanoparticle preparation.[3, 9, 12] In addition microgels are widely used in biotechnology for biosensing or bioseparation and hold great potential for biomedical applications such as drug delivery, as will be presented in the section 1.4 of this chapter.[9, 13-19]

Synthesis of Microgels

Since the first synthesis of microgels by Staudinger and Husemann almost 80 years ago,[20] many different methods have been developed to synthesize microgels. There exist two major strategies, either through physical or chemical cross-linking.[3, 5] In the physical method, existing polymers are processed into particles by cross-linking via hydrophobic interactions, for example by phase separation and spray drying, or via ionic interactions. This last strategy is in particular used for the preparation of microgels from bio-polyelectrolytes such as alginate or chitosan (Scheme 1.1). In the chemical method, cross-linking arises from the heterogeneous polymerization of monomers.[21, 22] Free radical polymerizations are mostly applied and different types of polymerization can be conducted such as precipitation, suspension or emulsion polymerization (Scheme 1.4). By definition, precipitation polymerization consists of the precipitation of a polymer which is insoluble in the continuous phase but obtained from soluble monomer and initiator. In suspension polymerization, the monomer and initiator are stabilized in the droplets of an emulsion upon mechanical agitation and polymerization occurs within the droplets leading to microgel formation. In emulsion polymerization, polymerization takes place in particles that form spontaneously in the continuous phase, are fed from the monomer contained in the droplets of an emulsion (reservoir) and are stabilized by a surfactant. Usually emulsion polymerization very advantageous since it yields microgels with narrow particles size distributions. For example, microgels of PNIPAAm are typically prepared by precipitation or emulsion polymerization at high temperatures (~ 70 °C) in the presence of a cross-linking agent.
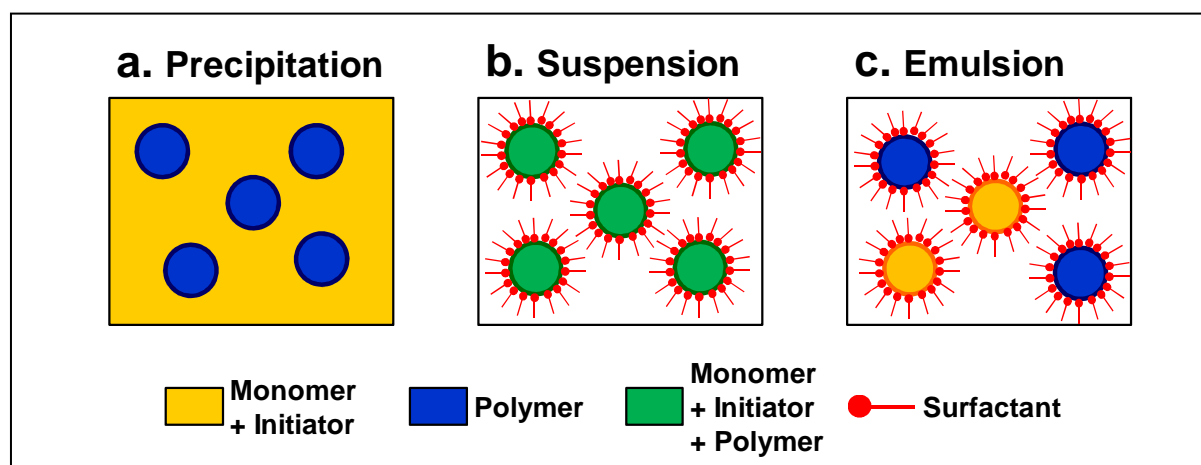
Scheme 1.4. *Principle of a. precipitation; b. suspension; and c. emulsion polymerizations.*

Functionalization of Microgels

Functional groups may already be intrinsically present on microgels, for example in the case of PAA microgels, or need to be incorporated for the foreseen applications. Different strategies can be adopted for the functionalization of microgels (Scheme 1.5).[21] Functional groups can be introduced during polymerization and microgel formation via heterofunctional initiators or surfactants or, as

mostly done, by co-polymerization with heterofunctional monomers. PNIPAAm is very frequently co-polymerized with other functional monomers such as, for instance, acrylic acid to obtain stimuli-sensitivity to both pH and temperature. Functional groups can also be incorporated after microgel formation. In this case surface modification can be conducted via three possible methods: simple organic reaction, polymerization or layer-by-layer (LbL) assembly. In the first case, functional groups which are already present on the microgels such as for PAA are further functionalized using standard reactions of organic chemistry. Using this method, small molecules and polymers can be "grafted-on" the surface of microgels. Functionalization can also be achieved by subsequent polymerization after adsorption of monomer on the surface of the microgels and lead to core-shell structures. Polymers are therefore "grafted-from" the surface of microgels. In the LbL process, oppositely charged polymers (polyelectrolytes) or nanoparticles are stepwise added on the surface of charged microgels. The polymerization method mostly leads to microgels depicting a "hairy layer" while the two other methods usually result in very thin and dense coatings (except for the "grafting-on" procedure with polymers).
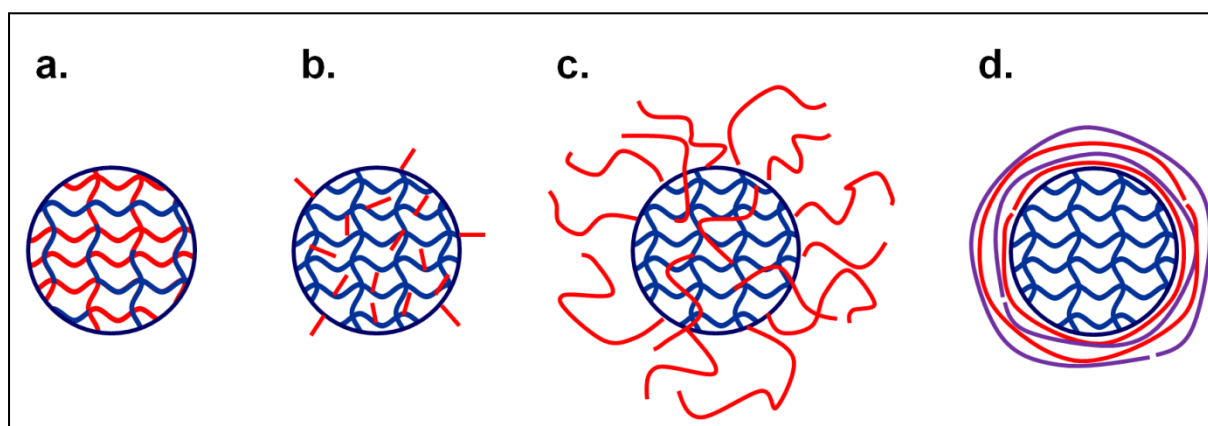
Scheme 1.5. *Different types of functional microgels obtained by a. co-polymerization; b. post-functionalization with small molecules; c. post-functionalization with polymers; and d. LbL assembly.*

Characterization of Microgels

Microgels can be characterized with a wide range of methods.[10, 23, 24] In the next paragraphs, some of the techniques also applied in this thesis will be briefly presented.

Optical Microscopy - This is the most versatile, user-friendly and inexpensive method for the examination of microgels larger than $1\,\mu m$. Information about size, shape, morphology and aggregation can be obtained.

Confocal Laser Scanning Microscopy (CLSM) - After labeling with fluorescent dyes, CLSM enables to evidence the presence and distribution of functional groups. This method is based on the selective

laser excitation of the fluorophores in the focal plane, emission of light from the fluorophore and point-to-point detection of the fluorescence in the focal plane. The resolution of both optical and CLSM microscopy is however limited to 1 - 2 µm with standard microscopes.[23]

Electron Microscopy - Images of higher resolution allowing for the visualization of detailed morphology and surface topology are gained by electron microscopy. The secondary electrons released upon impact of the electron beam and back-scattered electrons reflected from the incoming electron beam provide detailed information about the surface of the microgels (Scanning electron microscopy, SEM). The electrons transmitted through cross-sections of a few tens of nanometers of a sample enable to visualize the internal structure of microgels (Transmission electron microscopy, TEM). The disadvantage of SEM lies in the fact that dry samples are required for observation under vacuum. Under these conditions, microgels may completely collapse. For TEM, microgels are embedded in a resin and may not collapse but are not clearly visible due to the low electronic contrast between the polymeric matrix and microgels. In order to avoid drying and still promote a high contrast, cryogenic electron microscopy has been developed (cryo-SEM and cryo-TEM).[25] In this case, aqueous samples are rapidly frozen and observed under cryogenic temperatures, avoiding water sublimation under the high vacuum conditions required for electron microscopy. Microgels can thereby be observed in their original state in water. For cryo-SEM, microgels however need to be exposed on the surface of the frozen samples to enable observation. This is achieved by fracturing the sample with a knife (freeze-fracture) or shortly increasing temperature to promote the sublimation of the superficial layer of water (freeze-etching).[25]

ζ-potential Measurement - The presence of ionic groups or adsorbed ions and colloidal stability of microgels can be evidenced via the surface charge of the microgels. An evaluation of the surface charge can be provided by the ζ-potential which roughly corresponds to the electric potential between water and the surface of the aqueous layer rich in ions which is attached to the microgels (Stern layer). Measurement of the ζ-potential relies on particle electrophoresis, which involves the movement of charged particles in water under an electric field. The velocity of microgels can be measured and used for the determination of the surface charge using classical models such as the Smoluchowski model.[23]

UV-Adsorption/Titration - Colorimetric UV titrations using specific dyes allow for a quantification of the concentration of functional groups. The accuracy of this method is however limited if the concentration of microgels and/or of functional groups is low.

1.2. Porous Microgels

Definitions and Properties of Porous Microgels

Porous microgels are solid materials which present cavities and channels (so-called pores). These pores can have different shapes from round to cylindrical, can be closed when not connected to the surface, open in the opposite case, or interconnected when linked to other pores (Scheme 1.6). Pores laying on the surface of particles may be called external in opposition to the internal pores situated in the core of particles.[26] Pores can also have different sizes. By definition, pores of less than 2 nm are referred to as micropores, of 2 - 50 nm as mesopores and of more than 50 nm as macropores. Typically, there exist two classes of porosity which define porous materials and porous networks (Scheme 1.7).[27] Porous materials consist of a continuous solid material which surrounds finely dispersed, well defined pores. In porous networks however, the matrix and pores form interpenetrated, inseparable continuous phases.
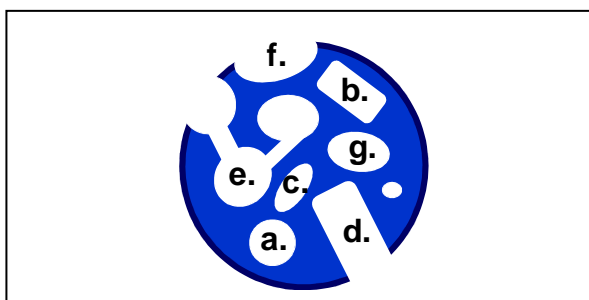
Scheme 1.6. *Types of pores: a. round; b. cylindrical; c. closed; d. open; e. interconnected; f. external; and g. internal.*

Basically, microgels can present both types of porosity. Due to their nature, they intrinsically feature a porous network resulting from the cross-linking of polymers. The intrinsic porosity of microgels is stimuli-sensitive since pores become larger upon microgel swelling and smaller upon shrinkage. The size of these pores and extent of pore enlargement can be fine-tuned by the rigidity of the microgels which is itself controlled by the chain length of the macromonomers and degree of cross-linking. Usually the size of intrinsic pores can reach several nanometers. In addition, distinct larger pores can be incorporated on microgels. Since this type of porosity is an additional feature of microgels, the expression "porous microgels" will refer, in the following, to microgels presenting both an intrinsic and additional porosity (Scheme 1.7). The introduction of pores however generates higher surface tensions which are thermodynamically disfavored. Such additional pores may therefore shrink and close by plastic deformation of the microgels. More generally, numerous, large pores may also dramatically alter the mechanical stability of the microgels. This is the reason why porous microgels are stiff and highly cross-linked in order to preserve mechanical stability.[28] In this case, the intrinsic porosity is reduced but the additional porosity is maintained. The most common porous microgels

synthesized so far are based on poly(styrene), poly(divinylbenzene) and the biocompatible and biodegradable polymer poly(lactic-co-glycolic acid) (PLGA) (Scheme 1.1).

Porous microgels are very attractive materials since they feature both high specific surface areas and high specific pore volumes. Large, accessible surfaces are desirable for adsorption and chemical reactions while large volumes can advantageously be used for the uptake and temporary confinement of substances. Moreover, microparticles featuring open interconnected pores are permeable and allow for the diffusion and faster transport of substances.
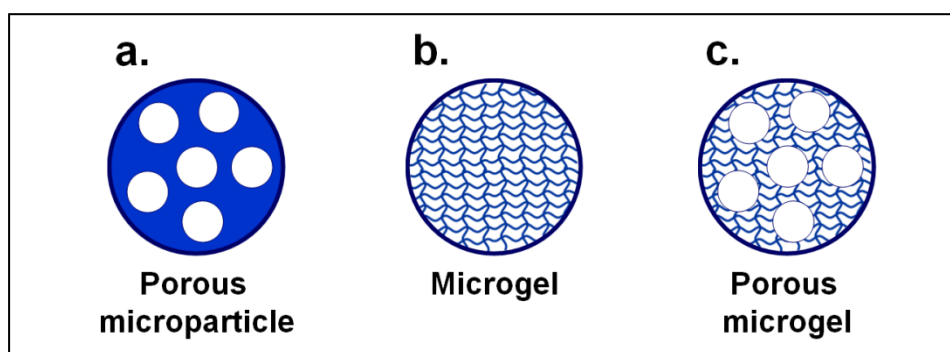
Scheme 1.7. *a. Porous microparticle; b. microgel (porous network); and c. porous microgel.*

Applications of Porous Microgels

Due to these advantageous features, porous microgels have been employed for a wide range of applications.[26, 28] These microgels were first commercialized for ion-exchange, especially in order to soften water and remove toxic heavy metals. Porous microgels have also found applications in chromatography, especially in size exclusion chromatography (SEC). Small polymers are able to permeate through the pores of the microgels and show longer retention times than larger polymers thereby resulting in the separation of polymers based on their size. The configurable pore size of the microgels enables to adapt porosity to the polymer mixture which needs to be separated and allows for improved separation performance. In addition, porous microgels can be used for high-performance and high-speed affinity chromatography for the purification of proteins, showing high column efficiency, high dynamic capacity and low flow resistance due to their porous nature. For both types of chromatography, porous microgels of agarose (Scheme 1.1) are commonly employed.[11, 29] Eventually porous microgels are also used in catalysis and currently developed for biomedical applications such as drug delivery (see section 1.4).[9, 13-18]

Synthesis of Porous Microgels

For most of these applications a well-defined porosity is required. Synthetic procedures have therefore been developed to control the porosity of the microgels in terms of size, shape, interconnectivity and resulting surface areas. In general, porous microgels are prepared employing the same techniques as for microgel synthesis such as suspension and precipitation polymerizations but by additionally introducing porogens.[26, 28, 30, 31] Porogens are pore-forming agents such as solvents, polymers or solid inorganic particles. The use of porogens leads to phase separation during polymerization in the microgels. After polymerization, porogens are removed and leave spaces which become the pores. For example, porous polystyrene microgels can be synthesized by suspension polymerization in water using the solvents toluene or n-heptane as porogen. Effervescent salts such as ammonium bicarbonate can also be used as porogens and generate gas which forces the formation of pores within microgels. Besides the use of porogens, the use of templates also allows for the preparation of porous microgels.[32-35]

By definition, templating consists of the inverse replication of one structure into another (Scheme 1.8).[32, 33, 35] Templates are therefore structure-directing agents and the generated material is expected to be a true inverse copy of their templates. After synthesis, templates are removed and leave spaces which become the pores. Templates can therefore be considered as porogens but all porogens are not templates. Compared to the use of porogens, templating methods generally allow for the formation of pores of different sizes, possibly interconnected, and for an overall improved control over the morphology and porosity due the inverse replication process. Generally, two types of templates can be used, either organic and soft or inorganic and hard. For example, emulsions containing hard particles can be used as soft templates. In this case, suspension polymerization takes place within the droplets in the presence of the hard particles. Removal of both emulsion and particles provide porous microgels. As hard templates, porous microparticles are used. The pores of the template microparticles are first filled with monomer and initiator, then polymerization takes place within the template in order to form hybrid template-microgel particles and the template is finally removed, leaving pores in the resulting microgels (Scheme 1.8). The use of hard templates usually leads to more successful replications than that of soft templates.[32, 34, 36, 37] Soft templates are thermodynamically less stable and more difficult to remove after synthesis. Hard templates in the form of porous inorganic particles are therefore preferable.
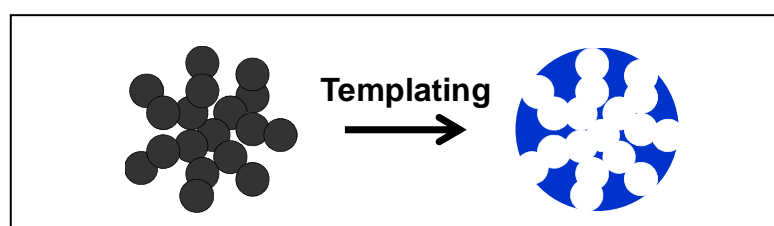
Scheme 1.8. *Principle of hard templating with porous microparticles.*

Characterization of Porous Microgels

The porosity of materials can be characterized with different methods.[24, 26, 28]

Small Angle X-Ray Scattering (SAXS) - Resulting from the interactions between X-rays and the electron shells of atoms in the sample, SAXS is used to evidence the presence of phase inhomogeneities in the nanometer range and thereby, the porosity of systems. For ordered systems, the form of the scattering signal also gives information about the shape and size of pores.

Electron Microscopy - The topology and internal morphology of microparticles as well as the shape, size and interconnection of pores can be visualized by SEM and TEM. The observation of pores smaller than 2 nm is however difficult, especially without high resolution TEM.

Gas Adsorption/Desorption - The surface area, total pore volume and pore size distribution can be measured by gas adsorption/desorption (N_2 mainly). With this method, the volume of gas which is adsorbed by and desorbed from porous materials is measured as a function of relative pressure. The above-mentioned information can be acquired from the measured isotherms using the Brunauer-Emmett-Teller (BET) model.

Mercury Intrusion - The surface area, total pore volume and pore size distribution can also be measured by mercury intrusion. These characteristics are obtained from the external pressure required to force the non-wetting liquid into porous materials. Gas adsorption/desorption and mercury intrusion are the most standard methods to characterize porous materials, with gas adsorption being more suitable for the characterization of micro- and mesopores and mercury absorption providing data only for meso- and macropores.

Most of these methods however require dry samples. SAXS measurements can be performed in solvent but only provide information if the contrast between the two phases, cross-linked polymer and solvent, is high enough. High contrast may not be obtained since the solvent is intrinsically present within the polymer network. Dry samples are therefore preferable for SAXS measurements. The structure of microgels may however be completely altered upon drying. This is the reason why standard methods for the characterization of porosity may not be applicable to microgels. Alternative methods such as cryo-SEM and cryo-TEM are therefore employed.

Permeability studies - Permeability studies employing fluorescent markers of different sizes and monitored by CLSM also enable to characterize porosity in the wet state. The diffusion of such markers into the microgels makes the particles fluorescent and proves the presence of interconnected

pores of a size larger than the size of the marker. Due to the resolution of CLSM, larger pores of a few microns can even be directly evidenced.

1.3. PEG Microgels

Definitions and Properties of PEG

Poly(ethylene glycol) (PEG) is the synthetic polyether deriving from ethylene oxide and is therefore also called poly(ethylene oxide) (PEO, Scheme 1.1). In general, the term "PEG" refers to polyether of molecular weights below 20 000 g.mol^{-1} while "PEO" refers to larger polymers.[38] PEG is mostly synthesized by anionic polymerization of ethylene oxide. Depending on the type of initiator used for the polymerization process, different terminal groups are present on PEG chains. For example, by using hydroxide ions polymerization leads to PEG chains presenting hydroxyl groups on both ends. PEG polymers are commercially available in a wide range of size and highly monodisperse PEG chains can be synthesized, showing polydispersity index as low as 1.01. In addition to linear PEG, other geometries are available such as branched, star or comb PEG.

PEG of low molecular weights, typically below 1000 g.mol^{-1} are colorless, viscous liquids while larger PEG are white, waxy solids at room temperature. The melting point of PEG increases with molecular weight but reaches a plateau at 67 °C.[38] This polymer is thermosensitive and becomes insoluble in water at temperatures higher than 100 °C.[39] In addition, PEG is amphiphilic and soluble not only in water but also in many organic solvents except for diethyl ether and hexane. Most of all, the high hydrophilicity and the neutral character of PEG are essential features and lead to the suppression of unspecific interactions with molecules such as proteins and their adsorption on PEG polymer.[40] In addition, PEG is biocompatible, non-toxic, non-immunogenic and has been approved by the American Food and Drug Administration (FDA) for internal consumption and clinical use.[40] Eventually the polyether is stable and non-biodegradable.

Applications of PEG

Due to this myriad of advantageous distinctive features, PEG has been used for many different applications.[40] Due to its ability to reduce unspecific interactions, PEG hydrogels have been used as support for solid phase synthesis as well as ultrafiltration. PEG has also been integrated in consumer products that we use in our everyday life. PEG chains have been attached to hydrophobic molecules in order to form surfactants employed in cosmetic products such as toothpaste, shampoos or soaps. The antifouling properties of PEG also led to its integration in contact lenses for the protection against bacteria and fungi. In addition, PEG is currently used in the biomedical field as excipient in pharmaceutical preparations as well as active principles in laxatives. Eventually, PEG is considered as

the "gold standard" polymer for cell culture, tissue engineering and drug delivery. In the particular case of drug delivery, PEG is used either for the coating of drug carriers or conjugation with drug molecules, in the process known as "PEGylation".[41-43] The presence of PEG provided an enhanced water solubility, reduced immunogenicity, stability and protection against enzymatic degradation. In addition, carriers and drugs functionalized with PEG present reduced interactions with proteins and blood components which avoids recognition by the immune system (opsonization) and results in prolonged blood circulation times (stealth effect). Drugs thereby present an enhanced bioavailability which enables to reduce the frequency of drug administration and the drug dosage.

Functionalization of PEG chains

In most applications PEG chains are either conjugated to drugs and materials or employed as hydrogels. Both uses require the functionalization of PEG terminal groups. End-group functionalization can be performed by the appropriate choice of initiator during polymerization. A more versatile method however consists of post-functionalization after polymerization. To this effect, the solubility of PEG in almost all organic solvents allows for using classical reactions of organic chemistry. Using this method, carboxylate, amine, thiol and azide could for example be incorporated on PEG chains. For the preparation of hydrogels acrylates and acrylamides have been introduced. PEG-diacrylate (PEG-dAA), PEG-dimethacrylate (PEG-dmAA) and PEG-diacrylamide (PEG-dAAm) are commercially available but usually show low purity (Scheme 1.9). For biomedical applications, PEG-dAAm is preferrable over the more common PEG-dAA since it is known to be more resistant to hydrolysis in water, amides being more stable linkages than esters.[44] PEG-dAAm can be synthesized following a procedure reported by Hartmann *et al.*, based on work by Elbert and Hubbell (Scheme 1.9).[44, 45] In brief, commercially available PEG-dihydroxyl is first functionalized with mesyl groups for complete conversion into amine by reaction with ammonia in a second step. The amines are finally reacted with acryloyl chloride to yield PEG-dAAm.
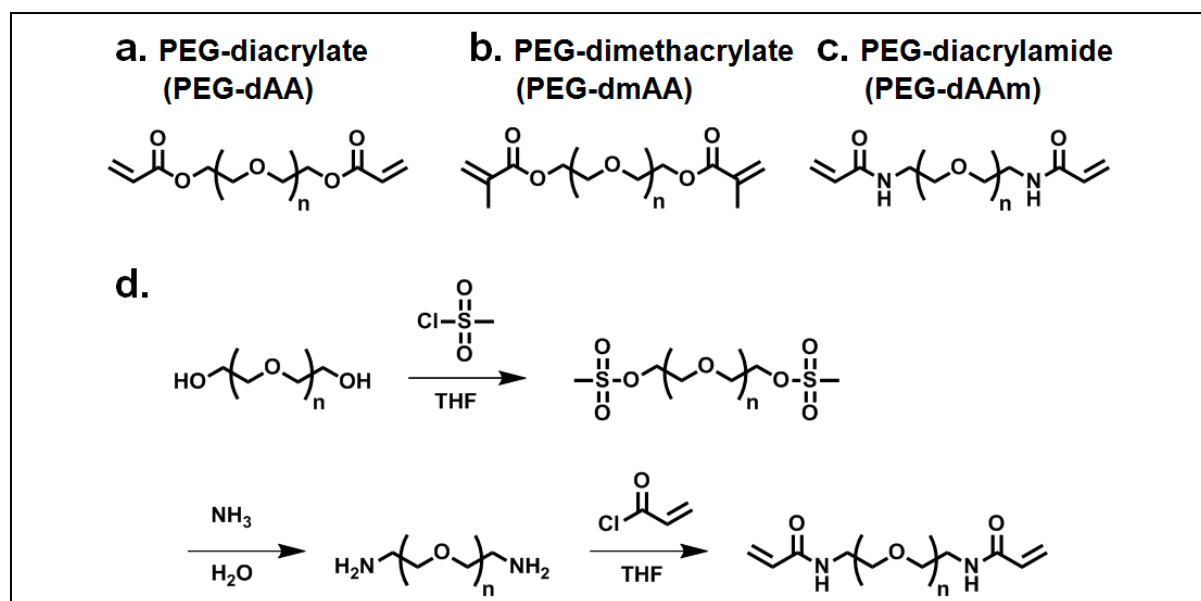
Scheme 1.9. *Structural formulas of a. PEG-dAA; b. PEG-dmAA; c. PEG-dAAm; and d. synthetic procedure for the functionalization of PEG-dAAm (THF: tetrahydrofuran).*

Synthesis of functional PEG hydrogels and microgels

PEG hydrogels are employed for cell cultures, tissue engineering and the formation of PEG microgels. A very common strategy for the synthesis of PEG hydrogels consists of PEG cross-linking by polymerization of telechelic PEG macromonomers (Scheme 1.10). Such molecules present functional groups on both ends which are capable of entering into further polymerization. After initiation, each PEG macromonomer can be simultaneously involved in the formation of two new polymer chains. During propagation of one chain, novel macromonomers are incorporated which are already involved in the propagation of other chains, thereby resulting in cross-linking. As usual, the rigidity of the microgels is controlled by the chain length of PEG macromonomers and degree of cross-linking. The degree of cross-linking depends on the concentration of radicals, itself determined by the concentration of monomer and initiator. As telechelic PEG macromonomers, PEG-dAA, PEG-dmAA and PEG-dAAm can be used, with PEG-dAAm leading to more stable hydrogels against hydrolysis.
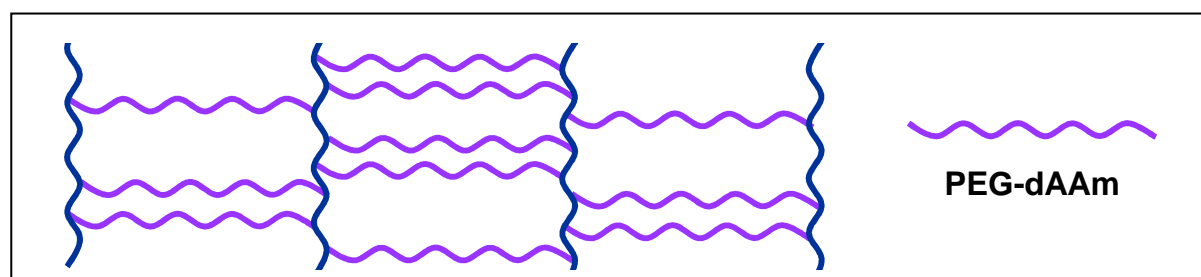
Scheme 1.10. *Cross-linking of telechelic PEG macromonomers (purple) leading to the formation of PEG hydrogels*

Non-porous PEG microgels can be synthesized using the thermosensitivity of PEG. The polymer is known for becoming insoluble in water at temperatures higher than 100 °C.[39] PEG thereby undergoes phase separation to produce spherical PEG-rich domains. By using kosmotropic salts such as sodium sulfate favoring the salting-out of polymers, the temperature where precipitation starts is decreased. The size of the resulting PEG droplets can finally be controlled by the molecular weight of polymers, concentrations of polymer, sodium sulfate salt and temperature.[46] After phase separation, PEG droplets are cross-linked upon UV irradiation using a water soluble photoinitiator. Non-porous PEG microgels can therefore be synthesized by polymerization after precipitation of PEG-dAAm in aqueous sodium sulfate solutions.[46-48]

Different strategies are available to achieve the functionalization of PEG hydrogels and microgels. For example, the macromonomers used for hydrogel synthesis can be co-polymerized with other heterofunctional monomers such as vinyl monomers or PEG macromonomers bearing a vinyl moiety at one end and another functional group at the other end.[47] These heterofunctional co-monomers however do not participate in the cross-linking process leading to the formation of a hydrogel network. This strategy therefore involves additional reaction optimizations to avoid changes in the resulting hydrogel properties such as cross-linking density and mechanical stability. In order to ensure formation of stable and rigid hydrogels, these co-monomers can only be introduced at low concentrations, which often results in low degrees of functionalization. In addition, the use of vinyl co-monomers may drastically alter the biocompatibility of the hydrogel. Therefore the modification of PEG hydrogels at a high degree of functionalization has turned to be an intricate task so far.

1.4. Microgels for Biotechnological and Biomedical Applications

Microgels present a wide range of advantageous properties which make them very valuable for both biotechnological and biomedical applications.[9, 14, 15] First, microgels are very versatile. They can be synthesized in a wide range of compositions and, in particular, from biocompatible and biodegradable hydrogels. They can be prepared in a wide range of sizes, with microgels above one micron enabling an easier handling. Microgels can also be prepared with a very low polydispersity which results in sharp physico-chemical properties as well as reliable and reproducible performance when it comes to applications. In addition, microgels can be functionalized to promote affinity-based interactions with molecules such as drugs or proteins and allow for active targeting. Moreover, microgels are soft, viscoelastic and colloidal stable, even in media of high ionic strength such as physiological fluids. Hydrophilic microgels therefore have the potential to mimic biological cells in size, degree of hydration, texture and colloidal stability, which makes them highly valuable.[49, 50] In addition, microgels show a stimuli-sensitive behavior. They are able to swell and shrink, allowing for

the entrapment and release of molecules by diffusion through the pores of the gel. Eventually, microgels, especially porous microgels, show high specific surface areas which are highly relevant for interactions with molecules, entrapment and targeting.

Because of this plethora of advantageous properties, microgels are widely used in the field of biotechnology.[9, 13] They are currently employed for biosensing as well as bioseparation of cells, proteins and DNA.[51-54] In addition, they hold great potential for biomedical applications, especially as biomaterials for regenerative medicine.[9, 14] For example, microgels can provide structural support for damaged soft tissues and enable their regeneration.[55] The potential of microgels as synthetic cells showing superior properties such as mechanical strength and ability of specific targeting or controlled release has also been discussed.[49] Eventually, an increasing amount of research has been done, in the past two decades, to develop microgels as carriers for drug delivery.[9, 13-16] To this regard, each mode of delivery requires a particular size of microgels. For instance, microparticles of more than one micron are well adapted for oral and transdermal delivery.[17, 18] Smaller sizes are required for example for intravenous delivery. In the following, the applications of microgels in bioseparation and drug delivery will be presented in more details.

Biosensing and bioseparation

One of the first major applications of microgels in biotechnology consists of the biosensing and bioseparation of cells, proteins and DNA.[51-54] For these applications, microgels are commonly called "beads". Such microgels are first functionalized with ligands which are able to specifically bind to the target. Typical ligands are biomolecules such as antibodies, antigens, other proteins such as streptavidin or DNA/RNA probes. The principle of the separation consists of the specific binding to the target, subsequent washing to remove the unbound material and purify the target, and finally removing the target from the microgel by elution. The washing step can be performed by different procedures: centrifugation, filtration or magnetic separation. In particular, magnetic separation allows for milder and faster purifications.[51-53, 56] For this application, microgels are made magnetic by loading with superparamagnetic nanoparticles (NPs). Such NPs show magnetic properties only when placed in a magnetic field but lose all magnetism and redisperse when removed from the field. The resulting microgels are therefore individually dispersed and can be collected with a magnet.

One of the first magnetic microgels used for biosensing and bioseparation applications have been synthesized by Ugelstad in the 1970[ies].[57] They consist of highly monodisperse, magnetic polystyrene beads of 2 to 5 µm. These microgels are nowadays commercialized under the trade name DYNABEADS and are still the most commonly used magnetic beads for magnetic separation of cells, proteins and DNA.[51, 54, 58-60] However, these particles are based on polystyrene and therefore are not

biocompatible but prone to unspecific interactions with proteins.[54] Hence, alternative hydrophilic and biocompatible microgels are currently under investigation.[56, 61-64]

<u>Drug delivery</u>

Microgels have also received considerable attention as potential carriers for drug delivery in the past two decades.[13, 15, 16, 18, 19] Carrier materials are designed to load drugs and release them in a controlled fashion at the targeted sites. In addition, such carriers enable to transport hydrophobic drugs under aqueous physiological conditions, protect them from enzymatic degradation and provide, in some cases, stealth behavior resulting in prolonged blood circulation times. Such properties enable to avoid side effects, maintain a continuous concentration of drugs and reduce dosage as well as frequency of administration.[65, 66] Typical carriers for drug delivery are micro- and nanoparticles, micelles and vesicles such as liposomes.[13] Compared to these carriers, microgels are more stable and their payload is less susceptible to leakage. In addition, they present a stimuli-sensitive behavior which is advantageously used for loading and release. Eventually, microgels show high loading capacity.[13, 15, 67]

Many different strategies exist for the loading and release of drugs using microgels. One common strategy applied for loading relies on the physical entrapment of drugs after diffusion through the intrinsic pores of the gel network. Since pores of the microgels can reach up to several nanometers, small drugs can be easily loaded. Release of the drugs is then achieved via different strategies.[65-67] For example, release can be obtained by simple diffusion under the same conditions as for loading (Scheme 1.11). Drugs can also be released via swelling of the microgels leading to pore opening or shrinkage of the microgels leading to the forced expulsion of drugs (Scheme 1.11). In this last case, thermosensitive or pH-sensitive microgels are most frequently used. Microgels of PNIPAAm swell at room temperature and can be used for the loading of drugs but they shrink close to body temperature and may thereby expel the drugs.[68] PAA has also been incorporated in microgels for oral drug delivery of insulin. Insulin was protected from the low pH of the stomach since it kept entrapped in the microgels but could be released upon pH increase after passage in the stomach, leading to the swelling of the microgels via electrostatic repulsion between acrylates.[17] The toxicity of these polymers, especially of PNIPAAm, may however prevent true biomedical applications.[69, 70] Eventually, release can also be triggered by degradation of the polymer network (Scheme 1.11). For this application, microgels of the biocompatible and biodegradable PLGA have been the most extensively investigated so far.[71, 72] In particular, large porous PLGA particles have been considered for pulmonary drug delivery.[73]
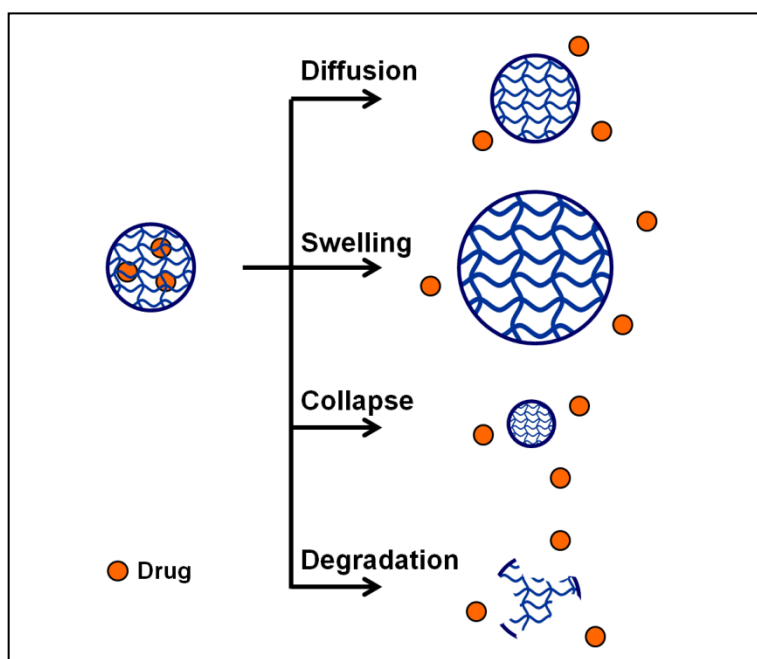
Scheme 1.11. *Possible mechanisms of release of physically-entrapped drugs in microgels.*

In addition to the physical entrapment, drugs can be loaded into microgels using chemical strategies. One common strategy consists of covalently attaching drugs to the microgels by using cleavable bonds, such as disulfide, hydrazine or acetal bonds.[74] Drugs can then be released by cleavage of the bond under reducing or acidic conditions, respectively (Scheme 1.12). This method is however complicated since synthetic procedures need to be adapted for the covalent binding of each new drug. This reaction may also require the use of solvents and reagents which are not biocompatible. A more straightforward and biocompatible method consists of loading and releasing charged molecules via electrostatic interactions in water (Scheme 1.12).[67, 75] For this, acidic and basic functional groups are introduced in the microgels. For the loading of a charged molecule, the pH of the system is adjusted to the values at which the microgels bear an opposite charge. By changing the pH value to switch the protonation state of the functional groups, the microgels turn neutral and can release the charged substance. For instance, carboxylates can be loaded with cations at pH above their pK_a and release them at pH below.[67] In the opposite case, amine groups can be loaded with anions at pH below their pK_a and release them at pH above.[67] As an example, cationic poly(amines) are used for complexing polynucleotides for gene delivery.[76]
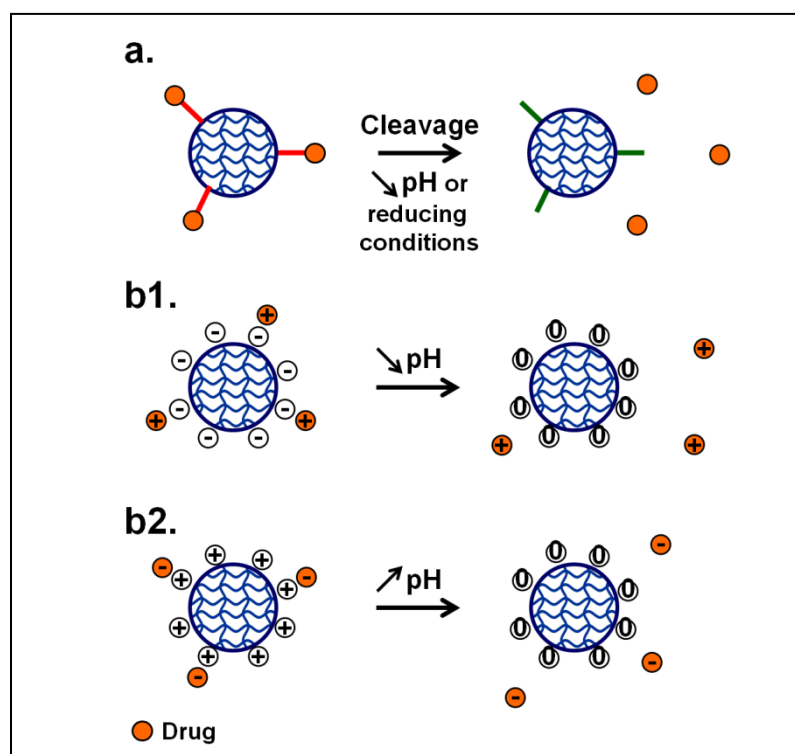
Scheme 1.12. *Release of drugs loaded in microgels by a. cleavage of a covalent bond; b. electrostatic interaction with carboxylates (b1) and amine groups (b2).*

Microgels for the treatment of bacteria

One important bio-related application of microgels encompasses the treatment of bacteria. Bacteria are single-celled microorganisms which are classified amongst prokaryotes since they lack a cell nucleus.[77] Their broad metabolic capabilities enable them to live in almost every environment as well as grow and divide very rapidly. Bacterial cells are composed of a cytoplasm which contains the genetic material, a membrane consisting of proteins and lipids and a rigid cell wall made of peptidoglycans (Scheme 1.13). Depending on the properties of the cell wall and its reaction to the "Gram" stain, two types of bacteria can be identified. Gram-positive bacteria present a thick cell wall composed of many layers of peptidoglycans. Gram-negative bacteria present a thinner cell wall composed of a few layers of peptidoglycans and surrounded by a second lipid membrane containing lipopolysaccharides and lipoproteins. Most bacteria are Gram-negative. Moreover, bacterial membranes are usually negatively-charged due to the presence of anionic lipids.[78] In addition, some bacteria present extracellular appendages such as flagella used for motility, or pili also called fimbriae which are straight, rigid appendages allowing them to adhere to surfaces (Scheme 1.13). The pili of some bacteria are constituted of proteins able to attach to specific carbohydrates present on the surface of other cells, via carbohydrate-protein interactions.[79-81]
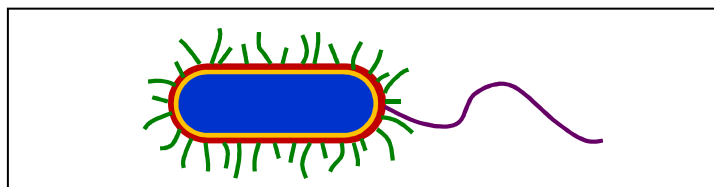
Scheme 1.13. *Simplified structure of a bacteria showing the cytoplasm (blue), the membrane (yellow), the cell wall (red), a flagellum (purple) and pili (green).*

Two types of bacteria can be differentiated: harmless or even beneficial bacteria on one side and pathogenic bacteria on the other side. First, bacteria are very valuable and useful microorganisms. For example in nature, they convert dead organic materials into nutrients, thereby fertilizing soils and sustaining higher life-forms.[77] Some bacteria are advantageously employed in industrial fermentation processes for food preparation. For instance, they participate in the conversion of milk into yogurt or cheese and in the preparation of sauerkraut and olives.[77, 82] Bacteria are also used for the production of chemicals, partly from sugar fermentation, and the isolation of enzymes such as amylases.[77, 83] Eventually, bacteria are used in the pharmaceutical industry for the production of antibiotics and recombinant drug proteins after genetic modification.[83, 84] To support these applications, magnetic microgels are currently used to purify enzymes and drug proteins. In addition, magnetic microgels can be employed to remove bacteria from the final product or microbial culture and release them for further applications. This is mostly interesting for the valuable genetically engineered bacteria or when mixtures of bacteria are employed and specific strains need to be removed.

On the other hand, a few species of bacteria, called pathogenic bacteria, are known for being harmful and causing severe infectious diseases. For example, pathogenic bacteria have found to be responsible for tuberculosis, pneumonia, cholera or plague.[77] The fact that bacteria can live in almost any environment and spread very rapidly, especially in water or food, critically increases their potential threat. Hence, microbial infections are still reported as one of the major causes of death, in particular in developing countries.[85, 86] The carbohydrate-binding proteins present on the surface of bacteria have been identified for being partially responsible for microbial adhesion to cells and infections.[79-81] Moreover, pathogenic bacteria can be recognized by the presence of specific antigens on their surface. Different strains of the same pathogenic bacteria may however exhibit different antigens. It is therefore crucial to detect and eliminate pathogenic bacteria from contaminated solutions or physiological fluids. Microgels have been employed to achieve these goals. For instance, magnetic beads such as DYNABEADS are used for the detection of pathogenic bacteria.[52, 53] Microgels are also currently developed for drug delivery applications, especially delivery of antibiotics.[13, 15, 16] However, due to the widespread resistance of bacteria to antimicrobials, alternative strategies for the elimination of bacteria are also required.[87-91] A surrogate option consists of the detection and magnetic removal of bacteria using microgels. Compared to filters used for the removal

of bacteria via unspecific size discrimination,[92-95] magnetic particles show a wider range of applicability and allow for an easy, rapid and, above all, specific removal of pathogenic bacteria, for example leaving other cells unaffected. Very high yields of loading and removal can be achieved with such particles however high amounts of magnetic beads are usually required.

One particularly important species of bacteria encompasses the bacteria *Escherichia coli* (*E. coli*). These Gram-negative, rod-shape bacteria are approximately 2 µm long, 0.5 µm wide and present carbohydrate-binding proteins located on their pili.[96-98] In particular, these bacteria are able to bind to the monosaccharide mannose.[79] *E. coli* are normal inhabitant of the intestinal tract of humans and animals and are in general harmless or even beneficial, for example producing vitamin K in the gut of their host.[99] These bacteria are also employed in biotechnological processes such as the production of recombinant drug proteins.[84] Moreover, *E. coli* are frequently used as model bacteria in microbiology studies, partially because cultivated strains are well-adapted to laboratory work and have lost their ability to thrive in the intestine.[100] However, a few pathogenic strains of *E. coli* have found to be involved in severe gastrointestinal infections, causing diarrhea and hemorrhagic colitis.[101] It could be demonstrated that the carbohydrate-binding proteins located on the pili of pathogenic *E. coli* bacteria play an important role in bacterial adhesion to cells and infections.[97] The strain O157:H7 has been identified as one of the major pathogenic strains of bacteria *E. coli*.[102] Detection of this particular strain is possible via the use of DYNABEADS.[103]

Overall, microgels have found many applications in the detection, retrieval and elimination of bacteria.[51-53] One of their key features consists of the specific targeting of bacteria strains. Different strategies have been developed to target bacteria so far. They rely either on polycations to target the anionic membranes of bacteria,[104, 105] antibodies to target the antigens of pathogenic bacteria,[53, 106-108] or carbohydrates to target the carbohydrate-binding proteins of bacteria.[79, 109-118] Using carbohydrate ligands could in principle target bacteria, discriminate between strains of bacteria presenting different receptors and selectively bind bacteria presenting large amounts of carbohydrate receptors. Compared to cationic materials, carbohydrates ligands enable the specific detection of bacteria strains. Compared to antibodies, carbohydrates are less prone to denaturation and generally present broader interaction specificity.[119] The use of carbohydrates should therefore allow for the detection of unanticipated or new bacteria strains,[79] and broadens the applicability of microgels in the treatment of bacteria.

All in all, microgels have already been employed in a huge range of applications, especially in industry. A considerable amount of research is still devoted to microgels and will extend the scope of their applications in the next decades, especially in the biotechnological and biomedical fields.

2. Aims and Outline

Microgels are usually defined as microparticles of 100 nm to 100 µm, which are composed of cross-linked polymers and capable of swelling in a good solvent.[2, 3] These microparticles are very attractive materials since they are versatile, easily handled, colloidally stable, viscoelastic and present large specific surface areas.[5] In addition, they exhibit an advantageous stimuli-sensitive swelling behavior. Microgels have therefore been employed for a wide range of applications such as surface coatings, oil recovery, separation by chromatography and solid phase synthesis in chemistry.[2, 3, 9, 10]

In addition, microgels are widely used in biotechnology for biosensing or bioseparation and hold great potential for biomedical applications such as oral and transdermal drug delivery.[9, 13-18] These microparticles can be easily functionalized *e.g.* with receptor-specific ligands for active targeting. The size of the employed microgels is generally in the range of a few micrometers, which is a good compromise for both an easy handling and the high specific surface areas needed for efficient targeting. The enthusiasm for microgels in bio-related applications partially arises from their potential to mimic biological cells in size, degree of hydration, texture and colloidal stability in physiological fluids. For drug delivery applications, the large swelling-collapse transitions of microgels are advantageously employed for the loading of small drugs by diffusion through the pores of the gel, protection from degradation and final release. Compared to other carriers such as vesicles, microgels are more stable and their payload is less susceptible to leakage.[13] Microgels of the thermosensitive polymer PNIPAAm have been the most extensively investigated in this context since they are capable of releasing entrapped drugs close to body temperature.[120]

One important bio-related application of microgels encompasses the treatment of bacteria. Bacteria are nowadays used for various applications in the food and pharmaceutical industry, such as fermentation processes or proteins production.[82-84] In that case, microgels are employed to remove bacteria from the final product or select, catch and release bacteria from microbial cultures. Under different conditions, microgels have also found applications in the detection, retrieval and elimination of pathogenic bacteria from contaminated solutions.[51-53] These pathogens can be either removed or killed via delivery of antibiotics using microgels.[15, 16, 19] For the retrieval of bacteria, the most widely used microgels are polystyrene-based resins, which are made magnetic and functionalized with ligands for bacteria targeting.[54, 103, 117, 121-124] These microgels are able to bind bacteria and can be removed by simply using a magnet. Compared to filtration techniques, the use of functional microgels presents a wider range of applicability and allows for easy, rapid and, above all, specific removal of bacteria.

However, the currently developed microgels present some fundamental limitations for bio-related applications and in particular for the manipulation of bacteria. One major restriction lies in the choice of polymeric materials since a compromise needs to be found between biocompatibility, stimuli-sensitivity and ease of synthesis and functionalization. Although broadly used, PNIPAAm is neurotoxic[69, 70] and polystyrene is not biocompatible but prone to unspecific adsorption of proteins, which limits their applicability.[54] A second major limitation of current microgels comes from their restricted loading capacity, which decreases their performance. For the retrieval of bacteria, a high concentration of magnetic microgels is usually required to achieve high yields of removal. This means that only few bacteria are bound per particle. For drug delivery, only small molecules can be loaded through the pores of the gel network. Eventually, an additional limitation of current microgels is that multicomponent, multifunctional microgels can only be achieved via the synthesis of complex structures, such as core-shell microgels.[6] Therefore, the next generation of microgels should present two very essential features: 1) a biocompatible, hydrophilic polymeric scaffold reducing unspecific interactions and allowing for surface functionalization, and 2) a higher loading capacity allowing for a straightforward incorporation of different entities of various sizes and natures, while still guaranteeing the integrity of the microgels.

Thus the aim of this work is to prepare a novel platform of microgels based on functional porous PEG hydrogel microparticles. 1) Concerning the first requirement of biocompatibility, PEG is an ideal candidate since it has been FDA approved and is the most frequently used polymer for biotechnological and biomedical applications.[40] In addition, a new protocol was recently established, enabling the functionalization of PEG microgels for targeting as well as stimuli-sensitive loading and release applications.[125, 126] 2) Concerning the second requirement, higher loading capacity will be achieved by introducing interconnected pores. Hierarchical microgels with pores of different sizes will allow for the loading of different components, based on their size. In this work, PEG microgels will feature internal pores of a few tens of nanometers allowing for the loading of large drugs or nanoparticles, as well as larger pores of a few microns on the surface of the particles for the binding of cells or bacteria. In order to test their potential for biotechnological and biomedical applications, they will then be used for the targeting and removal of bacteria as well as evaluated for a potential delivery of antibiotics to bacteria. Overall, functional porous PEG microgels also present great potential for a wider range of biotechnological and biomedical applications such as bioseparation of cells, detection of viruses and purification of proteins or catalysis.

Since control over the size and porosity of PEG microgels is a prerequisite, a hard templating method based on $CaCO_3$ microparticles will be applied for the synthesis (chapter 3). The obtained porous PEG microgels will thereafter be functionalized using radical chemistry with both carbohydrate ligands for bacteria targeting and cationic moieties for the loading of molecules and nanoparticles via

electrostatic interactions (chapter 4). The functional porous PEG microgels will then be made magnetic by introducing magnetic nanoparticles and tested for the specific detection and magnetic removal of bacteria, compared to the standard non-porous and non-biocompatible particles currently used for this application (chapter 5). Finally, the potential of these microgels for antibiotics delivery will be investigated via the introduction of a novel CO_2-sensitive, carbamate-based functionalization, enabling efficient electrostatic loading and release of charged dyes used as model drugs (chapter 6).

3. Synthesis of Porous PEG Microgels

The aim of this work is to prepare a novel platform of porous microgels and use them for the targeting and magnetic removal of bacteria as well as for a potential drug delivery. These microgels therefore have to present the two following features: 1) a biocompatible polymeric scaffold reducing unspecific interactions and allowing for surface functionalization, and 2) a higher loading capacity allowing for a straightforward incorporation of drugs and magnetic nanoparticles (NPs) as well as for the binding of a high number of bacteria. To achieve this aim, porous PEG microgels have been synthesized.

Concerning the first requirement of biocompatibility, microgels of poly(lactic-co-glycolic acid) have been extensively investigated for biomedical applications.[71] These hydrogels are not only biocompatible but also biodegradable, which makes them perfect candidates for drug delivery but prevents long-term applications, such as bacteria retrieval employing reusable microgels. As alternative, PEG is an ideal candidate since it is hydrophilic, neutral, biocompatible but not biodegradable, FDA-approved and prevents unspecific interactions with proteins. For these reasons PEG is one of the most frequently used polymers for biotechnological and biomedical applications.[40] However, in the past, the functionalization of PEG scaffolds was quite intricate and high degrees of functionalization could not be achieved. As a result, PEG has found more applications as coating for microgels than as a pure microgel.[41] Recently, a new protocol has been introduced to achieve easy and variable functionalization of PEG hydrogels, thereby extending possible applications of PEG microgels.[125, 126]

Concerning the second requirement, higher loading capacity will be achieved by introducing pores into the microgels. Porosity indeed increases the specific surface area available for the incorporation of drugs or NPs or the binding of bacteria. Pores are intrinsically present in the hydrogel network but are too small for the loading of large molecules or efficient binding of bacteria. Enlarging these pores could be achieved by increasing the chain length of the cross-linked polymers but this would result in very soft microgels and dramatic loss of mechanical stability. A more efficient strategy consists of introducing new, larger pores. In this case, the intrinsic pores of the hydrogel network remain intact and the stiffness of the gel can still be fine-tuned to maintain the mechanical stability. Another method to improve loading capacity by increasing the specific surface area would be to decrease the size of PEG microgels. However, porosity is preferred since the loaded drugs can be protected from their environment in the pores of microgels whereas they would be exposed to degradation on the surface of smaller microgels.

These new pores need to be interconnected to be fully accessible for loading from the exterior of the microgels and their size should be adjusted to the desired components to be loaded. In order to achieve multifunctional microgels, hierarchical microgels featuring different levels of porosity should be prepared. The presence of intrinsic pores and introduction of new pores already allows for the loading of different components based on their size. Furthermore, pores of different sizes can be incorporated. In this work, the porous PEG microgels should feature internal pores of a few tens of nanometers for the loading of large drugs or NPs and larger pores of one to two microns on the surface of the particles for the binding of bacteria. To the best of our knowledge, this is the first time that microgels exhibiting such elaborate porosity have been prepared.

In the following chapter, the synthesis and characterization of such porous PEG microgels will be described. To better control the porosity of PEG microgels, a hard templating method based on $CaCO_3$ microparticles was used. The principle of particle formation based on this method will be first explained in section 3.1. Then the experimental procedure will be detailed in section 3.2, emphasizing the critical synthetic conditions responsible for the final structure of PEG microgels. In the final section 3.3 of this chapter, the morphology and porosity of the resulting porous PEG microgels will be characterized and the possibility of a real structural control by the introduced procedure will be evaluated.

3.1. Principle

PEG microgels were synthesized from the telechelic macromonomer PEG-diacrylamide (PEG-dAAm, Scheme 3.1). It was preferred over the more common PEG-diacrylate since it is known to be more resistant to hydrolysis in water, amides being more stable linkages than esters.[44] PEG-dAAm was synthesized by D. Pussak following a procedure reported by Hartmann *et al.*, based on work by Elbert and Hubbell.[44, 45] Subsequent polymerization of PEG-dAAm in water was started by radical initiation upon UV irradiation using the water-soluble photoinitiator Irgacure 2959 (Scheme 3.1) and led to cross-linking and formation of PEG hydrogel.
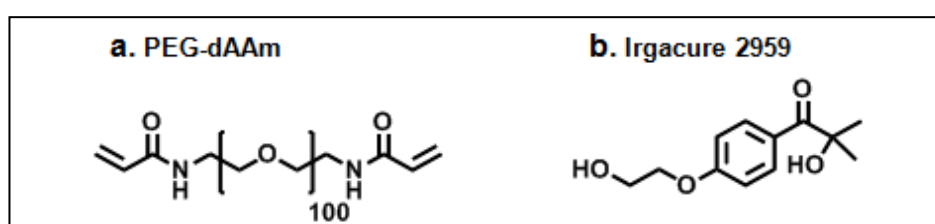
Scheme 3.1. *Structural formulas of the macromonomer PEG-dAAm and the water-soluble photoinitiator Irgacure 2959 used for the synthesis of PEG microgel.*

Non-porous PEG microgels have already been synthesized by precipitation polymerization of PEG-dAAm in aqueous sodium sulfate solutions.[46, 48] At high salt concentrations, PEG-dAAm undergoes phase separation to produce spherical PEG-rich domains, which were cross-linked upon UV irradiation using Irgacure 2959. The size of the resulting microgels could be controlled by the concentrations of polymer, sodium sulfate salt and temperature. Non-porous PEG microgels with an average diameter of 10 µm could be prepared by polymerization of a 0.5 M sodium sulfate solution containing 0.5 wt.% of PEG-dAAm at 70 °C (see Appendix, Figure 8.1). These microgels were used as negative control to the porous PEG microgels presented in this work.

Porous microgels are commonly prepared by suspension or precipitation polymerization in the presence of porogens,[26, 28, 30, 31] or by using templating techniques.[32-35] In this work, porosity was introduced by a templating method because it allows for the formation of interconnected pores of different sizes and for overall improved control over the morphology and porosity.

By definition, templating consists of the inverse replication of one structure into another.[32, 33, 35] Templates are therefore structure-directing agents and the generated material is expected to be a true inverse copy of its template. For thermodynamic and physicochemical reasons, the use of hard, inorganic templates usually leads to more successful replications into organic materials than that of soft, organic templates.[32, 34, 36, 37] Porous inorganic particles have therefore been used for the synthesis

of the porous PEG particles. The principle of this method is depicted in Scheme 3.2: first the pores of the template particles are filled with PEG hydrogel precursors, then PEG hydrogel is formed by polymerization and finally the template is removed, leaving pores in the resulting PEG particles.
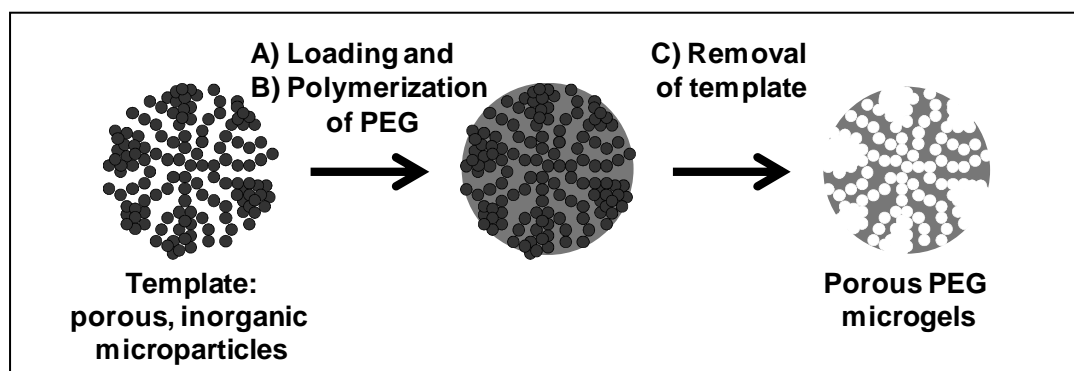
Scheme 3.2. Principle of hard templating for the synthesis of porous PEG microgels from porous, inorganic microparticles.

The choice of template is crucial since it will be responsible for the porosity of PEG microgels. The template particles should present the inverse morphology of the expected microgels, for which nano-sized, interconnected, internal pores and micro-sized external pores were envisioned. Thus, the template particles should be porous, constituted of small interconnected NPs and presenting larger aggregates on their surface. This particular structure is very uniquely presented by $CaCO_3$ microparticles, as revealed by scanning and transmission electron microscopy (SEM, TEM, Figure 3.1). $CaCO_3$ particles consist of crystallites of about several tens of nanometers in size, which are arranged in fibers radiating from the center of the particles.[127, 128] Depending on sample preparation, larger crystallite aggregates of several hundreds of nanometers up to 1 - 3 µm can be observed on the surface of $CaCO_3$ particles (Figure 3.1.e). The voids between these crystallites represent pores that are interconnected throughout the particles. Exact inverse replicates would therefore present a homogeneous channel-like structure with pores of the expected sizes.

In addition to their unique internal morphology, $CaCO_3$ microparticles are very attractive templates since they are non-toxic, relatively monodisperse, structurally uniform and easy to prepare. Furthermore, $CaCO_3$ can be decomposed under relatively mild conditions by complexation with EDTA salts (ethylenediaminetetraacetic acid) or at low pH values. This is very advantageous since other hard templates usually require harsh conditions for decomposition, such as HF etching for silica particles, which would severely alter the integrity and biocompatibility of PEG microgels.
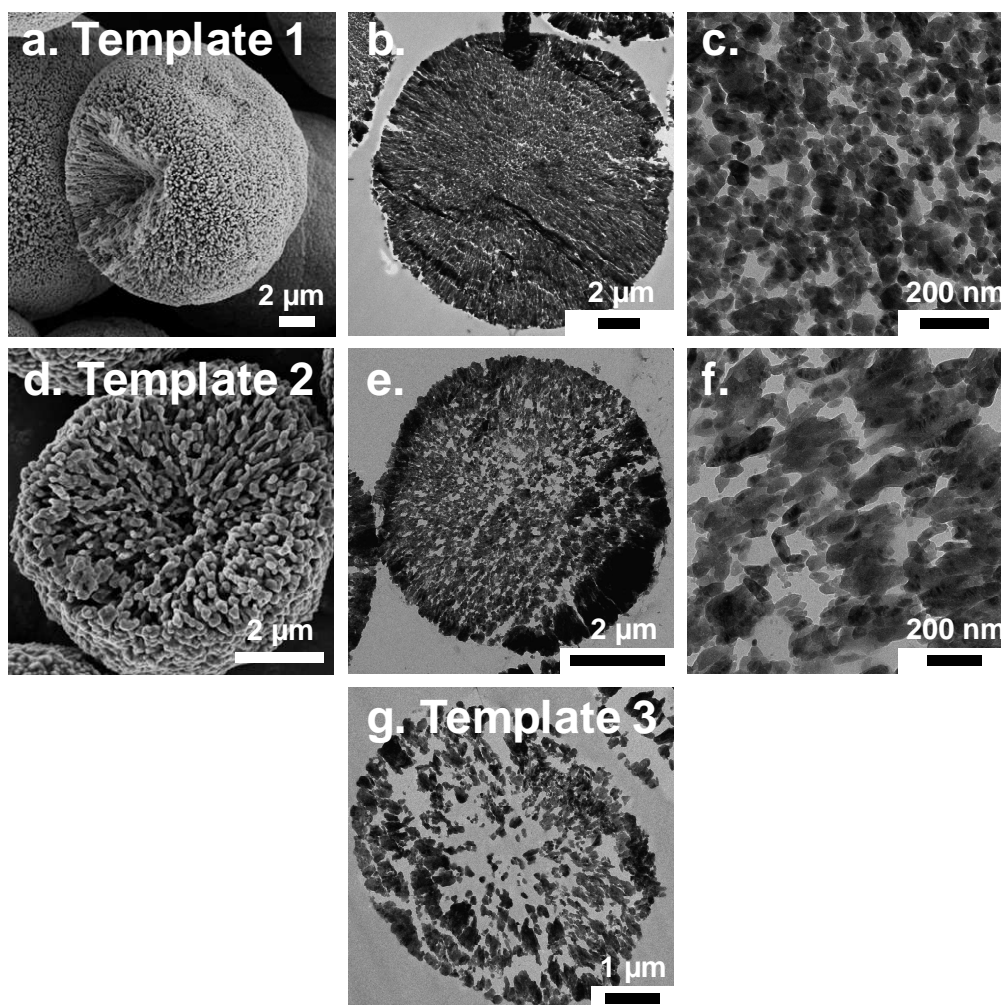
Figure 3.1. *Electron microscopy images of the CaCO₃ particles used as templates for the synthesis of porous PEG microgels: template 1 of 17.9 µm, template 2 of 6.9 µm and template 3 of 7.3 µm. a. SEM image of broken particles of template 1; b. and c. TEM images of cross-sections of particles of template 1. d. SEM image of broken particles of template 2; e. and f. TEM images of cross-sections of particles of template 2; g. TEM images of cross-sections of particles of template 3.*

In order to achieve the expected porosity in PEG microgels, three types of $CaCO_3$ microparticles differing in their diameter and density were tested. First, $CaCO_3$ particles of $17.9 \pm 3.4 \, \mu m$ with a uniform distribution of crystallites of 20 to 60 nm but relatively few surface aggregates were synthesized by Dr D. Volodkin (Figure 3.1.a-c).[129, 130] These particles were compared to two batches of commercial $CaCO_3$ microparticles of smaller sizes and lower density. One type of commercial particles presents an average diameter of $6.9 \pm 0.7 \, \mu m$, similar nano-crystallites and large aggregates of several hundreds of nanometers reaching up to 1 - 3 µm on their surface (Figure 3.1.d-f). The third type of particles of $7.3 \pm 1.2 \, \mu m$ presents the lowest density of all investigated templates featuring very few crystallites and aggregates (Figure 3.1.g). In the following

discussion, these templates and resulting PEG microgels will be referred to as sample 1 (17.9 µm, high density), sample 2 (6.9 µm, medium density) and sample 3 (7.3 µm, low density).

Porous $CaCO_3$ microparticles have already been used for hard templating applications. However, most often microcapsules have been formed by layer-by-layer physisorption of polyelectrolytes.[129-135] In these cases, the polymers were mostly deposited on the surface of $CaCO_3$ microparticles and little attention has been devoted to the infiltration of polymeric materials into the pores of $CaCO_3$ or to the resulting morphology of the infiltrated material. So far, only pure insulin particles have been synthesized by infiltrating the internal structure of $CaCO_3$ microparticles but they collapsed after template removal.[136, 137]

PEG hydrogels are also flexible networks, which may collapse upon introduction of pores into their structure. True inverse replication of $CaCO_3$ templates is therefore challenging since replicas can only be obtained if polymers are effectively and selectively loaded into the template and the obtained hydrogel is sufficiently rigid to maintain the structure of the microgels after template removal. The stiffness of the hydrogel is partially controlled by the cross-linking density, which is set by the concentration of radicals during cross-linking and chain length of PEG macromonomers. However, very rigid hydrogels are not desirable since they are not flexible enough for the envisioned presentation of ligands for bacteria targeting. Therefore, PEG of an intermediate size and an average molecular weight M_n of 4600 Da was chosen in this work (~ 100 ethylene glycol repeating units per macromolecule). All other parameters responsible for an exact replication could be controlled by the synthetic conditions. In the following section, the procedure for the infiltration of PEG hydrogel precursors in $CaCO_3$ microparticles and inverse replication into PEG microgels will be described.

3.2. Synthetic Procedure

As illustrated in Scheme 3.3, the general procedure for the synthesis of porous PEG microgels can be divided into three steps.[138] In the first step (A), PEG-dAAm and the photoinitiator Irgacure 2959 were loaded into $CaCO_3$ microparticles by a multistep process. In the second step (B), the resulting composite particles were irradiated with UV-visible light to polymerize PEG macromonomers and form a hydrogel inside the pores of the template. Finally, in the last step (C), the $CaCO_3$ templates were dissolved under acidic conditions, yielding porous PEG microgels.
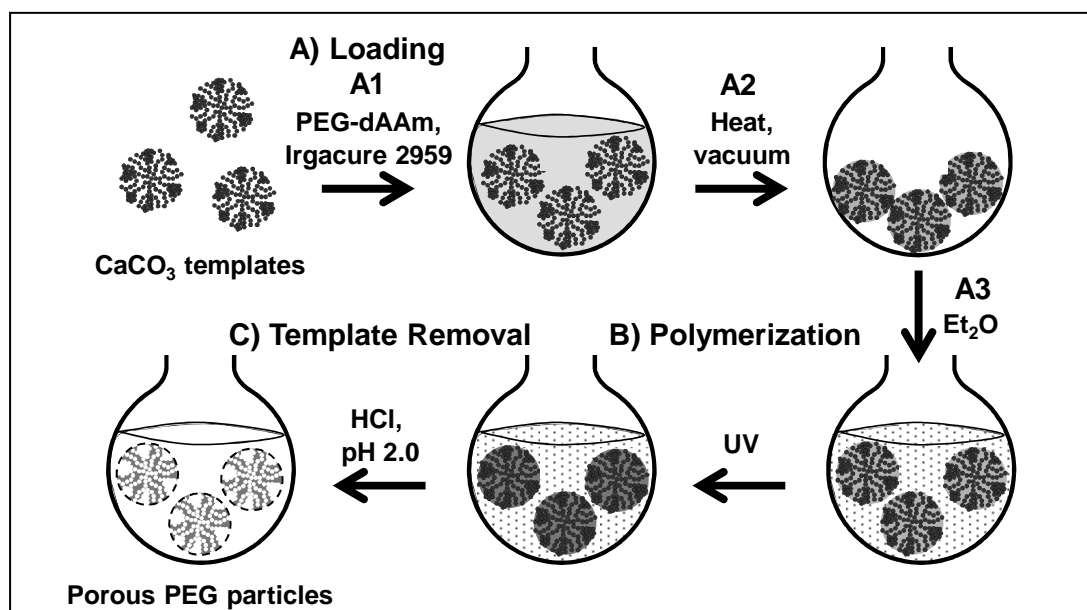
Scheme 3.3. *Procedure for the synthesis of porous PEG microgels by hard templating with CaCO₃ microparticles: A) Loading of precursors into the template; B) Polymerization of PEG macromonomers within the template and hydrogel formation; C) Removal of CaCO₃ template under acidic conditions.*

The first step of this templating process consists of the infiltration of CaCO₃ microparticles with PEG macromonomers and photoinitiator. This is the most critical step as there are several challenges and requirements to be met. Most importantly, PEG has to diffuse into the pores of the particles and completely fill them in order to form an inverse replica of the template and retain porosity after template removal. This means that PEG molecules should not only adsorb on the surface of the particles to avoid formation of hollow capsules, but also no excess PEG should accumulate on the surface to avoid blocking of pores, cross-linking between particles and aggregation.

The loading of hydrogel precursors was therefore performed in three steps (Scheme 3.4). In the first step A1, CaCO₃ microparticles were dispersed in an aqueous solution of PEG and UV-initiator. Then these compounds were transferred into the template particles by solvent evaporation under vacuum in the step A2. The exact mechanism of this loading is not yet fully understood. It is believed that the precursors are effectively transported from the bulk solution to the core of the particles by capillary forces during drying. Eventually, the dry composite particles were redispersed in solution in the step A3 to avoid cross-linking between particles during polymerization. Diethyl ether was used in this step since it is known to be a poor solvent for PEG and prevents the dissolution and diffusion of PEG out of the CaCO₃ templates.

A1: dispersion
(precursors in H₂O)

A2: evaporation

A3: redispersion
(Et₂O)
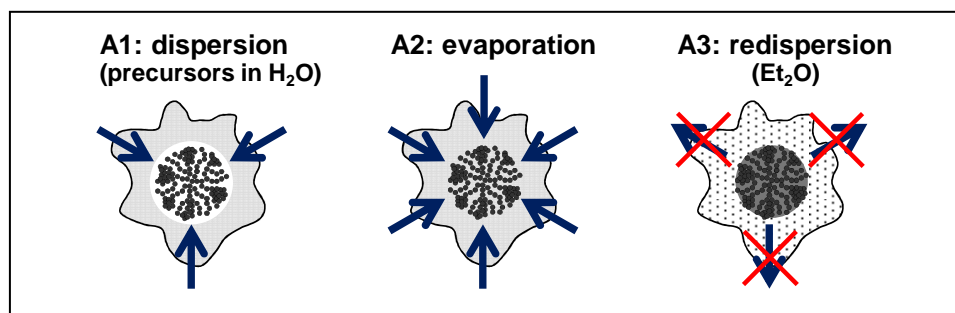
Scheme 3.4. Principle of the multistep loading of PEG hydrogel precursors into CaCO$_3$ template microparticles.

The amount of loaded PEG is another critical parameter. The pores of the template particles should be completely filled with polymer while avoiding accumulation of excess material on their surface. Since the CaCO$_3$ templates exhibit different porosities, different amounts of PEG had to be loaded, with particles of higher densities requiring less PEG. The amount of PEG could be adjusted by two parameters: the sample volume during drying and the concentration of PEG relative to that of CaCO$_3$. For template 1 which demonstrates the highest density, the amount of loaded PEG could be drastically reduced by spreading and drying the dispersion of particles and precursors over large surfaces (glass flasks, Table 3.1). In that case, PEG predominantly dried in the free space between particles, thereby reducing the amount of PEG drying inside the particles. In contrast, smaller volumes were applied for the loading of templates 2 and 3 of lower density (Eppendorf tubes of 1.5 ml, Table 3.1). In these cases, free space between particles was almost nonexistent so that PEG predominantly accumulated inside the particles. With this method high amounts of PEG could be loaded into the particles so that accumulation of PEG on the surface of particles had to be avoided by reducing the PEG/CaCO$_3$ weight ratio. Therefore 20 wt.% were required for template 3 of the lowest density, while the concentration had to be reduced to 5 wt.% for template 2 of medium density.

Table 3.1. Loading conditions for the synthesis of porous PEG microgels from different CaCO$_3$ templates.

Template	1	2	3
CaCO$_3$ template size	17.9 µm	6.9 µm	7.3 µm
Density	High	Medium	Low
Sample volume	Diluted, Glass flask	Concentrated, Eppendorf tube	Concentrated, Eppendorf tube
Ratio PEG/CaCO$_3$	20 wt.%	5 wt.%	20 wt.%

After successful loading of the precursors, PEG-dAAm macromonomers were polymerized by radical initiation upon UV irradiation, leading to cross-linking and hydrogel formation. Even though UV transmission through $CaCO_3$ templates is low, radicals can be formed at the surface of the composite particles and then diffuse into the inner parts, leading to efficient cross-linking of PEG throughout the particles. No aggregation was observed after UV irradiation, indicating the absence of excess PEG on the surface of the template particles.

In the last step, the $CaCO_3$ templates were dissolved in an aqueous solution of HCl (pH 2.0). Carbonate ions were converted into carbon dioxide gas and the remaining $CaCl_2$ salt was washed away with water. Acidification was preferred over complexation with EDTA since it resulted in a much faster decomposition of the template. Complete removal of the template was confirmed by energy-dispersive X-ray spectroscopy (EDS) which showed no calcium peak after washing (see Appendix, Figure 8.2). This last step finally led to the porous PEG microgels.

3.3. Characterization of Porous PEG Microgels

The resulting PEG microgels were then characterized to check if the expected porosity was obtained.[138] Their structure was also compared to that of $CaCO_3$ microparticles to determine if true inverse replicas have been synthesized by the templating method.

Light microscopy revealed that non-aggregated, spherical hydrogel particles were obtained (Figure 3.2.a-c). No major change in size was observed after template removal. PEG microgels synthesized from $CaCO_3$ templates of $17.9 \pm 3.4\,\mu m$ (sample 1), $6.9 \pm 0.7\,\mu m$ (sample 2) and $7.3 \pm 1.2\,\mu m$ (sample 3) presented an average diameter of $17.6 \pm 2.7\,\mu m$, $9.2 \pm 1.3\,\mu m$ and $8.3 \pm 0.8\,\mu m$, respectively. In addition, the size distribution of PEG microgels was determined from the diameter of hundred particles measured from optical microscopy images. PEG microgels were rather monodisperse and the small polydispersity observed could be mainly attributed to that of the template itself (Figure 3.2.d-e). Thus, PEG particle shape, size and polydispersity were very similar to those of the original $CaCO_3$ templates, giving a first indication that PEG microgels did not collapse after template removal and that true inverse replicas were obtained by the templating method.
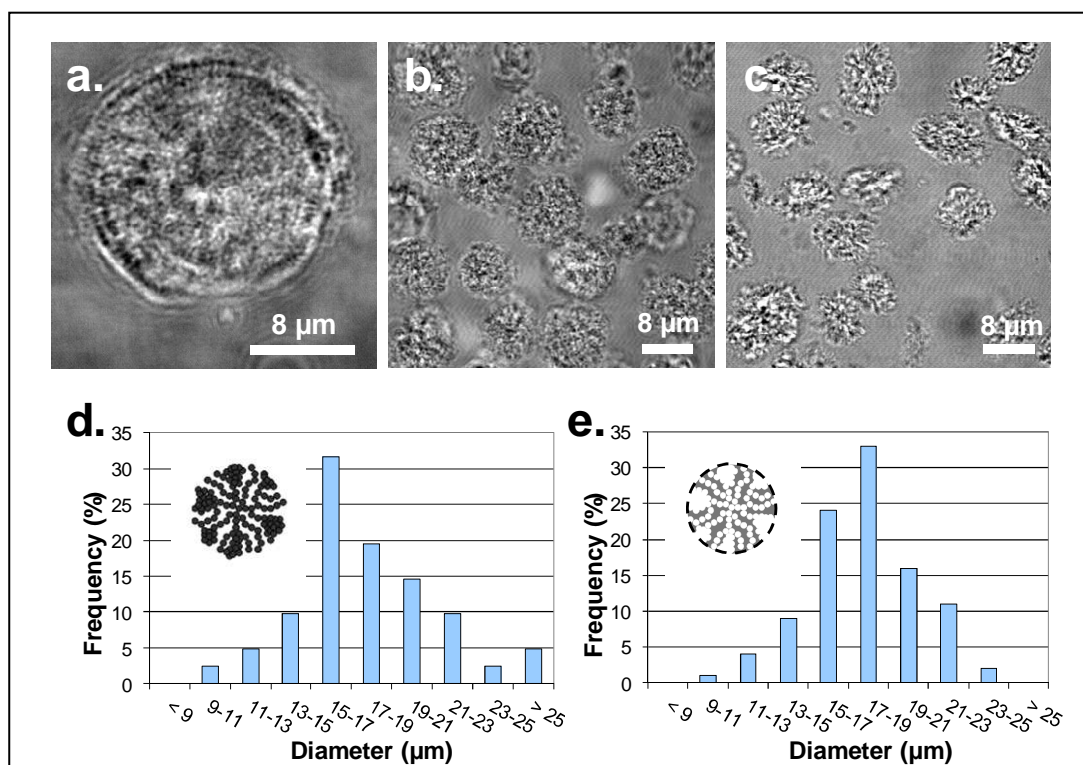
Figure 3.2. *Optical microscopy images of porous PEG microgels of a. 17.6 µm (microgels 1); b. 9.2 µm (microgels 2) and c. 8.3 µm (microgels 3). Note the apparent roughness of PEG microgels. Contrasts were enhanced with the program ImageJ. Particle size distribution of d. pure CaCO$_3$ microparticles of 17.9 µm (sample 1) and e. resulting pure porous PEG microgels of 17.6 µm after washes (sample 1).*

The porosity of PEG microgels was characterized in the next set of experiments. No characterizations could be performed in the dry state since PEG microgels collapsed and did not retain any porous structure upon drying or freeze-drying, as revealed by SEM (Figure 3.3.a and b). To explain the origin of this collapse, the water content of PEG microgels was calculated as the ratio of the average volume of water per particle to that of swollen particles V$_{swollen}$ (Table 3.2). The volume of water was determined as the difference between the volume of swollen particles and the volume of PEG corresponding to that of dry particles V$_{dry}$. V$_{swollen}$ was therefore calculated from the radius of PEG microgels measured from optical microscopy images, while V$_{dry}$ was measured by atomic force microscopy (AFM, see Appendix, Figure 8.3). Taken as example, PEG microgels 1 of 17.6 µm exhibited a water content of 99%, which is typical for hydrophilic polymer hydrogels. PEG microgels were therefore mainly composed of water, which could explain their collapse upon drying. For this reason the porosity of PEG microgels had to be characterized in water, for fully swollen microgels.

Table 3.2. *Definition and characterization of the water content of porous PEG microgels of 17.6 μm (sample 1).*

	Definition	Value
Average volume, swollen particles	$V_{swollen}$	3065 μm³
Average volume, dry particles	V_{dry}	27 μm³
Water content	$\dfrac{V_{swollen} - V_{dry}}{V_{swollen}}$	99%

The presence of pores on the surface of PEG microgels in water could be readily evidenced by optical microscopy, revealing a very rough surface of PEG microgels (Figure 3.2). Further characterization was performed by cryo-SEM on aqueous dispersions of PEG microgels. Compared to standard SEM measured on dry samples under high vacuum, cryo-SEM allows for the observation of frozen aqueous dispersions. High vacuum conditions are still applied but the cryogenic temperatures prevent solvent sublimation. Cryo-SEM was performed on PEG microgels 2 and revealed pores in the range of several hundreds of nanometers, as expected from the templating process (Figure 3.3.c-f). However, smaller pores could not be observed, even though they would be expected if perfect templating had been obtained. Their absence could be related to sample preparation, since the frozen dispersions had to be freeze-etched by slightly increasing temperatures in order to make PEG microgels visible. As soon as freeze-etching started, PEG microgels began to dry due to water sublimation and started collapsing. Under these conditions, the observation of pores in the range of tens of nanometers would be very difficult since pores were either still embedded in ice, not visible, or collapsed as soon as freeze-etching started. On the contrary, larger pores of several hundreds of nanometers are more stable, which is the reason why they could be evidenced on PEG microgels 2.
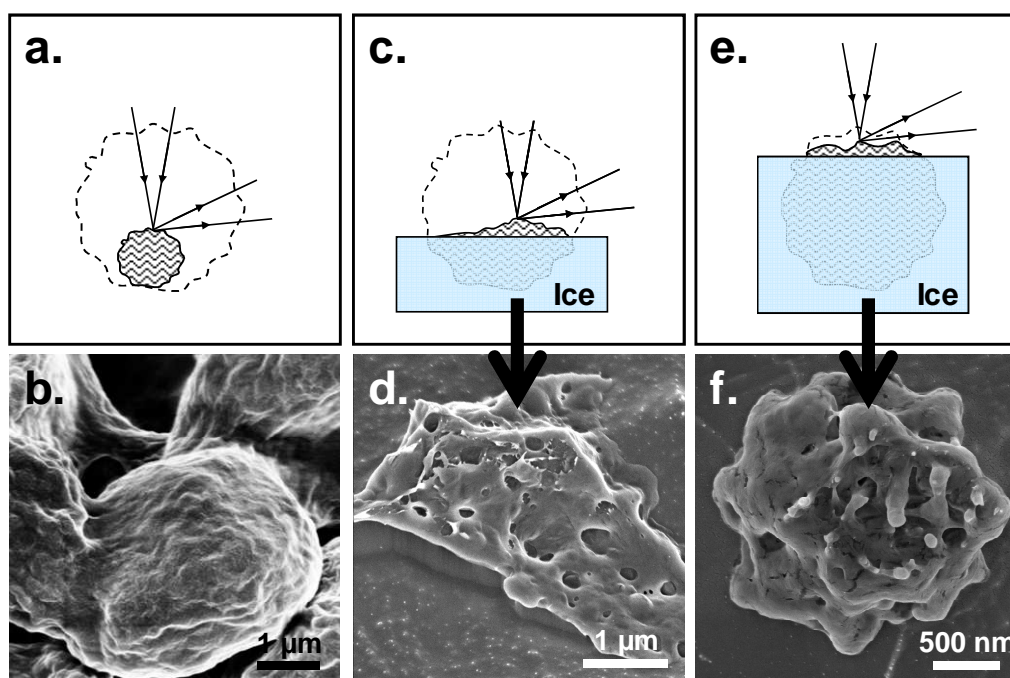
Figure 3.3. SEM images of porous PEG microgels of 9.2 µm (sample 2) and associated interpretation schemes: a. and b. SEM of freeze-dried particles; c. and d. cryo-SEM after long freeze-etching; e. and f. cryo-SEM after short freeze-etching. With too short freeze-etching no particle is visible, whereas with too long freeze-etching, particles completely collapsed.

More detailed characterization, especially of internal porosity, was more complicated. Traditional methods, such as gas adsorption, were precluded since they require dry samples. No signal could be obtained by small-angle X-ray scattering (SAXS), since the contrast between the two phases of water and fully-hydrated hydrogel was too low. TEM on cross-sections of PEG microgels embedded in a polyacrylic resin could not provide any further information, since the contrast between the PEG hydrogel and the resin was again too low. However, internal porosity could be indirectly characterized via a permeability study using fluorescent markers. To this end, three different fluorescently-labeled dextran samples of molecular weights 70 kDa, 500 kDa and 2000 kDa were used. These polymers are known for presenting a globular structure in water with hydrodynamic diameters of 12 nm, 29 nm and 56 nm, respectively.[139] The diffusion of these polymers into PEG microgels would make the particles fluorescent and demonstrate the presence of interconnected pores of a size larger than that of the marker.[140] The fluorescence of the microgels was detected by confocal laser scanning microscopy (CLSM). Permeability was here represented as the ratio of fluorescence intensity between the microgels and the surrounding solution measured from the CLSM images with the program ImageJ.
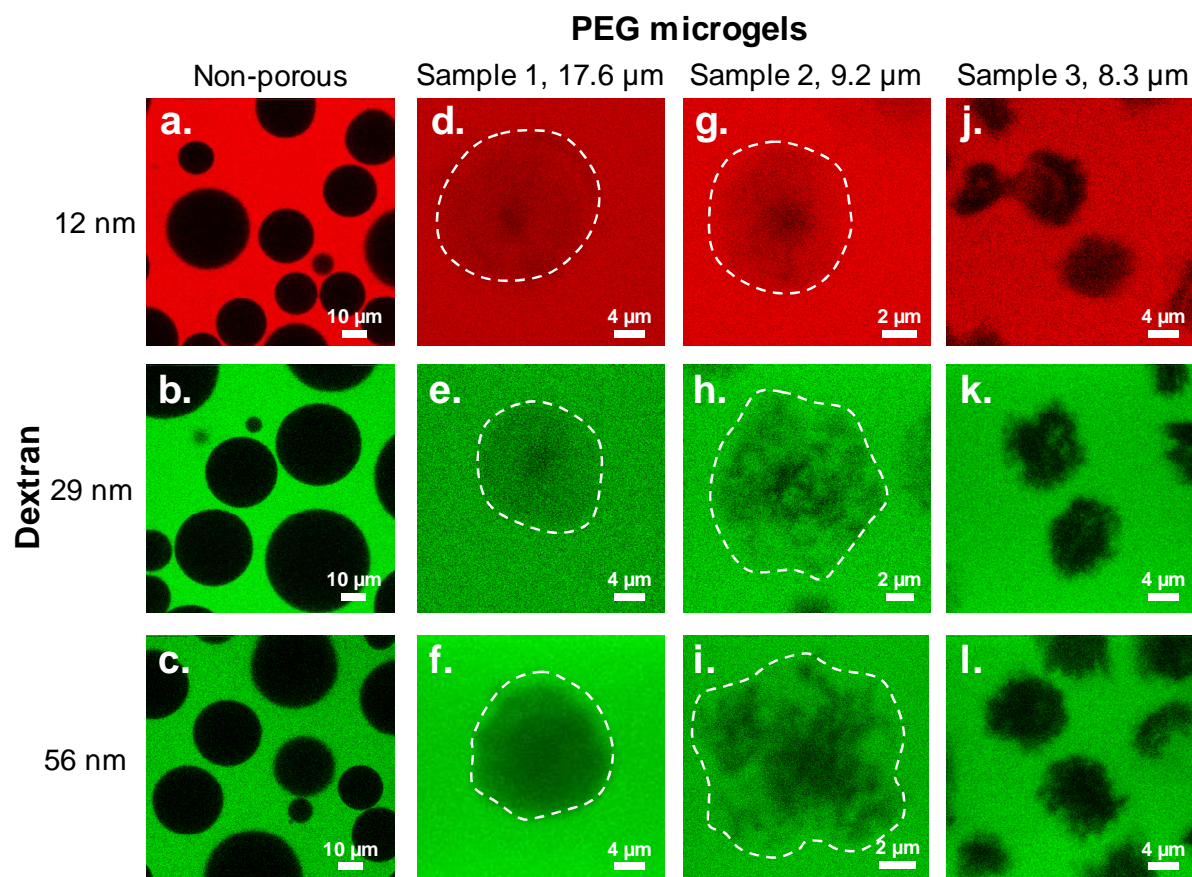
Figure 3.4. *CLSM images of non-porous PEG microgels (a., b. and c.), porous PEG microgels of 17.6 µm (sample 1, d., e. and f.), porous PEG microgels of 9.2 µm (sample 2, g., h. and i.) and porous PEG microgels of 8.3 µm (sample 3, j., k. and l.) 2 hours after addition of fluorescently labeled dextran of 12 nm, 29 nm and 56 nm, respectively.*

Overall, microgels 1 and 2 exhibited a much higher permeability to dextran than microgel 3 (Figure 3.4). As a control, non-porous PEG microgels showed no permeability at all. These results indicate that microgels 1 and 2 present interconnected pores of a few tens of nanometers while microgels 3 either present pores smaller than 12 nm or no interconnected pores or even no pores at all. This reduced porosity of microgel 3 could be explained by the structure of template 3, which exhibits the lowest density (Figure 3.1.g). By inverse replication, PEG microgels 3 must be very dense and present fewer pores. Therefore, PEG microgels 3 were not further investigated.
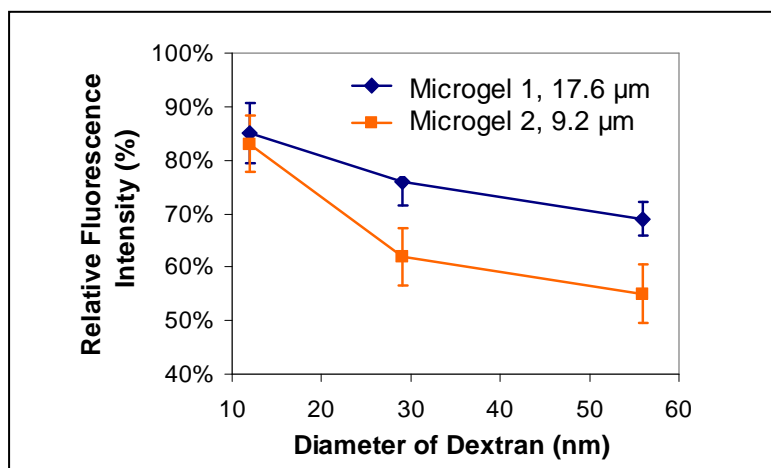
Figure 3.5. *Permeability (diffusion of dextran) of porous PEG microgels as a function of hydrodynamic diameter of dextran and type of PEG microgels (sample 1 of 17.6 µm and sample 2 of 9.2 µm). PEG microgels present internal, interconnected pores of a few tens of nanometers.*

For both microgels 1 and 2 permeability was almost maximal for the smallest dextran of 12 nm and gradually decreased with increasing size of dextran (Figure 3.4 and Figure 3.5). These results proved that microgels 1 and 2 present interconnected pores within a range of 20 to 60 nm at least, which corresponds to the size of the crystallites in $CaCO_3$ templates 1 and 2 (Figure 3.1.c and f). In addition, differences of permeability were observed between microgels 1 and 2, mainly apparent for the diffusion of the largest dextran of 56 nm. For the microgels 1, the diffusion of the 56 nm dextran was homogeneous (Figure 3.4.f). This indicated a relatively homogeneous distribution of highly interconnected pores, which could be attributed to the uniform distribution of crystallites within $CaCO_3$ template 1 (Figure 3.1.a-c). In contrast, the microgels 2 showed relatively inhomogeneous distributions of the fluorescent marker, as the 56 nm dextran could completely enter large parts of the microgels (Figure 3.4.i). This indicated the presence of larger pores on the surface of the microgels and confirmed the observations made by cryo-SEM on microgel 2. From the CLSM images these pores appeared to be as large as several hundreds of nanometers. The exact size of these pores could not be measured from cryo-SEM images since partial collapse occurred during sample preparation. To determine this size more precisely, fluorescent polystyrene beads of 450 nm and 1000 nm were used as diffusion markers. It could be shown that both types of beads were able to diffuse into the microgels 2, revealing the presence of external pores as large as 1 to 3 µm (Figure 3.6). This porosity was in good agreement with the original structure of template 2, presenting large crystallite aggregates of the same size, on their surface (Figure 3.1.d-f).
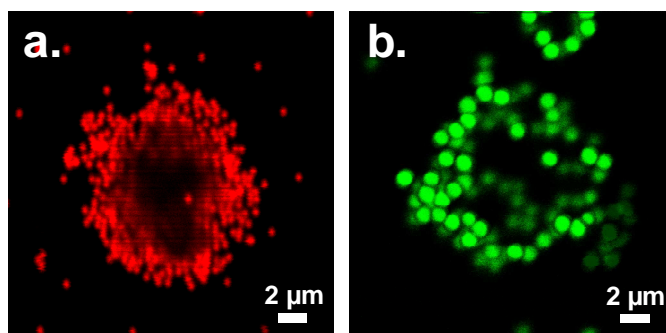
Figure 3.6. *CLSM images of porous PEG microgels of 9.2 µm (microgels 2) after immediate addition of fluorescent polystyrene beads of a. 450 nm; and b. 1 µm. PEG microgels present external pores of up to 1-3 µm at least.*

In conclusion, porous PEG microgels could be successfully synthesized by hard templating with porous $CaCO_3$ microparticles. Combined with an efficient three-step loading procedure, this method allowed for true inverse replication of $CaCO_3$ microparticles into PEG microgels and control over the final porosity. Employing structurally different templates, three types of PEG microgels with varying diameters and porosities were obtained. PEG microgels resulting from template 2 exhibit an average diameter of 9.2 µm and the expected porosity, with internal interconnected pores of 20 to 60 nm and external pores reaching up to 3 µm. Furthermore, permeability studies demonstrated that, due to their dual porosity, these microgels allowed for the passive loading not only of polymers and NPs but also of microparticles. They therefore represent an ideal material for the loading and release of drugs or magnetic NPs and targeting of bacteria. For these reasons PEG microgel sample 2 was selected for further work towards the foreseen applications.

4. Functionalization of Porous PEG Microgels

The aim of this work is to prepare porous PEG microgels and use them for the magnetic removal of bacteria as well as for a potential drug delivery. In the previous chapter, PEG microgels of 9.2 µm featuring internal, interconnected pores of 20 to 60 nm and external pores reaching up to 3 µm have been synthesized. It is expected that their small pores should allow for a more efficient loading by diffusion of drugs or magnetic nanoparticles (NPs) whereas the larger pores should allow for the binding of a high number of bacteria. The next step towards the development of these microgels requires the introduction of functional groups. Such groups are needed for a stable loading and controlled release as well as targeting applications. The functionalization of the porous PEG microgels will therefore be presented in the following chapter. Cationic amines will be introduced for the loading and release of drugs or magnetic NPs via electrostatic interactions and carbohydrate ligands will be incorporated for targeting of bacteria via carbohydrate-protein interactions.

Different strategies are available to achieve the functionalization of PEG hydrogels. For example, PEG macromonomers can be co-polymerized with other heterofunctional monomers such as vinyl monomers or PEG macromonomers bearing an acrylamide moiety at one end and another functional group at the other end.[47] However, these heterofunctional co-monomers do not participate in the cross-linking process which leads to the hydrogel network. This strategy therefore involves additional reaction optimization to avoid changes in the resulting hydrogel properties such as cross-linking density and mechanical stability. In order to ensure formation of stable and rigid hydrogels, these co-monomers can only be introduced at low concentrations thus resulting in low degrees of functionalization. In addition, the use of vinyl co-monomers may drastically alter the biocompatibility of the hydrogel.

Recently, a more versatile method allowing for the functionalization of readily prepared PEG hydrogel has been developed.[125, 126] This method is based on radical surface chemistry using benzophenone to graft functional monomers on PEG networks. Originally introduced by D. Pussak on non-porous PEG particles, this strategy has been here adapted to the porous PEG microgels. The novelty of this work lies in the fact that higher degrees of functionalization could be reached, asymmetrical functionalization with specific functionalization of the particles surface has been obtained and different functional groups could be simultaneously incorporated in a one-pot synthesis.

The functionalization of the porous PEG microgels was performed in two steps. The first step consisted of grafting carboxyl groups via the benzophenone-based radical surface chemistry and will

be presented in section 4.1. In the second step, the resulting PEG-COOH microgels were used to introduce the desired functional groups via the formation of an amide bond. On the one hand, the addition of cationic amines for loading and release applications will be detailed in section 4.2. In particular, an asymmetrical functionalization showing a very high concentration of amines on the surface of the microgels will be achieved using poly(amines). On the other hand, the introduction of carbohydrate ligands for targeting applications will be described in section 4.3. The simultaneous incorporation of both functional groups will also be presented in this last section. PEG microgel functionalization will be characterized by three different methods: the presence and uniform distribution of functional groups will be verified by CLSM after fluorescent labeling, the resulting surface charge of the particles will be indicated by measurement of ζ-potential at pH 6.5 and the degree of functionalization will be determined by UV titration.

4.1. Introduction of Carboxylates

The functionalization of PEG microgels is based on radical surface chemistry using benzophenone to graft functional monomers on PEG networks. The principle of this method consists of a side chain polymerization initiated by benzophenone used as a type II photoinitiator (Scheme 4.1). By irradiation with UV light, benzophenone is first excited to the triplet state and then abstracts hydrogen from polymers, thereby generating a radical on the polymeric backbone. A grafting polymerization can then start from this radical, leading to the formation of polymeric side chains.[141, 142]

Benzophenone-based chemistry has recently been used for the grafting on PEG hydrogel surfaces,[125] and was introduced for the bulk functionalization of non-porous PEG hydrogel particles by Pussak *et al.*[126] In the latest procedure, an ethanolic dispersion of PEG microgels was mixed with benzophenone and acrylic monomers, flushed with argon to prevent oxygen inhibition during radical polymerization and finally irradiated with UV-visible light. The monomers acrylic acid (AA) and 2-aminoethyl methacrylate (AEMA) were employed to graft carboxyl and amine groups, respectively (Scheme 4.1). After reaction optimization in order to reach the highest possible degree of functionalization, Pussak *et al.* obtained non-porous PEG-COOH microgels with a maximum concentration of 120 µmol of functional groups per gram of microgels.[126]
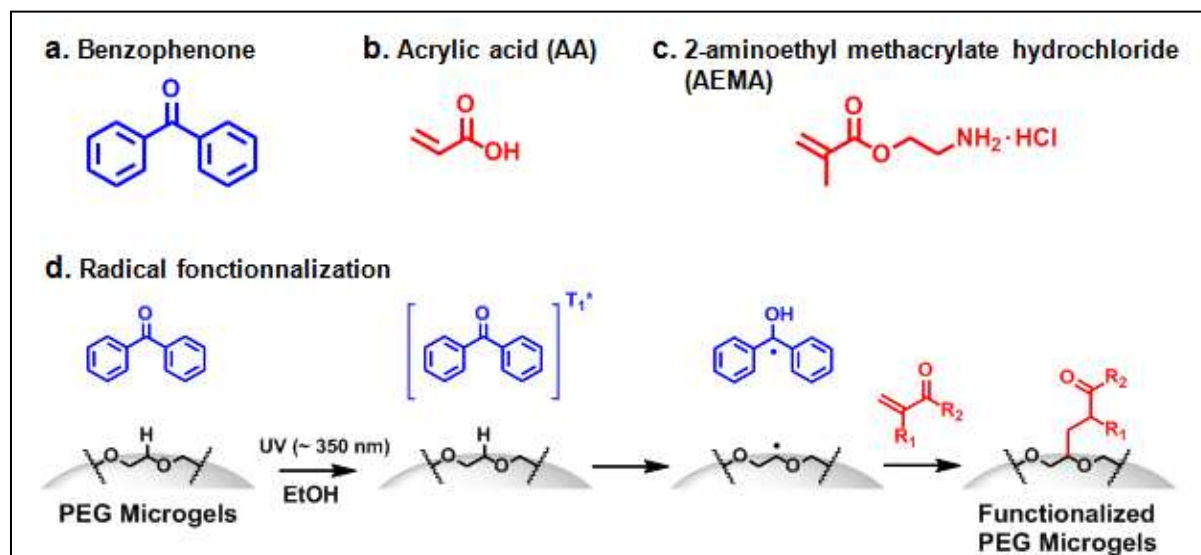
Scheme 4.1. *a., b., and c. Structural formulas of the photoinitiator benzophenone and grafting agents AA and AEMA used for the first step of PEG microgel functionalization; d. Mechanism of radical surface functionalization using benzophenone and acrylic monomers.*

The porous PEG microgels were functionalized following a similar procedure.[143] Functionalization with both acrylic monomers was tested: the use of AA led to high degrees of functionalization whereas only very low yields were achieved with AEMA. This was probably due to the low solubility of AEMA in organic solvents such as ethanol, even in the deprotonated form. Therefore, the porous PEG microgels were first functionalized with AA into PEG-COOH microgels and the carboxyl groups were used for further incorporation of amine groups and carbohydrate ligands via amide bond formation.
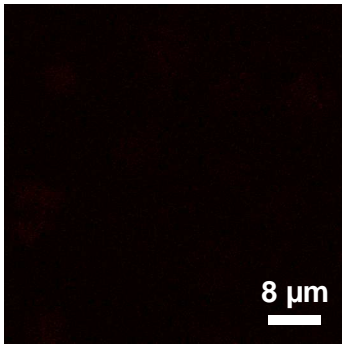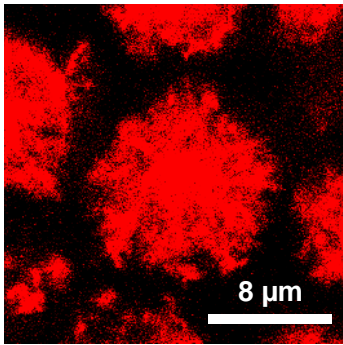
In order to obtain, in the second step, the highest possible concentration of amines and carbohydrate ligands for effective loading and targeting applications, reaction parameters of the first step were optimized to obtain the highest possible degree of carboxylate functionalization. The concentration of carboxyl groups could be tuned by the concentration of AA and of radicals, itself controlled by the concentration of benzophenone and irradiation time. While the concentration of benzophenone was kept constant, increased concentrations of AA or increased irradiation times led to aggregation of the microgels. This was most likely due to undesired bulk polymerization and termination between poly(acrylic acid) (PAA) chains of two distinct particles. The optimal conditions leading to the highest degree of functionalization without aggregation were found to be a concentration of 2.5 wt.% of benzophenone and 5 vol.% of AA, for a total irradiation time of 450 seconds. Aggregation was temporarily observed upon transfer of the particles from ethanol to water, most probably due to hydrogen bonds between neutral and deprotonated carboxyl groups. However, PEG-COOH microgels could easily be redispersed in water under basic conditions (10^{-2} M NaOH), which promoted electrostatic repulsion between the anionic carboxylate groups.

The presence of anionic carboxyl groups could be evidenced by a negative ζ-potential of -50.8 ± 5.9 mV at pH 6.5 (Table 4.1). By comparison, the unfunctionalized porous PEG microgels exhibited a higher ζ-potential of -26.2 ± 5.1 mV. The distribution of carboxylates was visualized by labeling with the cationic fluorescent dye Rhodamine 6G.[144, 145] CLSM revealed homogeneous fluorescence of the labeled PEG-COOH microgels, indicating a uniform functionalization at the resolution given by CLSM (Table 4.1). As control no fluorescence was observed with unfunctionalized PEG microgels.

The concentration of carboxyl groups was determined via colorimetric titration using the cationic dye toluidine blue O (TBO).[146] The concentration was found to be 1200 ± 200 µmol per gram of particles and corresponds to one carboxyl group for 20 ethylene oxide repeating unit (Table 4.1). Remarkably, porous PEG-COOH microgels showed a degree of functionalization ten times higher than non-porous PEG-COOH particles.[126] This could be attributed to the larger specific surface area of the porous particles. Such a high functionalization resulted either in a high

concentration of small PAA chains or in longer PAA chains grafted at a lower concentration. In order to prove that the formed PAA chains did not block the pores of PEG microgels, the permeability study with fluorescently labeled dextran was performed again, now on the functionalized particles. Since the diffusion profiles were very similar to the non-functionalized microgels, it could be assumed that the porosity of PEG microgels was retained. The benzophenone-based functionalization of porous PEG microgels therefore led, without aggregation and pore blocking, to PEG-COOH particles presenting a high degree of functionalization.

Table 4.1. Characterization of the porous PEG-COOH microgels and comparison to unfunctionalized PEG microgels (control) based on fluorescent labeling with the cationic dye Rhodamine 6G (CLSM images), ζ-potential at pH 6.5 and concentration of carboxylates measured by titration with the cationic dye TBO.

	PEG (control)	PEG-COOH
Labeling with Rhodamine 6G		
ζ-Potential (mV)	- 26.2 ± 5.1	- 50.8 ± 5.9
Concentration (μmol/g) (TBO titration)	20 ± 4	1200 ± 200

4.2. Introduction of Amines and Poly(amines)

In the second step, cationic amines were introduced for the loading and release of drugs and magnetic NPs via electrostatic interactions as well as for the potential unspecific targeting of bacteria.[143] The previously functionalized PEG-COOH microgels were thereby used for further functionalization via amide bond formation (Scheme 4.2). Oligo(amines) were employed, using at least one amine group for amide bond formation. Amine functionalization was thereby provided by the remaining free amines which did not react. Oligo(amines) of different sizes were investigated with the aim of increasing the concentration of amines for effective loading and targeting applications. Functionalization with the small molecule ethylenediamine (EDA) will be presented first and then compared to the functionalization with larger oligo(amines).
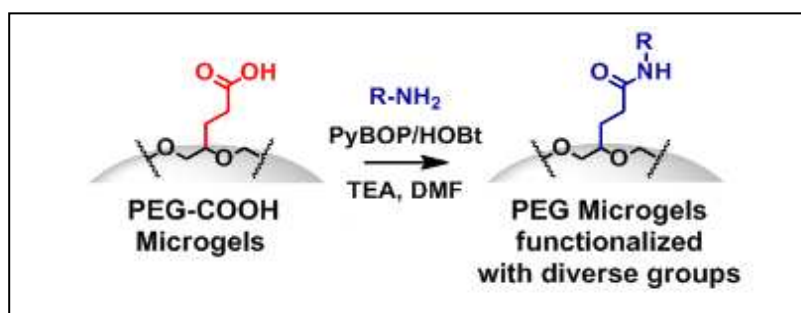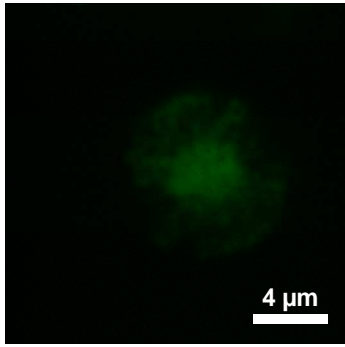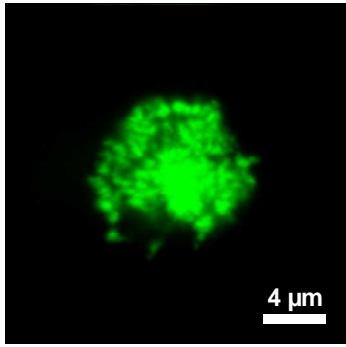
Scheme 4.2. *Principle of the functionalization of PEG-COOH microgels via formation of an amide bond, leading to the introduction of amines and carbohydrate ligands.*

EDA was coupled to the carboxyl groups of PEG-COOH microgels applying standard peptide coupling chemistry with PyBOP (benzotriazole-1-yl-oxy-tris-pyrrolidinophosphonium hexafluorophosphate) and HOBt (1-hydroxybenzotriazole) in DMF (N,N-Dimethylformamide, Scheme 4.2). Complete conversion was difficult to obtain since the carboxyl functionalities within the PEG network seem to be less accessible for further modifications than the functionalities on the surface of the particle and the pores. Therefore, high excesses of the coupling reagents were used to ensure high conversion. Similarly to PEG-COOH microgels, temporary aggregation occurred after transfer to water but redispersion could be achieved now under acidic conditions (10^{-2} M HCl).

The obtained microgels showed a positive ζ-potential of $+13.3 \pm 5.8$ mV at pH 6.5 (Table 4.2). This was an increase of 39.5 mV compared to unfunctionalized PEG microgels and indicated the presence of cationic groups. The distribution of amine groups was visualized by labeling with fluorescein isothiocyanate (FITC). CLSM revealed a uniform functionalization throughout the PEG-NH$_2$ microgels whereas no fluorescence was observed with the controls, unfunctionalized PEG and PEG-COOH microgels (Table 4.2). The quantification of amine groups by titration was however difficult. No accurate measurements could be done since the concentration of porous PEG microgels decreased after the two functionalization steps, resulting in too low concentration of amines and mass of particles per sample. The degree of functionalization was therefore extrapolated from that measured on non-porous PEG-NH$_2$ microgels functionalized under similar conditions and available in higher quantities.[126] In this case, the amount of amines was determined by titration with the dye 2,4,6-trinitrobenzenesulfonic acid (TNBS) and compared to that of carboxyl groups measured by TBO titration on non-porous PEG-COOH microgels. A conversion of 87% of carboxyl groups into amines was found for non-porous PEG microgels. Since similar conditions were used for the porous PEG microgels, it could be assumed that a concentration of about 1100 ± 200 µmol of amines per gram of particles was obtained.

Table 4.2. *Characterization of the porous PEG-NH$_2$ microgels obtained from functionalization with EDA and comparison to unfunctionalized PEG microgels (control) based on fluorescent labeling with FITC (CLSM images) and ζ-potential at pH 6.5.*

	PEG (control)	PEG-NH$_2$ from EDA
Labeling with FITC	4 µm	4 µm
ζ-Potential (mV)	- 26.2 ± 5.1	+ 13.3 ± 5.8

In order to increase the concentration of amine groups for effective loading and targeting applications, oligo- and poly(amines) were anchored on the porous PEG microgels and compared to EDA.[147] Four poly(amines) of different sizes and structures have been investigated in order to achieve the highest possible degree of functionalization. These poly(amines) are listed in Table 4.3 and consist of a small oligo(amidoamine) (OAMAM) composed of four lysine residues and synthesized following a protocol reported by Hartmann *et al.*,[148] poly(amidoamine) (PAMAM) dendrimer generation 4.0,[149] poly(allylamine) (PAH, M_w = 56 000) and poly(L-lysine) (PLL, M_w = 150 000-300 000). The average number of primary amine groups increases gradually from OAMAM bearing 8 amines to PLL bearing more than 1200 amines. In addition, all poly(amines) present a linear structure except for PAMAM dendrimer, which shows a globular one.[149]
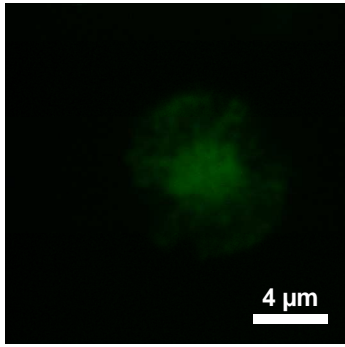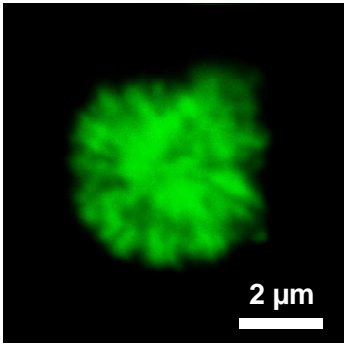
At first glance, poly(amines) with the highest molecular weight should be the most effective since it can be expected that many amines are still available after functionalization. However, functionalization with such long polymer chains may present two major problems: 1) several amines of the same chain can react with different PEG-COOH microgels, thereby leading to particle aggregation and 2) large polymer chains cannot diffuse into the intrinsic pores of PEG hydrogel so that only the surface of the hydrogel can be functionalized. Under the tested conditions, functionalization with high excess of PAH and PLL always led to particle aggregation. Therefore functionalization with the smaller poly(amines) OAMAM and PAMAM was preferred.

Table 4.3. *Name and intrinsic properties (formula, structure, number of primary amines) of all oligo(amines) investigated for the functionalization of PEG microgels.*

Name and structural formula	Number of NH$_2$
A. Ethylenediamine EDA Structure: linear	2
B. Oligo(amidoamine) OAMAM Structure: almost linear	8
C. Poly(amidoamine) dendrimer, generation 4.0, PAMAM Structure: globular	64
D. Poly(allylamine), PAH, M$_w$ = 56 000 Structure: linear	~ 600
E. Poly(L-lysine), PLL, M$_w$ = 150 000-300 000 Structure: linear	≥ 1200

Functionalization with the smallest oligo(amine) OAMAM led to non-aggregated microgels which were slightly positive, giving a ζ-potential of $+ 19.2 \pm 4.8$ mV at pH 6.5, comparable to that obtained with EDA. In comparison, functionalization with PAMAM dendrimer led to slightly aggregated microgels, which showed a higher ζ-potential of $+ 35.4 \pm 10.2$ mV (Table 4.4). This higher surface functionalization could be attributed to the fact that PAMAM features eight times more amines than OAMAM.
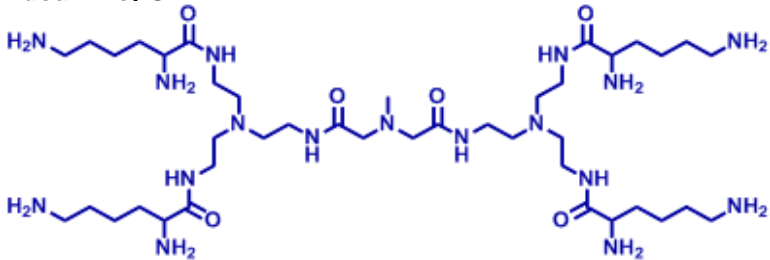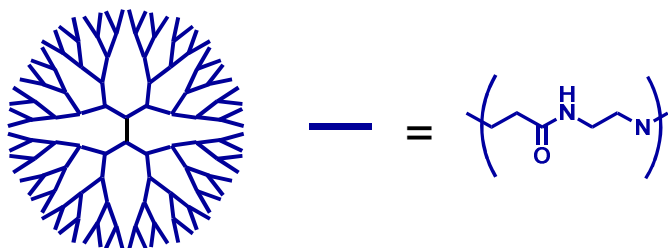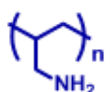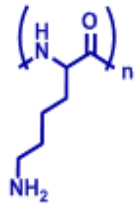
Table 4.4. *Characterization of the porous PEG-NH$_2$ microgels obtained from functionalization with PAMAM dendrimer and comparison to unfunctionalized PEG microgels (control) based on fluorescent labeling with FITC (CLSM images) and ζ-potential at pH 6.5.*

	PEG (control)	PEG-NH$_2$ from PAMAM
Labeling with FITC	4 µm	2 µm
ζ-Potential (mV)	- 26.2 ± 5.1	+ 35.4 ± 10.2

The uniformity of amine functionalization with PAMAM dendrimer was further investigated to determine if the dendrimer functionalized the core of PEG hydrogel. CLSM after labeling with FITC revealed a uniform functionalization throughout PEG microgels (Table 4.4), but the resolution of this method could not guarantee that the core of PEG hydrogel was functionalized. The amines were therefore titrated with TNBS. If the surface of the microgels was only functionalized, it could be expected that the concentration of amines would be much lower with PAMAM than with EDA. Contrary to EDA, titration on PEG-NH$_2$ from PAMAM was possible since functionalization with poly(amines) increased the concentration of functional groups and mass of PEG microgels, thereby allowing for accurate measurements. The concentration of amines was measured to be 150 ± 20 µmol/g particles. This value was lower than the functionalization degree obtained with EDA and could be explained by the fact that PAMAM did not functionalize the core of PEG hydrogels. Tomalia *et al.* reported that PAMAM dendrimer generation 4.0 presents a diameter of ~ 4 nm,[149] while the mesh size of the prepared PEG hydrogel has been estimated to be 8 nm.[150] In this case, the functionalization of the external layer of PEG hydrogel may prevent further diffusion of PAMAM dendrimer toward the core of the hydrogel. Therefore, as compared to EDA and OAMAM, PAMAM dendrimer led to a higher surface functionalization but most probably to a lower internal functionalization.
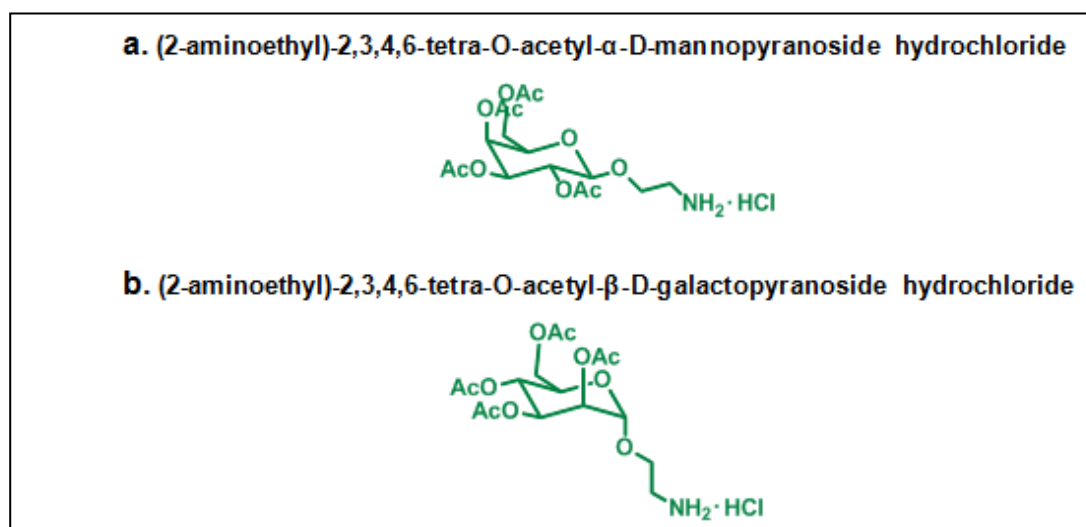
Overall, functionalization of porous PEG microgels into PEG-NH$_2$ was possible with EDA, OAMAM and PAMAM. EDA led to uniform functionalization with a very high total concentration of amine groups but relatively low surface functionalization. In comparison, PAMAM led to asymmetrical functionalization, with a very high surface functionalization but most probably non-

existent internal functionalization. Use of OAMAM resulted in microgels with intermediate properties. For loading applications, a high surface functionalization is more important than a high total concentration of amine groups, since large drugs or NPs may not be able to diffuse into PEG hydrogels and may be mostly loaded on the surface. The loading of magnetic NPs however does not need to be maximal to impart magnetic properties to the microgels. Therefore all types of porous PEG-NH$_2$ microgels are well adapted for this application. Nevertheless, it is highly beneficial to maximize the loading of drugs. In this case, porous PEG-NH$_2$ microgels from PAMAM dendrimer seem to be more advantageous.

4.3. Introduction of Carbohydrate Ligands

For the specific targeting of bacteria, carbohydrate ligands have been incorporated into the porous PEG microgels.[143] It has been proven that bacteria carry carbohydrate-binding proteins on their pili and certain strains of *E. coli* in particular are able to specifically bind to the monosaccharide mannose (Man) but not to other carbohydrates such as galactose (Gal).[79-81, 96-98] Compared to antibodies also used for bacteria targeting, carbohydrate ligands are advantageous since they are more stable and present a broader interaction specificity. Man was therefore introduced on the porous PEG microgels and the ability of the resulting particles to bind to Man-binding receptors was investigated. In order to prove the specificity of this binding, Gal was also incorporated on the porous PEG microgels and the resulting particles were used as negative control in the binding study.

Similar to the functionalization with poly(amines) described in the previous section, PEG-COOH microgels were used for carbohydrate functionalization via amide bond formation. Acetate-protected Man and Gal ligands presenting a short amine-linker at the anomeric position were employed (Scheme 4.3). This amine linker was used for amide bond formation and should be flexible enough to allow for the free presentation of the carbohydrate ligands on PEG microgels. The monosaccharides had to be protected to avoid side reactions between their hydroxyl functional groups and the carboxyl groups on PEG. These ligands have been synthesized by S. Mosca, partially following a protocol from Ponader *et al*.[151] Functionalization was achieved using standard peptide coupling chemistry based on PyBOP, HOBt and high excesses of the ligands (Scheme 4.2). After coupling, the carbohydrates were deprotected with sodium methoxide (MeONa) and the final PEG-Man and PEG-Gal microgels could be readily redispersed in water.

a. (2-aminoethyl)-2,3,4,6-tetra-O-acetyl-α-D-mannopyranoside hydrochloride

b. (2-aminoethyl)-2,3,4,6-tetra-O-acetyl-β-D-galactopyranoside hydrochloride
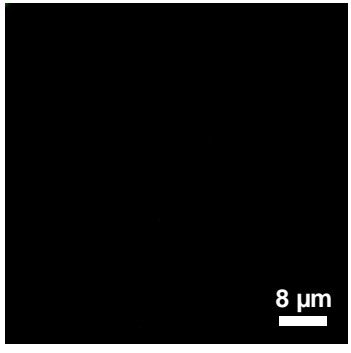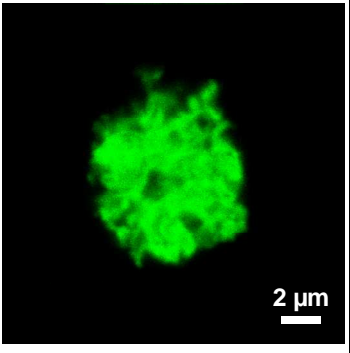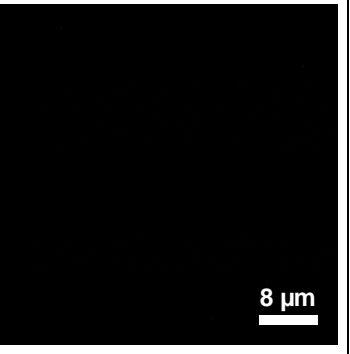
Scheme 4.3. *Structural formulas of the protected Man and Gal ligands with a short amine-linker used for the functionalization of PEG microgels.*

The resulting microgels showed a ζ-potential of - 19.4 ± 4.7 mV for PEG-Man particles and - 25.1 ± 5.8 mV for PEG-Gal particles at pH 6.5 (Table 4.5). This was an increase from the value measured for PEG-COOH back to the initial value for unfunctionalized PEG microgels (- 26.2 ± 5.1 mV). This charge compensation proved the successful incorporation of the neutral carbohydrate ligands and indicated almost complete conversion of carboxyl groups. Usually, direct quantification of carbohydrates can be performed for example with the phenol/sulfuric acid method.[152] However, similarly to the functionalization with the small EDA molecules, direct titration of carbohydrates on the porous PEG microgels turned to be difficult because the mass concentration of sample was relatively low after the two functionalization steps. A concentration of 1100 ± 200 μmol of carbohydrates per gram of microgels could however be estimated assuming a conversion of 87%. This conversion was extrapolated from the yield of amide formation between PEG-COOH microgels and EDA performed under similar conditions. Such an extrapolation was allowed because the reactivity of the amino-terminated carbohydrate ligands and EDA were most probably similar, since these reagents all react with an ethyleneamine moiety ($R-CH_2-CH_2-NH_2$).

The distribution of carbohydrate ligands as well as their ability to specifically bind protein receptors was visualized by incubation with fluorescently labeled Concanavalin A (FITC-ConA), a Man-binding protein (lectin). After incubation in a lectin-binding buffer, CLSM revealed uniform fluorescence of PEG-Man microgels proving homogenous functionalization and binding of FITC-ConA (Table 4.5). The binding of proteins to carbohydrates is usually very weak but can be considerably strengthened by multiple presentations of carbohydrate ligands to promote several binding events simultaneously (so-called multivalency effect).[153-155] Therefore, the observed binding was most probably favored by a high concentration of Man ligands and/or the multivalent presentation

of these ligands in the form of polymeric chains, resulting from the functionalization of the PAA chains.

Table 4.5. *Characterization of the porous PEG-Man as well as PEG-Gal microgels and comparison to unfunctionalized PEG microgels (control) based on fluorescent labeling with FITC-ConA (CLSM images) and ζ-potential at pH 6.5.*

	PEG (control)	PEG-Man	PEG-Gal
Labeling with FITC-ConA	8 µm	2 µm	8 µm
ζ-Potential (mV)	- 26.2 ± 5.1	- 19.4 ± 4.7	- 25.1 ± 5.8

In order to prove that the binding of FITC-ConA to PEG-Man microgels was specific, the unfunctionalized PEG, PEG-COOH and PEG-Gal microgels were used as controls for the incubation experiments. As expected, none of these particles became fluorescent and no binding of ConA was observed (Table 4.5). To further confirm the specificity of binding, an inhibition experiment with methyl α-D-mannopyranoside (Me-Man) was performed. Me-Man is a competitor to the Man moieties on PEG microgels, which also binds to FITC-ConA and thus should lead to a release of the fluorescent protein from the PEG-Man microgels. PEG-Man particles indeed lost their fluorescence after incubation with Me-Man (Figure 4.1), proving that the binding of FITC-ConA was specific. In addition, a minimal concentration of Me-Man ten times higher than that of Man ligand on PEG microgels had to be added to observe detachment of FITC-ConA. This was an additional indication that binding occurred via a multivalent presentation of the Man ligands. Functionalization therefore led to high concentrations of Man ligands which promoted a strong binding of ConA. This demonstrated that PEG-Man microgels should be very well adapted for specific and efficient targeting of bacteria.
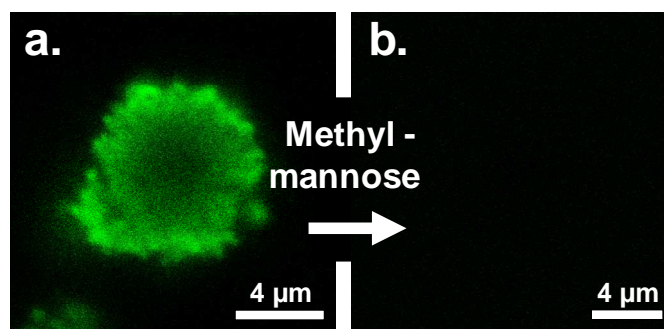
Figure 4.1. *CLSM image of the porous PEG-Man microgels after first labeling with FITC-ConA (a.) and then addition of a 2 M solution of Me-Man (b.).*

In order to be able to load antibiotics and magnetic NPs, target bacteria and release antibiotics with the same microgels, it is also of interest to combine functionalization with carbohydrate ligands and cationic amines. Porous PEG-COOH microgels were therefore functionalized with both groups by adding stoichiometric amounts of EDA and the Man ligand in a one-step procedure.[143] On the one hand, the presence of uniformly dispersed NH_2 groups throughout PEG microgels was demonstrated by CLSM after FITC labeling (Table 4.6). On the other hand, the homogeneous presence of Man ligands was evidenced after incubation with FITC-ConA (Table 4.6). The ζ-potential of PEG-Man/NH_2 microgels reached $+ 16.1 \pm 5.8$ mV at pH 6.5 due to the presence of the cationic amines, which was consistent with the value obtained for the pure PEG-NH_2 microgels functionalized with EDA (Table 4.6). In conclusion, both amine and carbohydrate groups could be incorporated on the porous PEG microgels. Moreover, their concentrations were still high enough to guarantee a positive charge at the surface of the particles as well as their ability to bind to proteins. These microgels therefore show great potential for loading, release and targeting applications.

Table 4.6. *Characterization of the porous PEG-Man/NH_2 microgels based on fluorescent labeling with ConA and FITC (CLSM images) and ζ-potential at pH 6.5.*

	PEG-Man/NH_2	
Labeling with ConA (Man) and FITC (NH_2)		
ζ-Potential (mV)	$+ 16.1 \pm 5.8$	

In conclusion, the two-step functionalization procedure relying on benzophenone-based radical surface chemistry allowed for the incorporation of both cationic amines and carbohydrate ligands on the porous PEG microgels (Scheme 4.4). Combination of amines and carbohydrates was also possible in a one-pot procedure. Compared to the degree of functionalization already obtained with this procedure, a ten-fold higher concentration of functional groups could be reached due to the porosity of PEG microgels. Even higher degrees of surface functionalization and asymmetrical functionalization could be obtained using large molecules such PAMAM dendrimer.
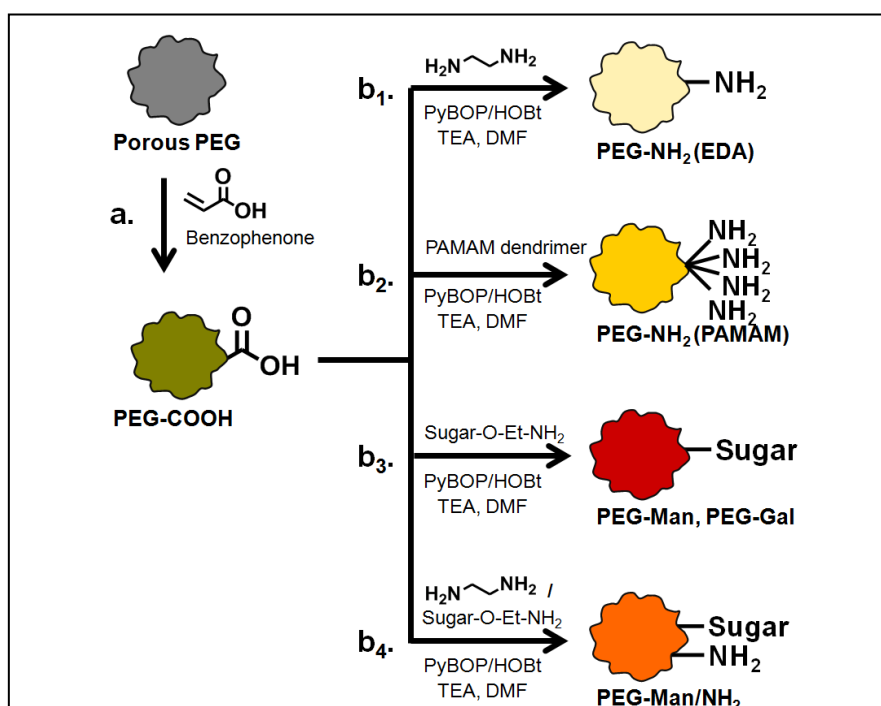
Scheme 4.4. *List of all the functionalized PEG microgels prepared in this work and associated synthetic procedures.*

The amine-functionalized porous PEG microgels showed a positive surface charge and should allow for the loading of magnetic NPs as well as drugs via electrostatic interactions. Moreover, the Man-functionalized microgels were able to bind to proteins, which indicates that they should be able to specifically target bacteria via their carbohydrate ligands. Unspecific targeting may also be possible via their cationic functionalization. Thus, the functional porous PEG microgels can now be employed for the magnetic removal of bacteria as well as for a potential drug delivery.

5. Functional Porous PEG Microgels for the Magnetic Removal of Bacteria

In the previous chapters, porous PEG microgels of 9.2 µm featuring internal interconnected pores of several tens of nanometers and larger external pores of a few microns have been synthesized. Moreover, these microgels could be functionalized with amine groups and carbohydrate ligands. In order to test their potential for biotechnological applications, they will be evaluated as a novel microgel platform for the selective targeting and efficient magnetic removal of bacteria.

Bacteria can be classified into two different types: harmless or even beneficial on one side and pathogenic on the other side. For both types, the removal of bacteria is of high importance for various biotechnological applications. For example, bacteria are employed in fermentation processes in the food industry or for the production of enzymes and recombinant drug proteins in the pharmaceutical industry.[82-84] In these cases, it is profitable to selectively remove bacteria from the final product or microbial culture and release them for further applications. In a biomedical setting, it is often crucial to detect and remove pathogenic bacteria from contaminated solutions or physiological fluids for analysis or treatment.

One of the most common strategies employed for the specific detection and removal of bacteria relies on magnetic separation.[51-53] This technique is based on the use of magnetic beads which are functionalized with ligands, such as antibodies, able to specifically bind to the target. These beads selectively bind bacteria via their ligand functionalization and can remove them from solution by simply using a magnet (Scheme 5.1). Compared to filters also used for the removal of bacteria,[92-95] magnetic beads show a wider range of applicability and allow for an easy, rapid and, above all, specific removal.[51-53]

The most widely used magnetic beads employed for the detection and removal of bacteria are magnetic polystyrene beads of 2 to 5 µm commercialized under the trade name DYNABEADS.[54, 103, 117, 121-124] However, these particles are not biocompatible but prone to unspecific interactions and therefore present limited applicability.[54] In addition, high concentrations of magnetic beads are usually required for high yields of removal since there are only few bacteria bound per particle. The restricted loading capacity is therefore another factor limiting the performance of current magnetic beads.

The functional porous PEG microgels synthesized in this work will now be evaluated as an alternative to the current polystyrene beads. On the one hand, PEG is known to be a hydrophilic, biocompatible polymer which prevents non-specific interactions and thus should allow for a wide range of biotechnological and biomedical applications.[40] On the other hand, the external pores which are comparable in size to bacteria will increase the specific surface area available for binding, thereby increasing the capacity for the loading of bacteria. Higher yields of bacteria binding and removal are therefore expected with the novel porous PEG microgels. To the best of our knowledge, this is the first time that magnetic beads combining biocompatibility and porosity have been used for the isolation of bacteria.

In order to achieve selective magnetic removal of bacteria, two important features need to be introduced to the porous PEG microgels: magnetic properties and specific bacteria targeting. Firstly, magnetic properties will be incorporated by loading with anionic, superparamagnetic nanoparticles (NPs) via electrostatic interactions with the cationic amines of PEG microgels. Secondly, specific targeting and binding of bacteria will be achieved by carbohydrate ligands grafted on PEG microgels. Bacteria are indeed known for presenting carbohydrate-binding proteins on their pili. In particular, a strain of bacteria *Escherichia coli* (*E. coli*) will be targeted via mannose ligands (Man). The resulting magnetic, porous, sugar-functionalized (MaPoS) PEG microgels will be finally used for the selective binding and magnetic removal of bacteria *E. coli* from solution (Scheme 5.1).

Addition of **MaPoS** particles to a solution of bacteria — Incubation: binding of bacteria — Magnetic collection of particles with bound bacteria — Magnetic removal of particles with bound bacteria
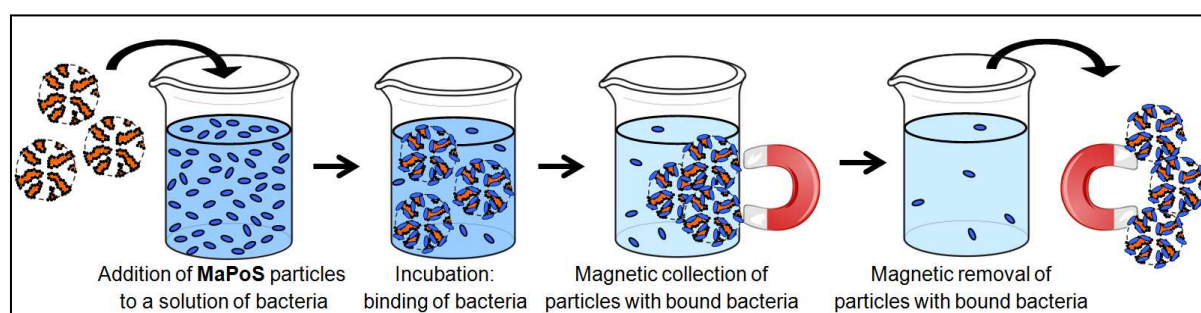
Scheme 5.1. *Principle of the magnetic removal of bacteria using MaPoS PEG microgels. During incubation, bacteria bind to the particles via carbohydrate-protein interactions. Then MaPoS microgels and the bacteria bound to them can be removed with the help of a magnet.*

The course of this study will be divided in three steps, as presented in Scheme 5.2. The two functionalities, magnetic properties and binding of bacteria, will be first evaluated separately. In the first step A shown in section 5.1, magnetism will be obtained with PEG-NH$_3^+$ microgels. In the second step B presented in section 5.2, the specificity and efficiency of the binding of bacteria to PEG-Man microgels will be investigated. Eventually, in the last step A+B, both features will be combined on MaPoS microgels prepared from PEG-Man/NH$_3^+$ particles. The efficiency of bacteria removal using MaPoS microgels will be investigated and compared to non-porous beads in section 5.3.
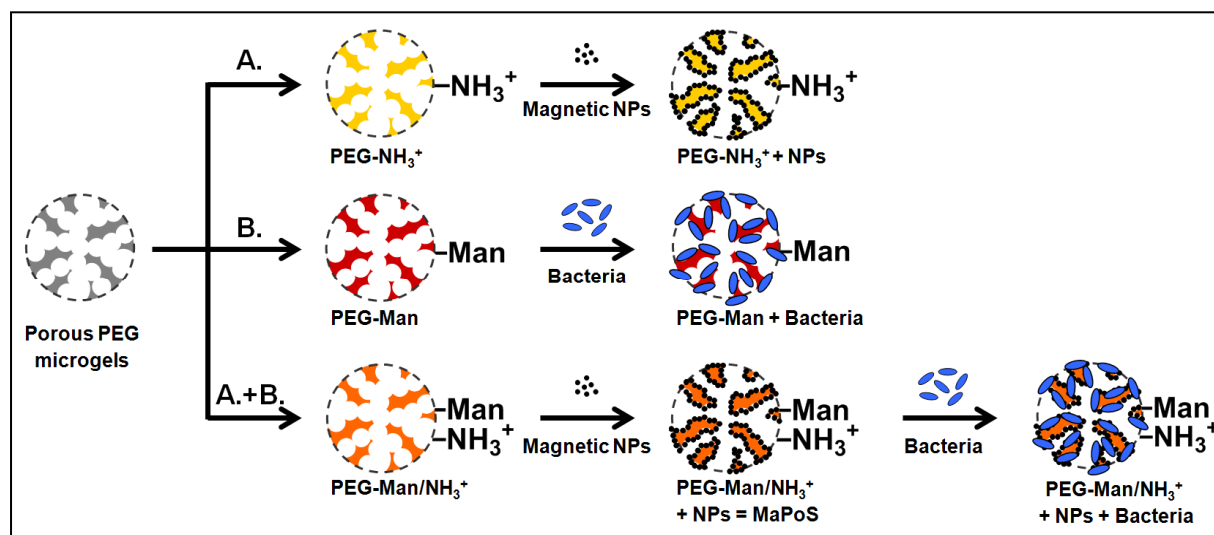
Scheme 5.2. *Schematic presentation of the course of this study leading to the magnetic removal of bacteria using MaPoS PEG microgels. The cationic amines incorporated on PEG microgels were used for the loading of anionic, superparamagnetic NPs via electrostatic interactions, while the Man ligands were used for the targeting of bacteria. The magnetism (A.) and binding of bacteria (B.) were first investigated separately on PEG-NH$_3^+$ and PEG-Man microgels, respectively, and both features were finally combined on PEG-Man/NH$_3^+$ microgels for the removal of bacteria (A.+B.).*

5.1. Introduction of Magnetism

At first, magnetic microgels were prepared by loading superparamagnetic iron oxide NPs.[143] One possible strategy is to incorporate the NPs during the synthesis of the porous PEG microgels. The solution containing PEG hydrogel precursors was therefore mixed with the NPs and loaded into the $CaCO_3$ template particles following the procedure described in chapter 3. However, the resulting PEG microgels had poor magnetic properties since only low concentrations of NPs could be loaded in order to preserve the structure and mechanical stability of PEG microgels.
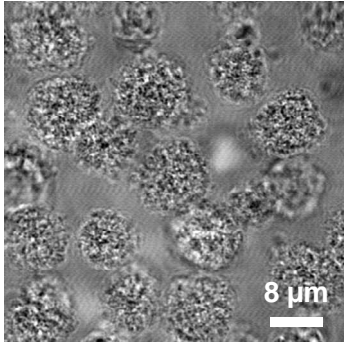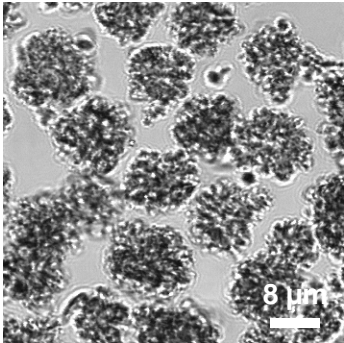
A more straightforward method consists of loading the NPs into the pores of PEG microgels. In order to achieve a high, strong and stable loading over time, the NPs were loaded via electrostatic interactions (Scheme 5.2.A). The NPs would first diffuse through the pores of PEG microgels and then coat their surface via electrostatic attraction. To this aim, cationic $PEG-NH_3^+$ microgels and superparamagnetic iron oxide NPs presenting an anionic coating were applied.

For this application $PEG-NH_2$ microgels resulting from functionalization with EDA were chosen (*cf.* chapter 4). As NPs, commercially available oleate-coated Fe_3O_4 (magnetite) NPs of 8 ± 3 nm were applied. However, loading with these NPs led to the aggregation of PEG microgels. This was most probably due to the hydrophobization of the microgels as a result of the presence of oleate groups. The more hydrophilic citrate-coated Fe_3O_4 NPs were therefore synthesized in the range of 8-15 nm by Dr. M. Chanana (see Appendix, Figure 8.4) and loaded into the cationic $PEG-NH_3^+$ microgels. In this case no aggregation was observed using a 2 mg.mL^{-1} aqueous solution of NPs (Table 5.1).

The incorporation of NPs was first demonstrated by optical microscopy since the resulting microgels exhibited a higher contrast to water compared to the unloaded microgels (Table 5.1). Confirmation of loading was provided by the ζ-potential which switched from $+ 13.3 \pm 5.8$ mV for pure $PEG-NH_3^+$ to $- 31.7 \pm 6.3$ mV for $PEG-NH_3^+$ + NPs microgels at pH 6.5 (Table 5.1). This charge reversal could be attributed to the presence of excess citrate groups. Eventually, the loaded PEG microgels were magnetic and could be completely isolated from solution by applying a magnet for 30 seconds (Figure 5.1).

Generally, the final amount of loaded NPs could be controlled by the concentration of NPs during the loading step. Using a 2 mg.mL^{-1} solution of NPs, the final concentration of loaded NPs was estimated to be 65 wt% from the UV-absorption of the solution before and after loading (for calibration curve, see Appendix, Figure 8.5). Concentrations as low as 0.2 mg.mL^{-1} of NPs could be applied, still resulting in magnetic microgels. Below this critical concentration, the microgels obtained after loading were no longer magnetic.

Table 5.1. *Characterization of porous PEG-NH$_3^+$ microgels loaded with citrate-coated iron oxide NPs and comparison to unloaded PEG-NH$_3^+$ microgels (control) based on contrast by optical microscopy and ζ-potential at pH 6.5.*

	PEG-NH$_3^+$ (control)	PEG-NH$_3^+$ + NPs
Optical microscopy	(similar to unfunctionalized PEG)	
ζ-Potential (mV)	+ 13.3 ± 5.8	- 31.7 ± 6.3

The loading of NPs proved to be stable in PBS buffer (pH 7.4) over at least 12 weeks. The microgels retained their magnetic properties and no leaking of NPs was observed with UV-visible spectroscopy. Such stability in a medium of high ionic strength was due to the electrostatic interactions but most probably also to the formation of coordination bonds between the amines of PEG microgels and iron of NPs.
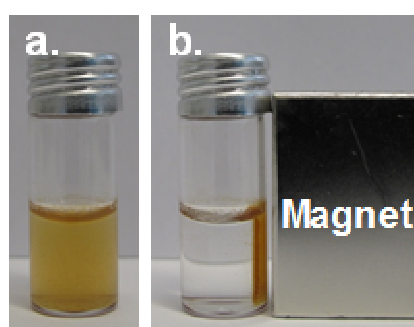
Figure 5.1. *Pictures of the magnetism of PEG-NH$_3^+$ microgels loaded with superparamagnetic iron oxide NPs (a. without magnet and b. with a magnet). The microgels were completely attracted by the magnet within 30 seconds.*

Additional characterizations with electron microscopy provided very interesting information. The presence of NPs on the surface of the microgels was evidenced by cryo-SEM, showing a rougher surface compared to unloaded PEG microgels (Figure 5.2.a-b). In addition, cross-sections of microgels observed by TEM revealed that the NPs were homogeneously loaded into the pores of the particles

(Figure 5.2.c-e). Remarkably, this data also allowed for direct observation of the core of the porous PEG microgels. Normally, the contrast of TEM imaging is too low to clearly visualize pure PEG microgels but was considerably enhanced with the physisorbed iron oxide NPs. These NPs were bound to PEG hydrogel but could not diffuse into the hydrogel network due to their size.[150] The NPs could therefore be used to visualize the interface between PEG hydrogel and the pores and reveal the internal morphology of PEG microgels. Thus, this method now directly confirmed that the porous PEG microgels were exact inverse replicas of their CaCO$_3$ microparticle templates (compare Figure 5.2.c-e to f-h).
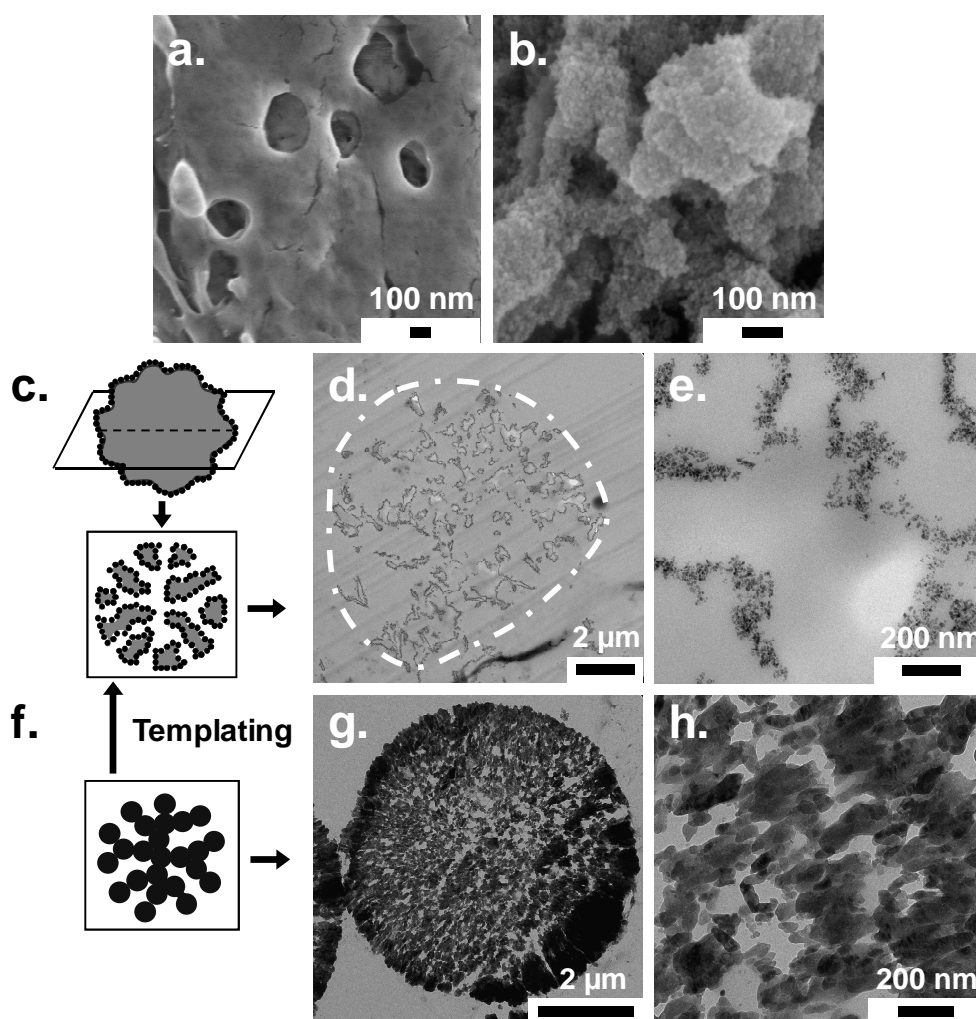
Figure 5.2. *Cryo-SEM images of a. unloaded porous PEG microgels and b. PEG-NH$_3^+$ microgels loaded with iron oxide NPs; Schematic representation and associated TEM images at different magnifications of a cross-section of PEG-NH$_3^+$ microgels loaded with iron oxide NPs (c.-e.) and of the CaCO$_3$ particles used as templates for the synthesis of the porous PEG microgels (f.-h.). PEG microgels were exact inverse replicas of their CaCO$_3$ microparticle templates.*

5.2. Binding of Bacteria

Targeting and binding of bacteria were achieved via carbohydrate-protein interactions, using the Man ligands introduced on the porous PEG microgels (Scheme 5.2.B).[143] Bacteria are indeed known for carrying carbohydrate-binding proteins, which are responsible for microbial adhesion to cells and infections.[79-81] Using carbohydrate ligands could in principle target bacteria, discriminate between strains presenting different receptors and selectively bind bacteria presenting large amount of carbohydrate receptors.[79, 109-117] So far, most systems used for the targeting of bacteria rely on either specific interactions based on antibodies,[53, 106-108] or on unspecific interactions based on cationic materials.[104, 105] Carbohydrate ligands are more specific compared to cationic materials. They are also advantageous compared to antibodies, as they are less prone to denaturation and generally present broader interaction specificity. The use of carbohydrate ligands should therefore allow for the detection of unanticipated or new bacteria strains.

For biotechnological and biomedical applications, targeting of the bacteria *Escherichia coli* (*E. coli*) is highly desirable. These bacteria are frequently used in biotechnological processes such as the production of recombinant drug proteins. A few pathogenic strains of these bacteria are also involved in severe infections. *E. coli* bacteria usually present carbohydrate-binding proteins on organelles, called pili, located on their surface.[96-98, 118] In this study, the strain ORN178 of *E. coli* was used as model bacteria.[156, 157] The bacteria of this strain are known for presenting proteins which specifically bind to Man, as well as a phenotypic stability of piliation which makes all bacteria ORN178 able to bind to Man moieties.[156, 157] Man ligands were therefore employed for specific targeting of the bacterial pili of *E. coli*.

All biological experiments have been performed in collaboration with Dr. N. Azzouz. In order to test the ability of PEG-Man microgels to bind bacteria *E. coli* ORN178, the particles were incubated in a suspension of bacteria in PBS buffer for one hour and then washed with buffer. The bacteria were stained with the fluorescent dye DAPI (4',6-diamidino-2-phenylindole dihydrochloride) to detect if bacteria bound to the microgels via CLSM. CLSM images showed strong fluorescence of PEG-Man microgels, indicating that a large number of bacteria attached to the particles (Figure 5.3.a). With light microscopy and SEM, single bacteria bound to PEG microgels were also visible (Figure 5.3.b-c). As discussed in chapter 4, the binding of carbohydrates to proteins is usually very weak but can be considerably strengthened by the multiple presentations of carbohydrate ligands, leading to the multivalency effect.[153-155] Similar to the binding of the protein ConA observed in chapter 4, binding of the bacteria probably resulted from a high concentration of Man ligands and/or the multivalent presentation of these ligands as polymeric chains.[109, 153]
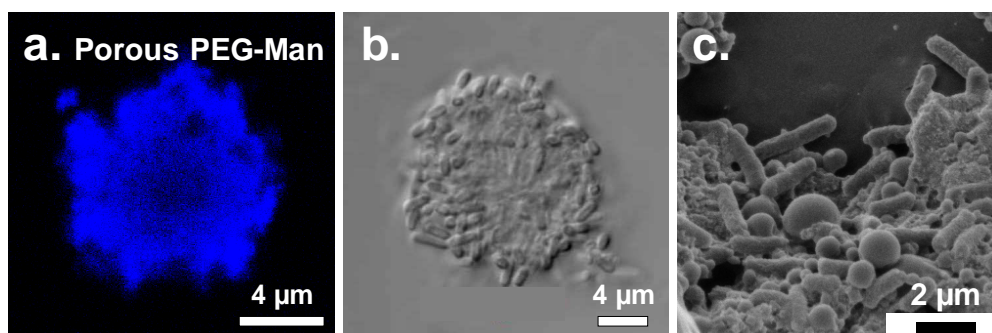
Figure 5.3. *a. CLSM and b. optical microscopy images of porous PEG-Man microgels after incubation with bacteria E. coli ORN178 in PBS buffer, staining with DAPI and washes with PBS; c. SEM image of porous PEG-Man microgels after incubation with bacteria E. coli ORN178 and washes. Upon drying PEG microgels collapsed but bacteria were still visible on the surface of the hydrogel.*

In order to prove that binding also occurs in more complex, protein-containing media, where a protein corona preventing bacteria binding may form on the particles,[158, 159] incubation experiments were performed in PBS and DMEM (Dulbecco's Modified Eagle Medium) solutions containing 1 wt% of BSA (bovine serum albumin protein). CLSM revealed that the bacteria were still able to attach to PEG microgels in the presence of BSA. This was most probably due to the nature of PEG hydrogel limiting unspecific adsorption of proteins.

As a negative control, no binding of bacteria was observed with unfunctionalized PEG and PEG-COOH microgels (Figure 5.4), proving that the binding was not due to unspecific interactions with the hydrogel scaffold. For the final removal of bacteria, PEG microgels will be functionalized with both cationic amines and carbohydrate ligands. In order to prove that no unspecific targeting will occur with the cationic functionalization, binding was also tested with PEG-NH$_3^+$ microgels. Again, no binding of bacteria could be observed (Figure 5.4).

Figure 5.4. *CLSM images of porous PEG microgels after incubation with bacteria E. coli ORN178 in PBS buffer, staining with DAPI and washes with PBS: a. porous unfunctionalized PEG; b. porous PEG-COOH; c. porous PEG-NH$_3^+$ microgels.*

To further prove that the binding of bacteria was due to specific ligand-receptor interactions, PEG-Gal particles were incubated with bacteria *E. coli* ORN178 under the same conditions. Gal cannot bind to the Man-binding receptors of *E. coli* ORN178 and indeed, no binding of bacteria to PEG-Gal microgels was observed (Figure 5.5.a). In another control experiment, instead of *E. coli* ORN178, a mutant *E. coli* strain ORN208, which does not bind to Man, was used.[156, 157] As expected, no binding to PEG-Man microgels was observed (Figure 5.5.b). A similar selectivity was maintained by incubating PEG-Man particles with a 50/50 mixture of bacteria ORN178 and ORN208, showing that only the bacteria ORN178 were able to attach to the particles (Figure 5.5.c-d). These experiments all confirmed that the binding of bacteria was due to the specific interactions between the Man ligands on PEG microgels and the carbohydrate-binding receptors on bacteria *E. coli* ORN178. Thus, the Man-functionalized PEG microgels could be used not only for the binding of bacteria but also for the discrimination between different strains.

Figure 5.5. *CLSM images of a. porous PEG-Gal microgels after incubation with bacteria E. coli ORN178 in PBS buffer, staining with DAPI and washes with PBS; b. porous PEG-Man microgels after incubation with bacteria E. coli ORN208 (mutant strain which does not bind Man); CLSM images of porous PEG-Man microgels after incubation in a 50/50 mixture of bacteria ORN178 labeled with the dye SYBR and ORN 208 labeled with acridine orange at emission wavelengths of c. 500 – 520 nm and d. 500 – 600 nm. Bacteria ORN 178 labeled with SYBR are not fluorescent in the emission range 500 – 520 nm but in the range 500 – 600 nm while bacteria ORN 208 labeled with acridine orange are always fluorescent on both ranges. Binding was only observed between PEG-Man and E. coli bacteria ORN178, proving its specificity.*

Since bacteria *E. coli* ORN178 are 2.1 ± 0.4 µm long and 0.8 ± 0.1 µm wide, they should be able to penetrate the external pores of 1 to 3 µm of the porous PEG microgels. In order to demonstrate the better binding capacities of the porous structure, the binding efficiency of the porous PEG microgels was compared with that of non-porous analogues. For this, the non-porous PEG microgels of 10 µm were functionalized with Man ligands. CLSM and optical microscopy were used to visualize the bacteria bound to the non-porous particles. These images showed that the non-porous microgels bound bacteria only on their surface (Figure 5.6.a-b). For the porous microgels however, bacteria did not only bind to the outer surface but also partially diffused into the larger pores of the particles (Figure 5.3.a-b). Thus, a higher binding efficiency was obtained for the porous microgels, due to the greater surface area offering binding sites. For a more quantitative comparison, the area of fluorescence was calculated from CLSM images for the porous and non-porous particles, taking the 85% fluorescence intensity of the bright outer particle surface as a threshold. These calculations showed that the porous microgels could bind two to three times more bacteria than the non-porous microgels (Figure 5.6.c).

Bacteria binding (= area of fluorescence)	
Porous	**Non-porous**
92 +/- 4%	31 +/- 15%

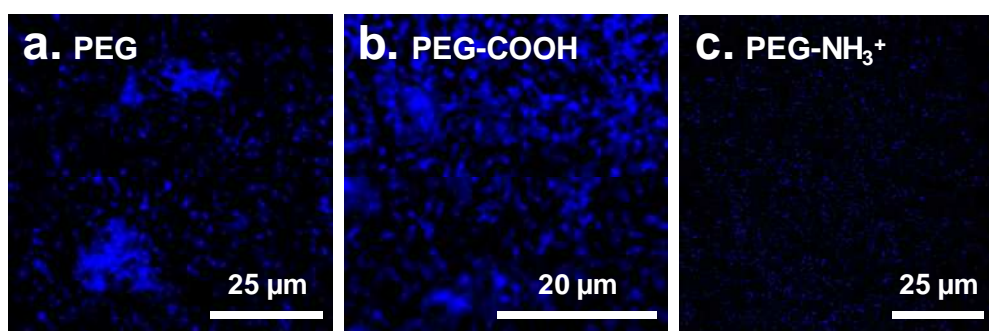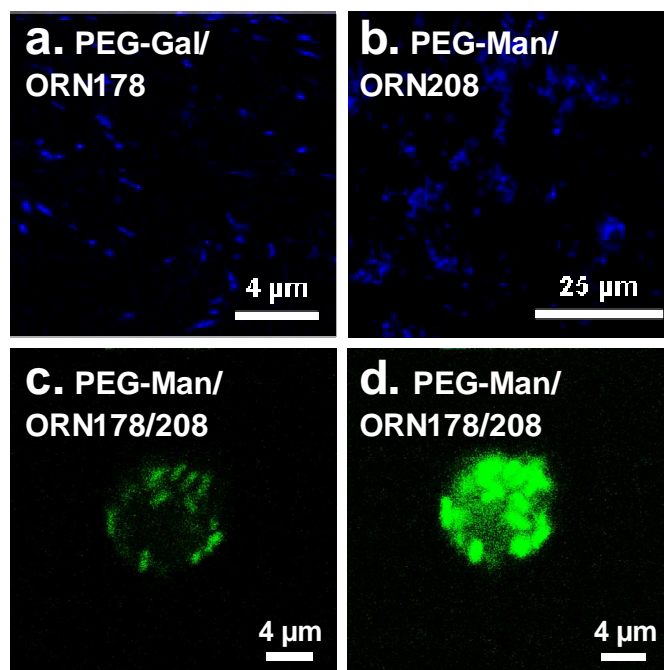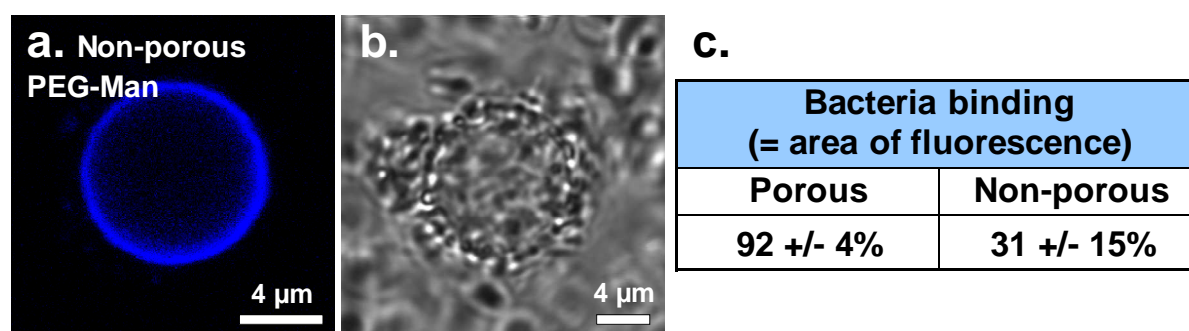*Figure 5.6. a. CLSM and b. optical microscopy image of non-porous PEG-Man microgels after incubation with bacteria E. coli ORN178 in PBS buffer, staining with DAPI and washes with PBS; c. Table presenting the efficiency of binding calculated from the area of fluorescence due to the bound, labeled bacteria for comparison between porous and non-porous PEG-Man microgels. Two to three times more bacteria bound to the porous particles.*

5.3. Removal of Bacteria

After successful incorporation and separate characterization of the two features, magnetic properties and ability to bind bacteria via carbohydrate ligands, both features were combined to obtain magnetic, porous, sugar-functionalized (MaPoS) PEG microgels (Scheme 5.2.A+B).[143] To this effect, the porous PEG-Man/NH$_3^+$ microgels were used and loaded with the superparamagnetic, citrate-coated iron oxide NPs. The combination of both features was however challenging since the presence of carbohydrate ligands may hinder the loading of NPs via electrostatic interactions and the presence of

NPs may prevent bacteria binding. Therefore, the accessibility of both functional groups for the loading of iron oxide NPs and binding of bacteria was first tested again on MaPoS particles.

In spite of the presence of the Man ligands, the PEG-Man/NH_3^+ microgels still exhibited a positive ζ-potential of $+ 16.1 \pm 5.8$ mV at pH 6.5 which was comparable to that of the PEG-NH_3^+ particles (Table 4.5). This surface charge was therefore suitable for the electrostatic loading of iron oxide NPs. Moreover, it was anticipated that too high concentrations of NPs should be avoided because they could lead to a full coverage of the microgels, hide Man groups and prevent final binding of bacteria. The initial amount of NPs available for loading was therefore reduced to a concentration of 0.2 mg.ml^{-1} which still conferred magnetism (Figure 5.7.a). The resulting concentration of loaded NPs was 41 wt%, as measured by UV-visible spectroscopy. MaPoS microgels stayed magnetic, not leaking NPs in PBS buffer (pH 7.4) for at least 12 weeks.
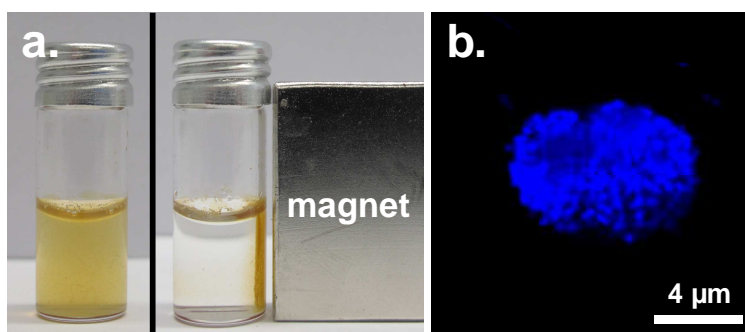
Figure 5.7. *a. Picture of the magnetism of MaPoS microgels; and b. CLSM image of MaPoS particles after incubation with bacteria E. coli ORN178 and staining with DAPI. Both magnetism and capacity for bacteria binding are preserved on MaPoS microgels.*

As for the accessibility of the Man ligands, incubation experiments with bacteria *E. coli* ORN178 showed binding of a large number of bacteria (Figure 5.7.b) comparable to the pure PEG-Man particles. Thus, binding occurred in spite of the presence of NPs most probably because part of the Man ligands were freely exposed on PEG microgels due to the low concentration of NPs and/or the pili of the bacteria were flexible enough to find the Man ligands hidden under the NPs. Even though it could be shown that no bacteria targeting could be done with the cationic amines of PEG microgels, it is most probable that their presence reinforced the binding initially established by carbohydrate-protein interactions. All in all, it could be concluded that the incorporation of both features, magnetism and specific bacteria binding, was possible.

MaPoS microgels were thereafter used for the removal of bacteria from aqueous solutions. They were incubated for one hour in a PBS buffer containing bacteria *E. coli* ORN178. Afterwards, the sample vials were set on a magnet, resulting in magnetically-driven sedimentation of microgels

with bound bacteria. Already with bare eye, a decrease in turbidity compared to the untreated bacteria solution could be observed, indicating the isolation of bacteria with MaPoS microgels (Figure 5.8.a, samples 2 and 3). In order to quantify the binding and removal efficiency of MaPoS particles, the supernatant was removed and the final concentration of bacteria in the supernatant was measured by flow cytometry. The yield of removal was then calculated from the concentration of bacteria in the supernatant after incubation and that of a control solution of bacteria incubated at the same concentrations but without PEG microgels.
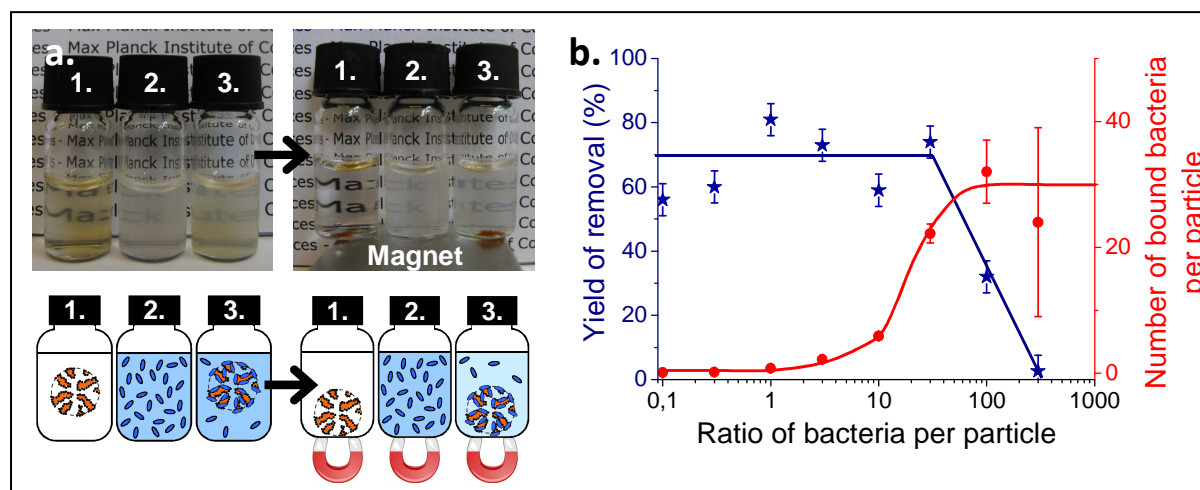
Figure 5.8. *a. Pictures of a solution of pure MaPoS microgels (vial 1), pure bacteria E. coli ORN178 (vial 2) and bacteria incubated with MaPoS microgels (vial 3) after incubation (left) and use of a magnet (right); b. Yield of removal (★) and number of bound bacteria per particle (•) as a function of the initial ratio of bacteria to MaPoS particles (concentration of particles: 1x10⁶ particles.mL⁻¹, concentrations of bacteria measured by flow cytometry, lines are no fits but a guide for the eye).*

The results for a series of isolation experiments at different initial ratios of bacteria per particle while keeping the particle concentration constant (10^6 particles.mL^{-1}) are shown in Figure 5.8.b. First, the evolution of the number of bacteria bound per particle was investigated. At lower initial ratios of bacteria to particle (less than 30/1), a strong correlation between the number of bacteria bound per particle and the concentration of bacteria in solution was observed. This could be attributed to the slow diffusion of bacteria in diluted samples, limiting the contact between bacteria and particles and therefore reducing the probability of a binding event. Only at higher initial concentrations of bacteria, all accessible binding sites of MaPoS microgels could bind bacteria and a maximum coverage of ~ 30 bacteria per particle was reached. Further increase in the initial concentration of bacteria in solution (ratios higher than 30/1) did not increase the number of bound bacteria since the maximum binding capacity has already been reached.

Secondly, the yield of bacteria removal was determined. An average efficiency in means of bacteria removed from solution of around 70% was observed for initial bacteria to particle ratios below 30/1. This yield was even increased to 90% by performing a second incubation with MaPoS microgels. Above the ratio of 30/1, the maximum coverage of bacteria per particle was reached and the yield of bacteria removal started decreasing. With these numbers in hand, it is now possible to calculate the optimal concentration of MaPoS microgels for the removal of bacteria from a solution of known bacteria concentration. If solutions of unknown bacteria concentrations are employed, a stepwise addition and removal of MaPoS microgels can be used to allow for maximum isolation of bacteria from the sample.

Up to now, the most commonly used magnetic beads for biotechnological applications are DYNABEADS. Generally, isolation and removal experiments using DYNABEADS are performed at low concentrations of bacteria ($< 10^6$ bacteria.mL^{-1}) and low initial ratios of bacteria per particle ($< 1/1$).[53, 103, 117, 121-123] Under these conditions, the yields obtained for MaPoS microgels are comparable to those described for DYNABEADS in literature.[117, 121-123] This can be explained by the fact that bacteria binding is essentially limited by the diffusion of bacteria in diluted samples. In this case, particle porosity does not play an important role. However, for the isolation and removal of bacteria from more concentrated solutions, DYNABEADS have to be applied in large quantities (*e.g.* ratio of bacteria per particle $< 1/1$) and the resulting yields of removal decrease.[53, 54, 123] For example, Hatch *et al.* reported less than 35% yield using Man-functionalized DYNABEADS for the removal of bacteria *E. coli* ORN178 at a concentration of 10^7 bacteria.mL^{-1}.[121] Here, MaPoS microgels still achieve high yields of removal while using small amounts of particles (70% yield for ratio of bacteria per particle up to 30/1). Solely comparing the conditions and yields described in literature, MaPoS microgels therefore showed higher binding and removal efficiency compared to non-porous particles. This better performance has been confirmed experimentally since it was already shown that MaPoS microgels were able to bind two to three times more bacteria, compared to non-porous PEG analogues (Figure 5.6).

In conclusion, the multifunctional, magnetic, porous, Man-functionalized PEG microgels were successfully used for the detection and removal of strains of bacteria *E. coli*. Using MaPoS microgels, bacteria were easily removed from solutions by simply applying a magnet. It has been shown that no unspecific binding occurred and that the carbohydrate ligands allowed for the specific detection of one strain of bacteria *E. coli*, even in a mixture of strains. Furthermore, MaPoS microgels allowed for the removal of 70% of bacteria, thereby showing higher efficiency compared to standard particles. This could mainly be attributed to their porous structure, allowing for a maximum binding efficiency of

around 30 bacteria per particle, which corresponds to two to three times more bacteria compared to non-porous beads. It is believed that due to the advantages of biocompatibility, reduced unspecific interactions and higher binding efficiency, MaPoS PEG microgels represent a novel generation of magnetic beads for the removal of bacteria, especially from fermented food or microbial cultures.
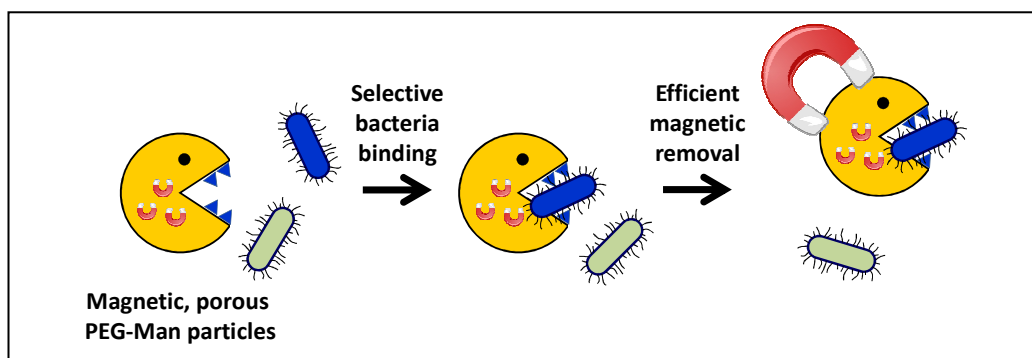
Targeting of other types of bacteria than *E. coli* should be allowed by incorporating different carbohydrate ligands using the straightforward functionalization of PEG microgels. For biotechnological applications where bacteria may be further used, carbohydrate-protein interactions should allow for a straightforward release of the bound bacteria from the microgels by inhibition *e.g.* with a methyl α-D-mannopyranoside solution, as was shown for the ConA receptor in chapter 4. The high number of small ligands in solution will compete with the binding of MaPoS microgels to the bacterial receptors and thus should lead to a detachment of the bacteria from the particles.

In addition to the bacteria removal presented in this chapter, it would be interesting to load drugs such as antibiotics into the microgels and release them upon contact with bacteria. A first step towards this application will be presented in the next and last chapter of this thesis.

6. Functional Porous PEG Microgels for the pH-sensitive Loading and Release of Charged Molecules

In the previous chapters, porous PEG microgels featuring interconnected pores of several tens of nanometers and larger pores on their surface have been synthesized and functionalized with amine groups and carbohydrate ligands. These microgels could be successfully used for the magnetic removal of bacteria and may find applications in biotechnological processes as well as in the detection and elimination of pathogenic bacteria. Further developing antibacterial materials, another obvious way to eliminate bacteria would be to deliver antibiotics. Therefore, the functional porous PEG microgels will be evaluated for a potential loading and release of drugs in the next chapter.

Microgels have received considerable attention for drug delivery applications in the past two decades.[13, 15, 16, 18] The most common strategy applied for the loading and release of drugs relies on the stimuli-sensitive swelling and collapse of microgels. For example, drugs can be loaded into the intrinsic pores of the hydrogel upon swelling and released when the microgels collapse. The major disadvantage of this method is that only small molecules can be loaded through the pores of the gel network. Microgels based on the thermosensitive polymer PNIPAAm have been the most extensively investigated for drug delivery since they are capable of releasing drugs close to body temperature.[120] However, the neurotoxicity of this polymer prevents true biomedical applications.[69, 70]

The functional porous PEG microgels synthesized in this work therefore present great potential as new carriers for drug delivery. PEG is a biocompatible polymer which has already been FDA approved and employed in a great variety of biomedical applications. In addition, the pores of several tens of nanometers in the microgels should allow for the loading of large drugs or drug conjugates, thereby increasing the loading capacity and protecting drugs from degradation. However, PEG microgels are not intrinsically stimuli-sensitive under physiological conditions of pH and temperature. This is the reason why no loading and release can be performed on pure PEG microgels. It is therefore of primary importance to incorporate a surface functionalization which will assume the task of loading and release. The new procedure for the functionalization of PEG hydrogels now allows for the potential use of PEG microgels as carriers for drug delivery. In this chapter, a novel, stimuli-sensitive functionalization will be introduced to the porous PEG microgels for potential drug loading and release applications.

Different kinds of functionalization have been developed to trigger the loading and release of drugs. One common strategy consists of covalently attaching drugs to their carriers and then using the reducing or acidic conditions present at the targeted sites to cleave them from their support.[74] This method is however complicated since synthetic procedures need to be adapted for the covalent binding of each new drug. Such synthesis may also require the use of solvents and reagents which are not biocompatible. A more straightforward and biocompatible method consists of loading and releasing molecules via electrostatic interactions in water. To this end, acidic and basic functional groups have been used. Under the pH conditions where these groups are charged, substances of opposite charge can be loaded. By changing the pH value to switch their protonation state, these groups turn neutral and can release the charged substances. For example, carboxylates can be loaded with cations at pH above their pK_a and release them at pH below.[67] Accordingly, amine groups can be loaded with anions at pH below their pK_a and release them at pH above.[67, 76]

This strategy however possesses some major disadvantages. Cations and anions cannot be loaded using the same functionalization. Furthermore, due to the pK_a of carboxylic acids and amines, release of cations is usually obtained at pH below 4 and of anions at pH above 9. Thus, release of substances in the more relevant physiological pH range of 5 to 7 is not possible. A major improvement would therefore be achieved by using a mixed functionalization presenting both acidic and basic groups of pK_a around 7.

Such a functionalization can be obtained from ammonium-carbamate groups prepared by reaction of CO_2 with amines. This functionalization presents both acidic and basic groups, with the carbamates exhibiting a pK_a around 7.[160] Wang *et al.* applied ammonium-carbamate species for the loading of anionic and cationic dyes but studied their release as a function of ionic strength only.[161] In the following chapter, an ammonium-carbamate functionalization will be presented and used for the loading of anionic and cationic molecules and their release as a function of pH. It will be shown that PEG microgels after modification with this functionalization can be used for potential delivery applications.

The concept of loading and release of PEG-ammonium-carbamate microgels is presented in Scheme 6.1. Porous PEG microgels will be first functionalized with poly(amines) and the unbound amines will be converted into ammonium-carbamates upon introduction of CO_2. The resulting microgels will then be loaded with cations at pH 10 via interactions with their carbamate moieties and release them at pH below 7.4 (path 1). The microgels will also be loaded with anions at pH 5 and will release them at higher pH values (path 2). The conditions for the formation of ammonium-carbamates in aqueous solutions will be preliminarily investigated in section 6.1. Then the porous PEG microgels will be functionalized with ammonium-carbamates in section 6.2. In the last section 6.3 of this

chapter, the pH-sensitive loading and release of both anions and cations using this functionalization will be investigated. In particular, the release from the zwitterionic PEG-ammonium-carbamate microgels will be compared to that of PEG microgels purely functionalized with either carboxylates or ammonium groups.
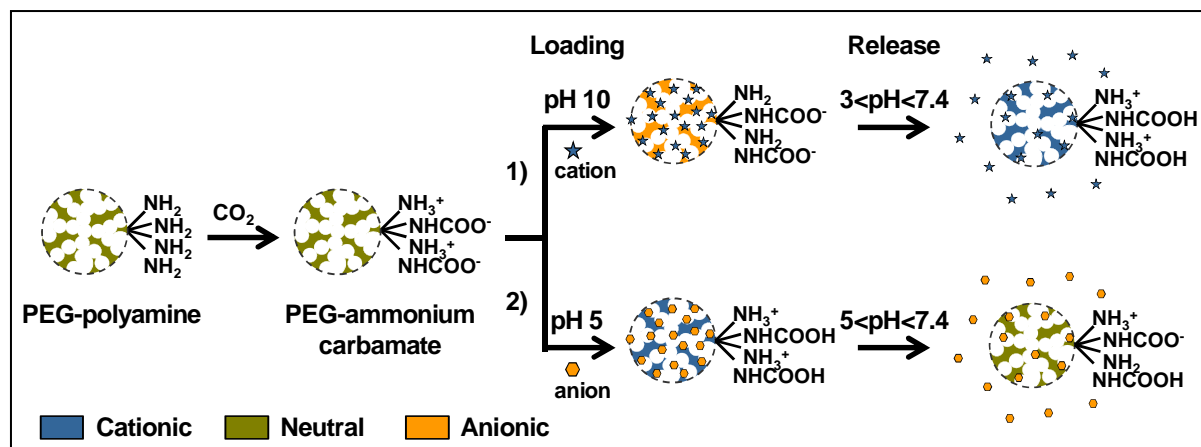
Scheme 6.1. *Principle of the loading and release of anionic and cationic molecules for PEG-ammonium-carbamate microgels.*

In order to achieve high loading of both anionic and cationic molecules, high concentrations of ammonium and carbamate groups are required. Since this number is directly correlated to the number of initial amines before reaction with CO_2, polymeric amines were used for functionalization of the particles. The porous PEG microgels have already been functionalized, in chapter 4, with four poly(amines) of different sizes, structures and pK_a (Table 6.1). Here, the formation of ammonium-carbamates and the effect of size, structure and pK_a on carbamate formation will be investigated for all four poly(amines).

Table 6.1. *Name and intrinsic properties (number of primary amines, structure and pK_a) of the four poly(amines) investigated for functionalization with ammonium-carbamates.*

Name and structural formula	Number of NH_2	Structure	pK_a
A. Oligo(amidoamine) OAMAM	8	Almost linear	~ 8.6
B. Poly(amidoamine) dendrimer, generation 4.0, PAMAM	64	Globular	~ 6.9
C. Poly(allylamine), PAH, $M_w = 56\ 000$	~ 600	Linear	~ 8.6
D. Poly(L-lysine), PLL, $M_w = 150\ 000\text{-}300\ 000$	≥ 1200	Linear	~ 10.5

6.1. Carbamate Formation on Poly(amines) in Solution

Before functionalization of PEG microgels, the ability of each poly(amine) to form ammonium-carbamates in aqueous solution was investigated. For the envisioned loading of anions and cations, both ammonium and carbamate groups should be formed at high concentration. This preliminary study therefore aimed at providing direct evidence and quantification of the ammonium and carbamate species in order to select the most suitable poly(amine) for further functionalization of PEG microgels.

As depicted in Scheme 6.2, carbamates are formed by the direct addition of gaseous CO_2 on nucleophilic amines which first leads to carbamic acids, which are then deprotonated into carbamates.[162, 163] However, a competitive reaction occurs in water: CO_2 gets solvated into carbonic acid (H_2CO_3), leading to a decrease in pH and protonation of the amines, which prevents carbamate formation. Ammonium ions are therefore easily formed from the deprotonation of carbonic and carbamic acids while the formation of carbamates is more delicate, reducing the proportion of carbamate groups relative to that of ammonium. Therefore, this study aimed at obtaining the highest possible yield of carbamation compared to that of protonation.
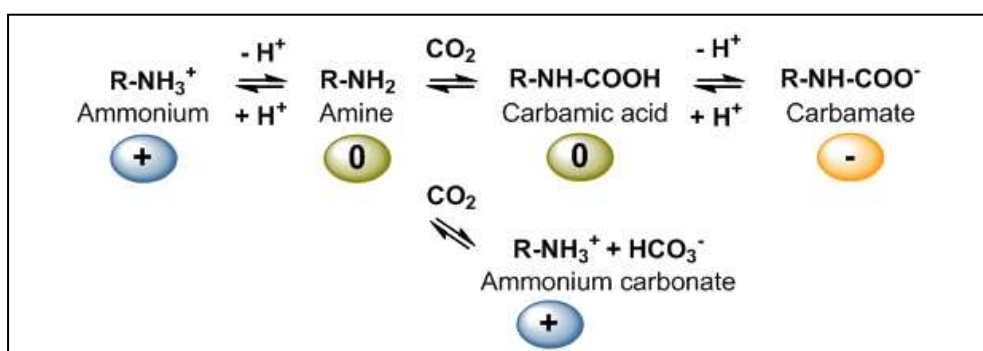
Scheme 6.2. *Presentation of the two competitive reactions of amines with CO_2 in water. Direct fixation of CO_2 on nucleophilic amines leads to the formation of carbamic acids and carbamates after deprotonation. Simultaneously solvation of CO_2 leads to carbonic acid and protonation of the amines into ammonium-carbonate species.*

In order to favor the formation of carbamates, poly(amines) were dissolved in a carbonate buffer prior to introduction of CO_2. A carbonate buffer was used because it is known to considerably increase the concentration of CO_2 compared to other buffers.[164] Moreover it was adjusted to pH 12 before addition of CO_2, so that the poly(amines) were fully deprotonated and the solution could longer buffer the introduction of carbonic acid. CO_2 was then bubbled into the solution for one minute and the pH rapidly decreased to 7.4. Afterwards the pH was slowly increased again in order to deprotonate

the amines and make them available for further carbamation reactions. It has been shown that nucleophilic amines are also able to react with bicarbonate ions.[160] Since too fast addition of base led to carbamate hydrolysis, the pH was slowly raised by adding drops of a carbonate buffer and KOH solution.

The presence of carbamates was demonstrated by Fourier transform infrared spectroscopy (FTIR) in water as well as proton and carbon nuclear magnetic resonance spectroscopy (^1H and ^{13}C NMR) in D_2O and is first exemplified with the poly(amine) OAMAM. Since many signals overlapped at lower pH, the pH was increased to 14 before each measurement to evidence the presence of new signals due to carbamate formation. FTIR spectroscopy after CO_2 bubbling revealed an increased intensity of the absorption band at 1565 cm^{-1}, which is commonly attributed to the COO^- asymmetric stretch of carbamates (Figure 6.1).[165, 166] A new peak appeared at 1080 cm^{-1} and may be attributed to the stretching of the C-N bond.[165, 167]
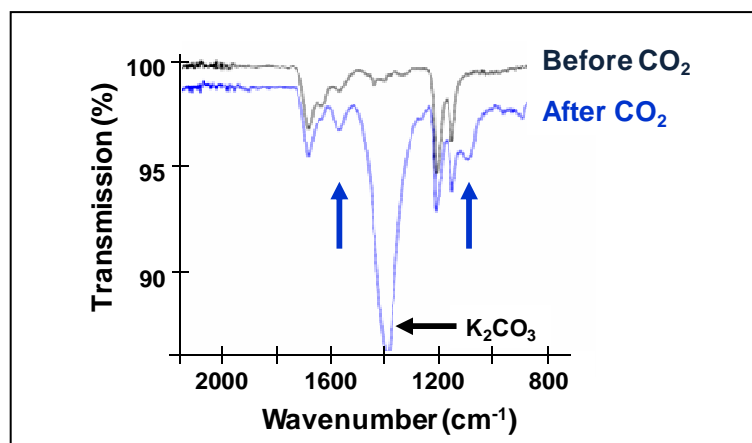
Figure 6.1. *FTIR spectra in H_2O at pH 14.0 of the poly(amine) OAMAM before (top) and after (bottom) treatment with CO_2.*

^1H NMR spectroscopy showed a decreased intensity of the peak at 2.55 ppm which is assigned to the methylene protons CH_2-NH_2 at the ε-amines of the lysine residues (Figure 6.2.a). Simultaneously, a new peak appeared at 2.96 ppm which can be attributed to the methylene protons in the vicinity of the carbamates CH_2-$NHCOO^-$. These protons were shifted downfield since they were de-shielded due to the high electronegativity of the carbamate groups. New peaks also appeared on ^{13}C NMR spectra in the range of 40.8 - 41.1 ppm for the ε-carbon and 29.1 - 29.5 ppm for the δ-carbon of the lysine residues which were carbamated (Figure 6.2.b). In addition, direct evidence of carbamation was provided by the formation of a new peak at 164.8 ppm which could be assigned to the carbon of the carbamates (Figure 6.2.c).[166, 168] Finally, this reaction was proven to be specific to CO_2 since no carbamates were formed without gas or when argon was bubbled instead of CO_2 (here, there is no need for final addition of buffer to increase pH).

^{1}H NMR spectroscopy also enabled to calculate yields of carbamation from the integration of the peaks for CH_2-$NHCOO^-$ and CH_2-NH_2. Yields of 75% for the ε-amines of the lysine residues were obtained for the poly(amine) OAMAM. Such high yields were obtained when the initial carbonate buffer was present at a molar ratio of carbonate to amine at least higher than 2. By decreasing this ratio, yields decreased as well, reaching 22% when no buffer was used. Therefore the presence of carbonate buffer had a crucial impact on the yields of carbamation. To determine the effect of the final step, where the pH was increased again after CO_2 bubbling, its contribution to the final yield was estimated. To do so, the carbonate buffer containing OAMAM was neutralized to pH 7 with HCl instead of bubbling CO_2 and then the pH was increased as before. Under these conditions, yields of 47% were obtained, demonstrating that the last pH-raising step of the procedure also had a strong influence on carbamation. Therefore, it could be concluded that carbamation yields as high as 75% could be obtained by the combination of three factors: use of a carbonate buffer, CO_2-bubbling and final increase of pH.

Extending this study to the other three poly(amines), similar observations could be made with ^{1}H NMR proving that carbamates were formed under the same conditions (Figure 6.3). For PAMAM dendrimer and PAH, up to 70% of carbamates were formed, similar to the yields obtained for OAMAM (Table 6.2). However, only 50% yields were obtained for PLL. PLL has the highest pK_a among all tested poly(amines) ($\sim$ 10.5).[169] Therefore a higher pH was required to get the nucleophilic amines able to form carbamates. However, the concentrations of CO_2 and bicarbonate ions are very low at high pH values and such pH could not be maintained upon introduction of CO_2. This explains why the reaction was more difficult and lower carbamation yields were obtained. All in all, it could be demonstrated that carbamate formation did not depend on the size or structure of the poly(amines) but solely on their pK_a.

Table 6.2. *Table of carbamation yields for all investigated poly(amines).*

Poly(amine)	OAMAM	PAMAM	PAH	PLL
Yields of carbamation (^{1}H NMR)	75%	70%	70%	50%
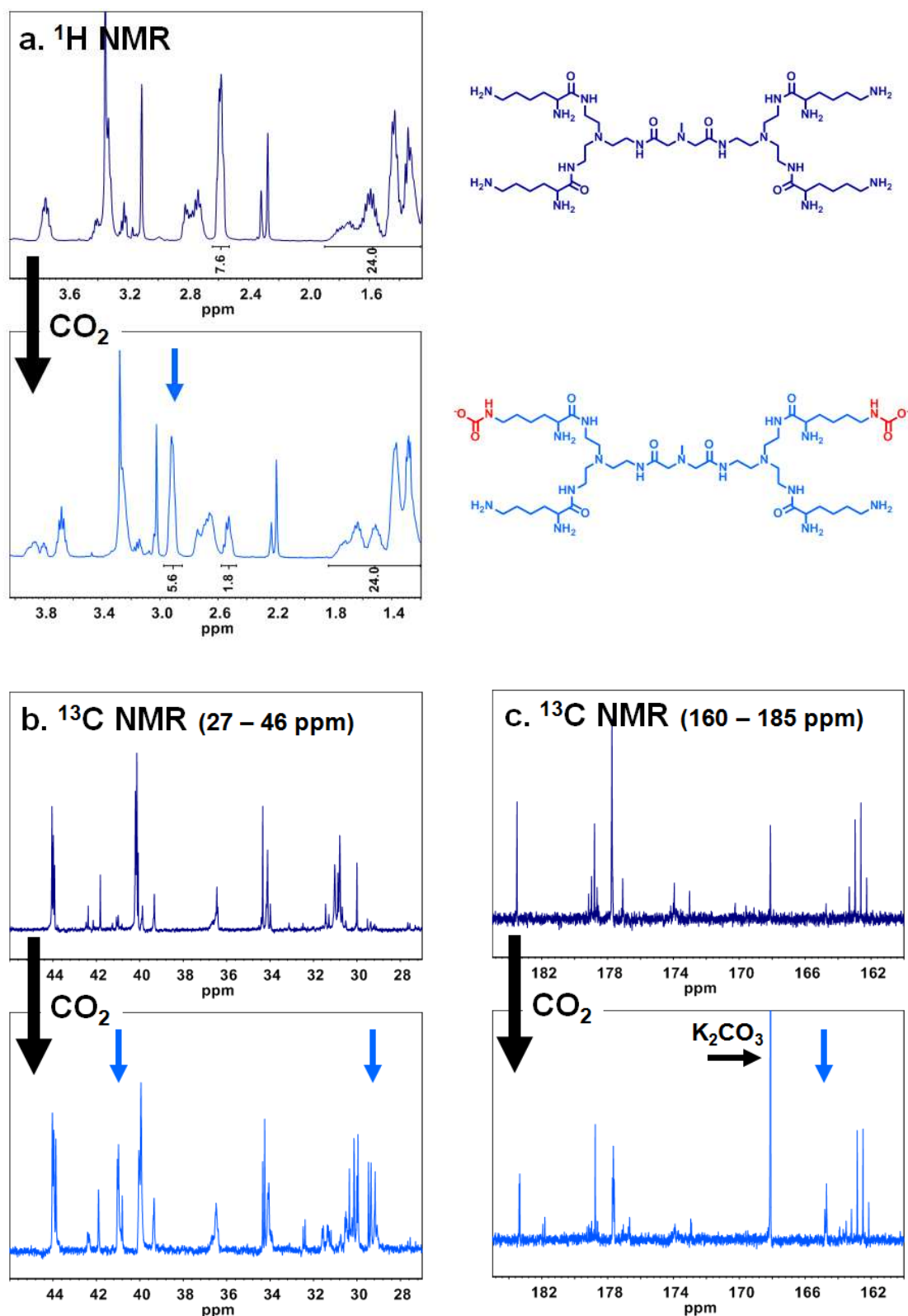
Figure 6.2. *a.* ^1H *NMR spectra (for chemical shifts between 1.2 ppm and 4.0 ppm); b.* ^{13}C *NMR spectra (for chemical shifts between 27 ppm and 46 ppm) and c.* ^{13}C *NMR spectra (for chemical shifts between 160 ppm and 185 ppm) in* D_2O *at pH 14.0 of the poly(amine) OAMAM before (top) and after (bottom) treatment with* CO_2. *Analysis of peak integrations with* ^1H *NMR allowed for the calculation of yields of carbamate formation.*
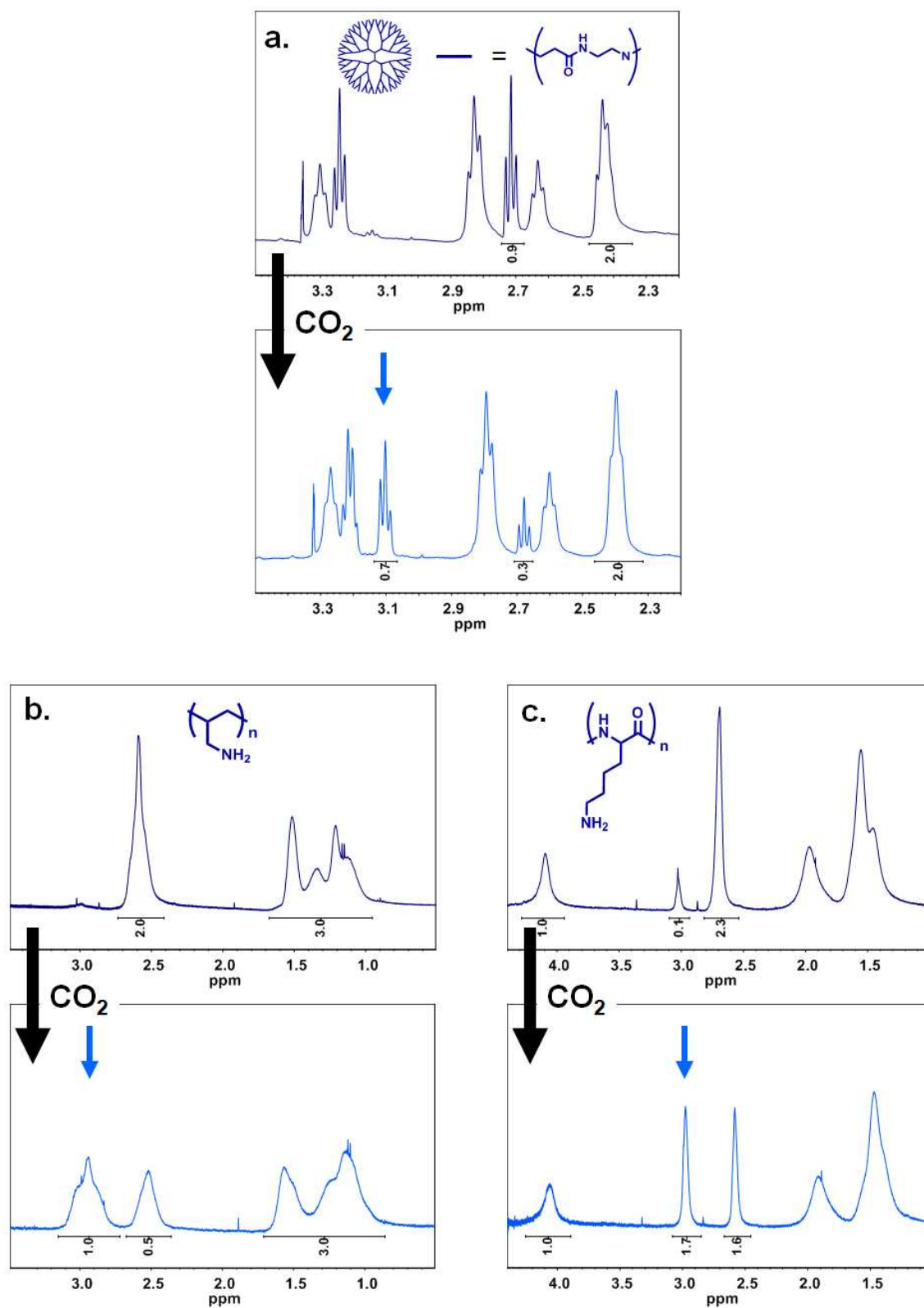
Figure 6.3. *^{1}H NMR spectra in D_2O at pH 14.0 of a. PAMAM dendrimer; b. PAH; and c. PLL before (top) and after (bottom) treatment with CO_2.*

The highest yields of carbamate formation were therefore obtained from OAMAM, PAMAM and PAH. In addition, it was shown in chapter 4 that functionalization with PAMAM dendrimer resulted in the highest surface functionalization of PEG microgels. Internal functionalization was most probably non-existent but is not relevant for the envisioned loading of drugs since large molecules may not be able to diffuse into PEG hydrogels and may be mostly loaded on the surface. From this point of view, functionalization with PAMAM seems to be the most advantageous. Another major advantage of PAMAM dendrimer lies in the low pK_a of its terminal amines (~ 6.9) allowing for a charge switch under physiological conditions.[149] PAMAM dendrimer was therefore chosen for the functionalization of the porous PEG microgels with ammonium-carbamates.

6.2. Ammonium-Carbamate Functionalization of Porous PEG Microgels

The ammonium-carbamate functionalization was achieved by first functionalizing PEG-COOH particles with PAMAM dendrimer and then converting the remaining amines into ammonium-carbamates with gaseous CO_2. The synthesis of PEG-PAMAM microgels has already been described in chapter 4.2. These microgels were thereafter modified to present ammonium-carbamate moieties using similar conditions to the ones applied in the preliminary study in section 6.1. The microgels were first dispersed in a carbonate buffer at pH 12, CO_2 was bubbled for 1 minute and the pH of the solution was finally raised to 14 by slow addition of base. The microgels were then washed three times with deionized water.

The presence of carbamate groups could not be directly evidenced, neither by FTIR spectroscopy since the associated absorption band was too weak, nor by NMR spectroscopy since no detectable signal for the functionalization on PEG microgels could be measured. Indirect proof was however provided by the ζ-potential of the particles measured in water after short treatment at pH 5.0 (Table 6.3). The initial PEG-PAMAM microgels presented a ζ-potential of $+ 23.0 \pm 7.3$ mV which was slightly lower than after treatment at pH 1.0 due to a reduced degree of protonation. The ζ-potential then decreased to $- 9.5 \pm 23.0$ mV after exposure to CO_2 but kept constant upon exposure to argon (control). Due to their low surface charge, these microgels slightly aggregated, which explains the higher error values (± 23.0 mV) for these measurements. The observed decrease in ζ-potential indicated that a CO_2-specific reaction leading to the formation of anionic species occurred and was interpreted as evidence for successful carbamate formation.

Table 6.3. *Characterization (ζ-potential, titration of functional groups) and loading of PEG-PAMAM microgels before and after CO_2.*

	PEG-PAMAM (control)	PEG-ammonium-carbamate
ζ-potential (mV)	+ 23.0 ± 7.3	- 9.5 ± 23.0
Concentration of NH$_2$ (µmol/g)	150 ± 20	100 ± 20
Concentration of TBO (µmol/g)	50 ± 10	100 ± 10
Concentration of MO (µmol/g)	1100 ± 100	2100 ± 300

The concentration of carbamates was indirectly determined by measuring, via TNBS titration, the concentration of amines which reacted with CO_2. Before addition of CO_2, the concentration of amines was 150 ± 20 µmol/g but decreased to 100 ± 20 µmol/g after introduction of CO_2 (Table 6.3). Thus, 50 µmol/g of amines were converted into carbamates giving a yield of carbamate formation of 33% on PEG-PAMAM microgels. This is only half of the yield obtained for PAMAM dendrimer in solution. This loss in yield might be correlated to the stability of carbamates. This stability was therefore investigated in solution with ^{1}H NMR spectroscopy. It could be observed that carbamation in solution reached 70% after a few minutes but decreased to 40% after a few hours (Figure 6.4). In spite of these lower yields, the ζ-potential of PEG particles decreased by nearly 30 mV due to the presence of carbamates and seemed to remain stable over days. Hence, the concentration of carbamates was still high enough to drastically and durably change the surface charge of PEG-PAMAM microgels.
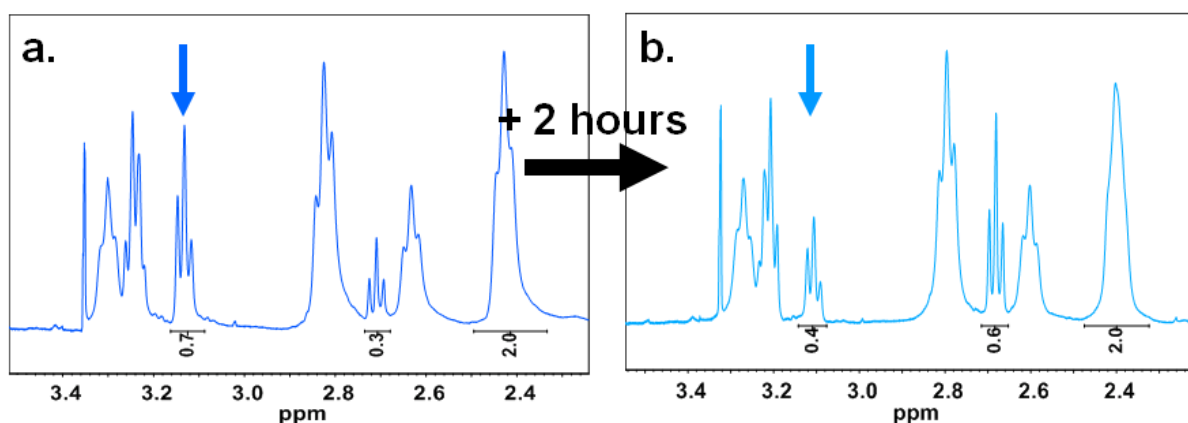
Figure 6.4. *^{1}H NMR spectra in D_2O at pH 14.0 of PAMAM dendrimer a. immediately after treatment with CO_2 and b. 2 hours after treatment.*

6.3. pH-sensitive Loading and Release of Anionic and Cationic Molecules

The porous PEG microgels functionalized with ammonium-carbamates were thereafter tested for the loading and release of charged model drugs. As a first step, the pH-sensitivity of the microgels was demonstrated. It was shown already that the PEG-ammonium-carbamate microgels contain 100 µmol/g of amine and 50 µmol/g of carbamate functionalization. Since both of these groups can be charged or neutral as a function of pH, they should confer a pH-sensitive charge to PEG microgels. The basic, primary amines of PAMAM dendrimer and acidic carbamates are known to present a pK_a around 6.9 and 7, respectively.[149, 160, 170] The ammonium-carbamate functionalization should therefore be cationic at pH values below 7 due to the protonated ammonium and neutral carbamic acids, but anionic at pH above 7 due to the carbamates and neutral amines (Scheme 6.3). Therefore PEG-ammonium-carbamate microgels should be able to switch their charge from positive to negative by increasing the pH and this change should occur around pH 7. This was confirmed by the ζ-potential of these particles switching from $+ 25.2 \pm 4.0$ mV at pH 5.0 to $- 19.8 \pm 5.1$ mV at pH 10.5. In the following section, such a charge switch will be used for the pH-sensitive, electrostatic loading and release of both anionic and cationic molecules.
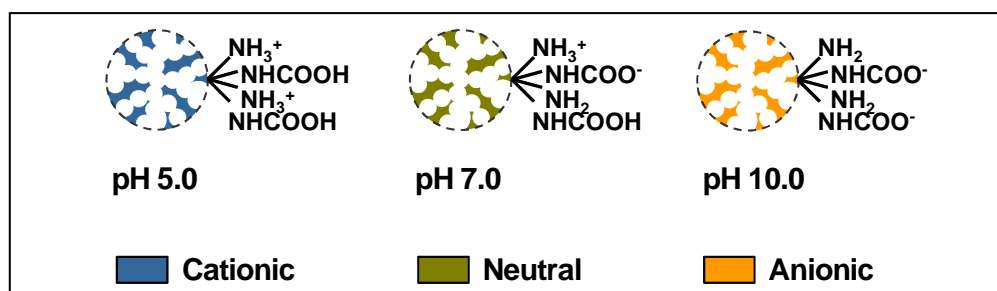
Scheme 6.3. *pH-sensitivity of PEG-ammonium-carbamate microgels.*

The concept of loading and release of cationic molecules using the ammonium-carbamate functionalization is presented in Scheme 6.1. Loading of cations was performed at pH 10.0 via electrostatic interactions with the anionic PEG-ammonium-carbamate microgels. The cationic dye toluidine blue O (TBO) was used as a model for cationic drugs (Figure 6.5). Within two hours of incubation, PEG-ammonium-carbamate microgels turned blue, indicating that the dye was taken up by the particles (Figure 6.7.a). In order to determine if the loading was homogeneous, the cationic fluorescent dye Rhodamine 6G (Figure 6.5) was loaded under the same conditions. CLSM confirmed that the loading was uniform throughout the microgels (Figure 6.6.a). As a control, the cationic PEG-PAMAM microgels which were not treated with CO_2 were also incubated with Rhodamine 6G and showed much less fluorescence (Figure 6.6.b). The little fluorescence observed was most probably due to the electrostatic interactions between the dye and residual carboxylates. It was indeed expected

that PAMAM dendrimer did not functionalize the core of the PEG hydrogel network, leaving unreacted carboxylates. The stronger fluorescence of PEG-ammonium-carbamate microgels however indicated that additional anionic carbamate groups were present on the microgels.
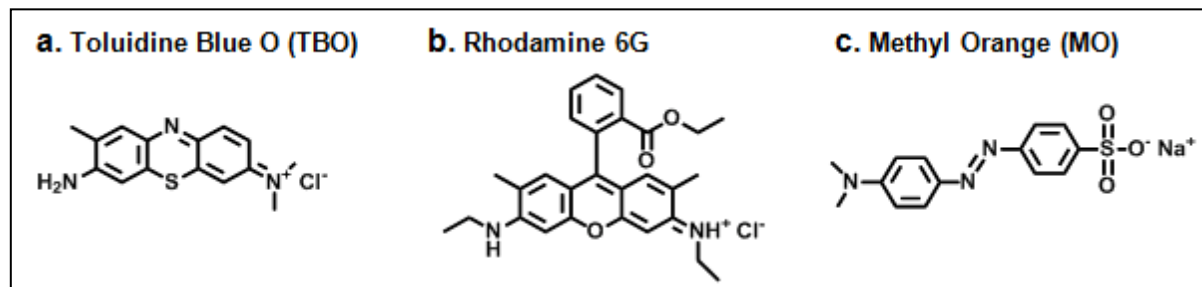
***Figure 6.5**.a., b. and c. Structural formulas of the cationic and anionic dyes used for loading and release from PEG-ammonium-carbamate microgels.*

In order to quantify the amount of loaded dye, UV-visible spectroscopy was performed on TBO solutions before and after loading, as well as on the supernatant after release of TBO at pH 1.0. Both methods confirmed that $100 \pm 10\ \mu mol/g$ of TBO was loaded into PEG-ammonium-carbamate microgels whereas only $50 \pm 10\ \mu mol/g$ of TBO was loaded into the untreated PEG-PAMAM microgels (Table 6.3). The loading of TBO observed on untreated PEG-PAMAM particles probably arose from the electrostatic interactions with the residual carboxylates. However, an excess of $50\ \mu mol/g$ of TBO was loaded into PEG-ammonium-carbamate microgels and can be attributed to the interactions with carbamate moieties. This value was also in good agreement with the concentration of $50 \pm 20\ \mu mol/g$ of carbamate groups obtained from TNBS titration. It is indeed usually assumed that TBO dye reacts in a 1/1 stoichiometry with anionic groups.[146] Furthermore, the loading proved to be stable over at least two weeks in water adjusted to pH 10 with NaOH, since only minimal release of dye was observed by UV-visible spectroscopy (Figure 6.8).
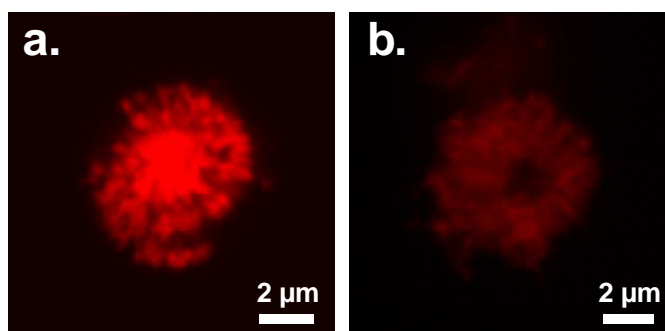
***Figure 6.6.** CLSM images of a. PEG-ammonium-carbamate microgels and b. PEG-PAMAM microgels (control) after loading of Rhodamine 6G.*

Release of the loaded dye was performed by decreasing the pH below 7.4 (Scheme 6.1). Under these conditions PEG-ammonium-carbamate microgels turned cationic, which resulted in the electrostatic repulsion of the loaded cationic dye. Release was studied at pH 7.4 in PBS buffer, pH 5.0 and pH 3.0 in a 0.1 M acetate buffer. Already at pH 7.4 the buffer turned blue after a few minutes in contact to the microgels, indicating that a release occurred (Figure 6.7.a). This release was quantified as a function of time. To do so, microgels were incubated in 1 mL of buffer and the absorbance of the supernatant was regularly measured by UV-visible spectroscopy. To evidence the influence of both carbamate and ammonium groups, release from PEG-ammonium-carbamate microgels was compared to that from PEG-COOH microgels. These microgels showed a purely anionic functionalization and were used for the loading and release of TBO under the same conditions.

The results for release at pH 7.4 and 5.0 are presented in Figure 6.7.b. The release plotted on the y-axis corresponds to the ratio between the amount of released TBO and the amount of TBO which was initially loaded. The presented values were measured after 60 minutes of release since release profiles seemed to reach a plateau within one hour for both types of microgels. At pH 7.4 as well as 5.0, TBO was released more efficiently from PEG-ammonium-carbamate than from PEG-COOH microgels. For example, 71% TBO was released from PEG-ammonium-carbamate at pH 5.0 whereas only 8% was released from PEG-COOH microgels, which corresponds to an eight-fold increase in release efficiency. The main reason for this difference is that PEG-ammonium-carbamate microgels are already cationic at pH below 7.4 due to the high pK_a of carbamate groups and presence of amines. On the other hand, PEG-COOH still remain anionic at these pH values ($pK_a \sim 4.4$). In addition, PEG-ammonium-carbamate microgels show an increased cationic charge at pH 5.0 compared to pH 7.4, which explained why release was even more efficient at pH 5.0 than 7.4. By further decreasing pH to 3.0 both types of microgels released 100% of the dye and no difference could be noted, since PEG-COOH turned neutral. However, under mild conditions (pH 5.0 - 7.4), ammonium-carbamate functionalization enabled a more efficient release compared to simple carboxylate functionalization.

Figure 6.7. a. Picture of TBO loading and release from PEG-ammonium-carbamate microgels at pH 7.4 in PBS buffer, after 3 minutes; b. Quantification of TBO release from PEG-ammonium-carbamate and control PEG-COOH microgels after 1 hour at pH 7.4 in PBS buffer and pH 5.0 in 0.1 M acetate buffer.

Following the same principle, also anionic molecules could be loaded into PEG-ammonium-carbamate microgels and released as a function of pH (Scheme 6.1). For this study, the anionic dye methyl orange (MO) was used as model for anionic drugs (Figure 6.5). MO could be successfully loaded into the cationic PEG-ammonium-carbamate microgels at pH 5.0, as indicated by the particles turning orange within two hours of incubation (Figure 6.9.a). The amount of loaded dye was quantified by UV-visible spectroscopy and compared to the one of control PEG-PAMAM microgels, which were not treated with CO_2 but loaded with the same dye. Such purely cationic microgels are indeed traditionally used for the loading of anionic molecules. For untreated PEG-PAMAM microgels, the amount of loaded MO was estimated to be 1100 ± 100 µmol/g (Table 6.3). This concentration was extremely high but similar to that already observed by Ghosh *et al.*[171] It could be shown that this loading did not result from interactions with PEG but mostly with PAMAM since only 320 ± 100 µmol/g of MO could be loaded into unfunctionalized PEG microgels. Such a high loading most probably resulted from the internalization of dye molecules into PAMAM dendrimer cavities by host-guest association, supported by electrostatic interactions, hydrogen bonding and/or hydrophobic interactions between PAMAM and the dye.[172] This concentration was expected to decrease when MO was loaded into PEG-ammonium-carbamate microgels, since less ammonium ions were available for attractive electrostatic interactions. However, the concentration of loaded MO was found to be even higher on PEG-ammonium-carbamate reaching 2100 ± 300 µmol/g (Table 6.3). One possible explanation for this higher loading is that carbamic acids induced stabilizing hydrogen bonds with MO sulfonate groups resulting in an additional loading. Carbamic acids were indeed not hydrolyzed at this pH, as could be seen on ^{1}H NMR spectra showing the same pattern before and after treatment at pH 5. Furthermore, the loading proved to be stable over two weeks in water adjusted to pH 5 since almost no release was observed by UV-visible spectroscopy (Figure 6.8).
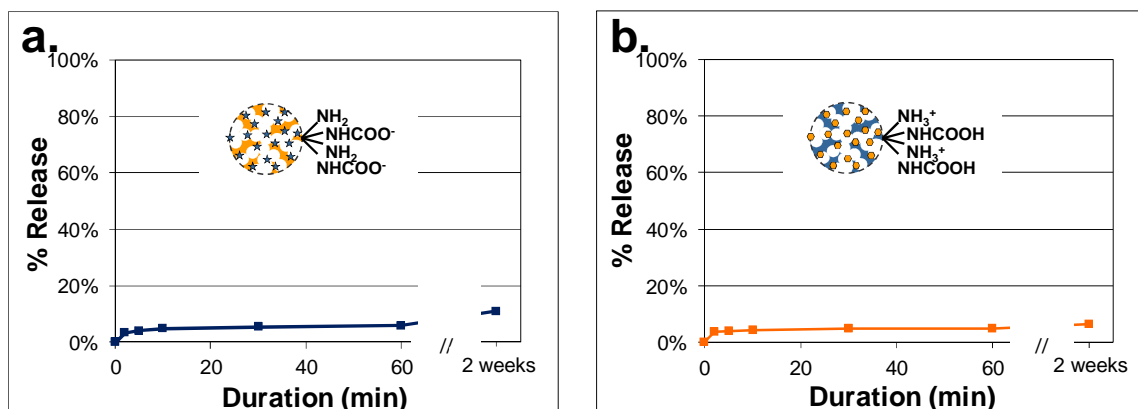
Figure 6.8. a. Stability of TBO loading in PEG-ammonium-carbamate microgels in water adjusted to pH 10 with NaOH, within 1 hour and up to 2 weeks; and b. Stability of MO loading in PEG-ammonium-carbamate microgels in water adjusted to pH 5 with HCl within 1 hour and up to 2 weeks.

Release of MO could be observed by increasing pH to 6.0 and 7.4, respectively (Figure 6.9.a). Under these conditions, PEG-ammonium-carbamate microgels slowly turned neutral, which induced release of the dye (Scheme 6.1). To evidence the influence of carbamates, this release was compared to release from untreated PEG-PAMAM microgels with purely cationic functionalization. The release reached a maximum at pH 7.4, where 100% of the loaded MO could be released for both PEG-ammonium-carbamate and PEG-PAMAM microgels (Figure 6.9.b). At the lower pH 6.0, MO release was not maximal but slightly more efficient from PEG-ammonium-carbamate since a higher proportion of loaded MO was released (Figure 6.9.b). This higher performance was most probably due to the electrostatic repulsion between the dye and the anionic carbamates.
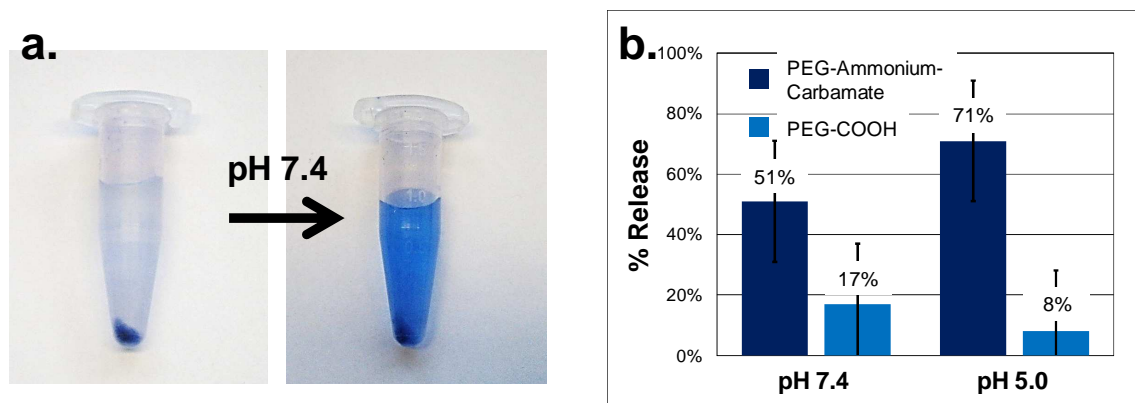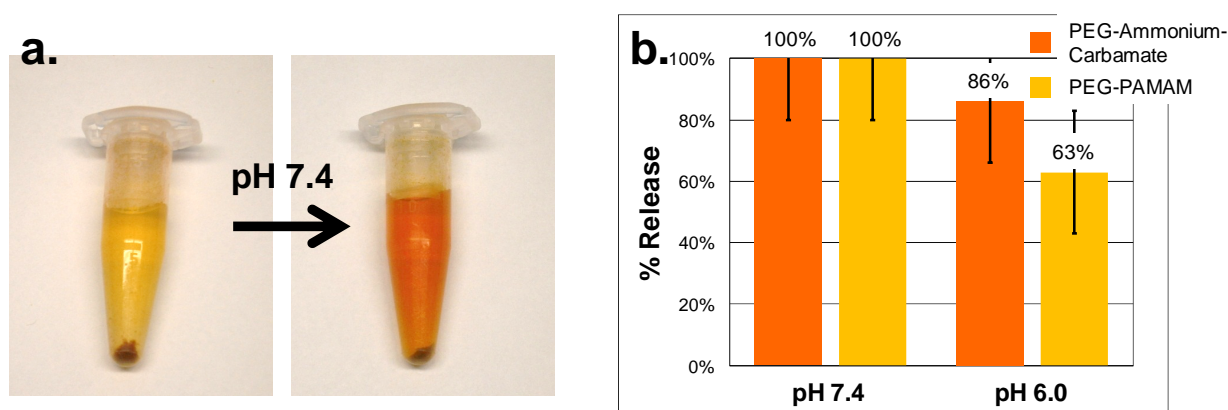

Figure 6.9. a. Picture of MO loading and release from PEG-ammonium-carbamate microgels at pH 7.4 in PBS buffer, after 3 minutes; b. Quantification of MO release from PEG-ammonium-carbamate and control PEG-PAMAM (no carbamates) microgels within 1 hour at pH 7.4 in PBS buffer and pH 6.0 in 0.1 M acetate buffer.

In conclusion, the porous PEG microgels could be made pH-sensitive by a novel functionalization based on ammonium-carbamate species and used for the loading and release of anionic and cationic model drugs. The ammonium-carbamate functionalization was obtained from the reaction of CO_2 with PAMAM dendrimer, giving 30% carbamate and 70% ammonium groups. The resulting functionalization switched from negative at pH 10 due to their carbamate moieties to positive at pH 5 due to their ammonium moieties. PEG-ammonium-carbamate microgels could therefore be loaded with both cations at pH 10 and anions at pH 5 via electrostatic interactions as well as release them at pH values between 5.0 and 7.4.

Compared to PEG microgels functionalized with pure carboxylate or ammonium groups, the PEG-ammonium-carbamate microgels enabled to load both anionic and cationic molecules. Since these molecules have been loaded under different conditions, only one type of molecules could be loaded at a time. Conditions for release were however similar, so that a simultaneous release of both anions and cations should be possible using a mixture of microgels, one type loaded with anions, the other type with cations.

Compared to pure carboxylate or ammonium, the zwitterionic PEG-ammonium-carbamate microgels also led to a release up to eight times more efficient at pH values between 5.0 and 7.4. More accurately, a higher proportion of the total amount of loaded molecules was released. This higher efficiency could be explained by two factors. Firstly, the pK_a of carbamates is higher than that of carboxylates, which allowed for a charge switch around pH 7 rather than 4 for carboxylates. Secondly, the functional group which was not used for the loading via electrostatic attraction can be employed to enhance the release via electrostatic repulsion. As a drawback, compared to a pure cationic or anionic functionalization, a lower total concentration of molecules can be loaded with the mixed ammonium-carbamate functionalization. This was for example the case for TBO (but not MO), but is compensated by a more efficient release. Therefore, PEG-ammonium-carbamate microgels overall represent a novel system especially suitable for the release of expensive molecules, since lower amounts are required for loading and a greater proportion is released.

It should be noted that loading was already effective with molecules bearing only one charge. However, stability of this loading could be only obtained in media of low ionic strength, since ions compete with the loaded molecules and lead to their release. It is however expected that the stability of the loading would be considerably improved in media of high ionic strength by loading molecules bearing multiple charges. For example, a wide range of antibiotics are oligo- or polycations. On-going work therefore focuses on loading polycationic antibiotics and testing the stability and release of this loading in media of high ionic strength such as PBS buffer and serum-containing media. Further work will also focus on obtaining a sustained release, for instance by coating the ammonium-carbamate

functionalized microgels with a semi-permeable membrane. It is believed that, by including such further improvements, the porous PEG-ammonium-carbamate microgels show great potential for the loading and release *e.g.* of antibiotics and could be advantageously combined with their magnetic, sugar-functionalized siblings.

7. Conclusions and Perspectives

In this thesis, the preparation of functional porous PEG microgels has been presented. Microgels have a great potential for biotechnological and biomedical applications such as the detection, retrieval and elimination of bacteria. The enthusiasm for microgels arises from their versatility, colloidal stability, stimuli-sensitivity and large specific surface area. The current microgels however present some major limitations since many systems are not biocompatible and/or show low performance due to their restricted loading capacity. This thesis therefore presents a new platform of microgels based on a biocompatible polymeric scaffold which reduces unspecific interactions, allows for surface functionalization and features a high loading capacity for a straightforward incorporation of large drugs or functional nanoparticles and binding of cells or bacteria.

To achieve this aim, PEG microgels presenting both internal nano-sized and external micro-sized interconnected pores have been synthesized and functionalized. Such porous PEG microgels have been prepared by a hard templating method based on porous $CaCO_3$ microparticles.[138] This method allowed for a precise control over the size and porosity of PEG microgels. The resulting microgels were exact inverse replicates of $CaCO_3$ microparticles, thereby presenting the expected porosity. Internal pores of 20 to 60 nm and external pores reaching up to 3 µm could be evidenced by a diffusion study, cryo-SEM and TEM. These porous PEG microgels were thereafter functionalized for targeting as well as loading and release applications. Radical surface chemistry based on benzophenone allowed for the grafting of carboxyl groups which could be used for further functionalization via amide bond formation.[126] Mannose ligands were thereby introduced for bacteria targeting and cationic amines were incorporated for the loading of molecules and nanoparticles via electrostatic interactions. Both functional groups could be added separately or simultaneously via a one-pot synthesis. The presence and uniform distribution of these groups was verified by CLSM after fluorescent labeling, the final surface charge of the microgels was determined via ζ-potential measurements and UV titrations were performed to determine the mass concentration of functional groups. The final degree of functionalization was as high as 1200 µmol per gram of particles, most probably due to the porosity of PEG microgels. The concentration of amines could even be increased on the surface of PEG microgels by functionalization with PAMAM dendrimers.

The potential of the resulting functional, porous PEG microgels was then tested in two important areas where microgels have been successfully applied: the detection and removal of bacteria as well as drug loading and release. First, porous functional PEG particles were employed for the detection and removal of bacteria.[143] Magnetic properties were introduced to the microgels by loading

citrate-coated, superparamagnetic iron oxide nanoparticles via electrostatic interactions with cationic amines. Mannose ligands were employed for the detection and binding of bacteria *E. coli* via carbohydrate-protein interactions. The resulting magnetic, porous, sugar-functionalized (MaPoS) PEG microgels were able to bind bacteria and remove them by simply using a magnet. As shown by CLSM, these microgels were able to selectively bind *E. coli* strain ORN178 but not the strain ORN208 known for not binding to mannose ligands. Similar selectivity was observed in a mixture of both strains. Flow cytometry indicated that up to 70% of bacteria ORN178 could be removed. This yield of removal could be even increased to 90% by performing a second incubation. Compared to the standard non-porous beads used for such applications (*e.g.* DYNABEADS), the biocompatible MaPoS PEG microgels allowed for the binding of two to three times more bacteria and showed higher yields of removal at high concentrations of bacteria. On-going work now focuses on targeting other types of bacteria by employing other carbohydrates but also on increasing the selectivity of targeting by using more complex carbohydrates.

In a second part, the potential of functional porous PEG microgels for the loading and release of drugs was investigated.[147] To achieve this, a novel, pH-sensitive functionalization was implemented on the microgels. This functionalization is based on the introduction of amine groups and their subsequent conversion into ammonium-carbamates via reaction with CO_2. The carbamates were employed for the loading and release of cationic molecules and the ammonium for the loading and release of anions. Successful functionalization of the microgels with various poly(amines) and ammonium-carbamate formation were proven by FTIR and NMR spectroscopies, CLSM, measurement of ζ-potential and UV titration. In particular, PEG microgels functionalized with PAMAM dendrimers showed 70% of ammonium and 30% of carbamate functionalities. ζ-potential measurements also revealed that this functionalization could switch its charge from -20 mV at pH 10 to $+25$ mV at pH 5. The resulting pH-sensitive PEG microgels could therefore be loaded with both cationic and anionic model drugs via electrostatic interactions at pH 10 and pH 5, respectively. Release was observed at pH values between 5 and 7.4. Compared to PEG microgels purely functionalized with carboxylate or ammonium groups, the zwitterionic PEG-ammonium-carbamate microgels allowed for a release up to eight times more efficient under physiological pH conditions. On-going work focuses on loading polycationic antibiotics and testing the stability and release of this loading in media of high ionic strength such as PBS buffer and serum-containing media. Further work will also be devoted to obtain a sustained release, for example by coating the PEG-ammonium-carbamate microgels with a semi-permeable membrane. Due to their size, such microgels could be adapted for transdermal delivery but for other types of delivery smaller microgels would be required. This could be achieved for instance by using smaller $CaCO_3$ templates or by switching to mesoporous silica nanoparticles.

Overall, the biocompatible, functional porous PEG microgels allowed for high performance in binding and retrieval of bacteria as well as loading and release of model drugs. This was due to the high surface area resulting from their porosity and high degree of functionalization. These microgels therefore show great potential for the treatment of bacteria but also for a wider range of biotechnological and, in long term, biomedical applications. Following the same principle as for bacteria retrieval, the magnetic, porous, functional PEG microgels may be used for the detection and removal of other pathogens such as viruses or the isolation and separation of cells. Moreover, these microgels can be employed for the separation of biomolecules such as proteins, as currently investigated in collaboration with Dr. D. Kolarich and Dr. C. Rademacher (MPIKG, Berlin). Combined with enzymes, the porous PEG microgels may also be used in catalysis, where PEG would advantageously provide a biocompatible protection to proteins. The hard templating procedure presented in this thesis could already be adapted to synthesize porous protein particles in cooperation with Dr. S. Schmidt (MPIKG, Golm).[173] Further work is now on-going in collaboration with the group of Dr. D. Volodkin (Fraunhoher IBMT, Golm) and Dr. R. Georgieva (Charité, Berlin) to develop mixed microgels composed of both PEG and proteins.

8. Appendix

8.1. Experimental Part

8.1.1. Materials

Benzophenone (99%) and ethylenediamine (99%) were purchased from Acros Organics, benzotriazole-1-yl-oxy-tris-pyrrolidinophosphonium hexafluorophosphate (PyBOP) from Novabiochem and 1-hydroxybenzotriazole monohydrate (HOBt·H_2O) from Iris Biotech GmbH. All other chemicals including PEG, acrylic acid (99%), 2-Hydroxy-4′-(2-hydroxyethoxy)-2-methylpropiophenone (Irgacure 2959, 98%), PAMAM dendrimer generation 4.0 with an ethylenediamine core (10 wt.% in methanol), poly(allylamine) solution (M_w = 56 000, 20 wt.% in H_2O), poly(L-lysine) hydrobromide (M_w = 150 000-300 000), fluorescein isothiocyanate-labeled Concanavalin A (Type IV from Canavalia ensiformis) and the different dyes were purchased from Sigma-Aldrich and used without further purification. A technical grade was used for gaseous carbon dioxide ($\geq$ 99.7 vol.%, Air Liquide).

$CaCO_3$ microparticles with an average diameter of 17.9 ± 3.4 µm (template 1) were kindly provided by Dr. D. Volodkin, synthesized referring to a protocol described by the same author.[130] $CaCO_3$ microparticles with an average diameter of 6.9 ± 0.7 µm (template 2) and 7.3 ± 1.2 µm (template 3) were purchased from PlasmaChem GmbH (Berlin). Templates 2 and 3 come from two different batches and do no exhibit the same density, template 2 presenting a higher density than template 3. PEG-dAAm (M_n = 4600 Da) was synthesized from PEG by D. Pussak following a procedure reported by Hartmann *et al.*[44, 45] (2-aminoethyl)-2,3,4,6-tetra-O-acetyl-α-D-mannopyranoside hydrochloride and (2-aminoethyl)-2,3,4,6-tetra-O-acetyl-β-D-galactopyranoside hydrochloride were synthesized by S. Mosca according to the protocol from Ponader *et al.*[151] The small oligo(amidoamine) OAMAM was synthesized by a procedure reported by Hartmann *et al.*[148] The citrate-coated magnetite (Fe_3O_4@citrate) nanoparticles were synthesized by Dr. M. Chanana according to a modified method published by Sahoo *et al.* and Racuciu *et al.*[174, 175]

8.1.2. Methods

Optical and **confocal laser scanning microscopy** (CLSM) images were taken with a TCLS system attached to an inverted microscope equipped with a 100x oil immersion objective (DM IRBE, Leica). The size, size distribution and average volume $V_{swollen}$ of swollen PEG microgels were determined by measuring the diameter of 100 particles, assimilated to perfect spheres. The diffusion of macromolecules into PEG microgels was studied via the solute exclusion method, using Rhodamine-labeled dextran of 70 kDa and FITC-labeled dextran of 500 kDa and 2000 kDa. The diffusion of dextran was evaluated as the ratio between the fluorescence intensity in the microgel core and that in the surrounding solution. The fluorescence intensity was determined as the grey value measured with the image processing program ImageJ.

Energy dispersive X-ray spectroscopy (EDS) was performed by Dr. J. Hartmann using a scanning electron microscope (DSM 940 A, Carl Zeiss, Germany), equipped with an EDS link ISIS-system (Oxford Instruments). These measurements were carried out at a voltage of 20 kV and under high vacuum conditions. The energy resolution of the link ISIS-system was 133 eV.

Atomic force microscopy (AFM) was conducted to measure the volume V_{dry} of dry particles and determine the water content in PEG microgels. Measurements were performed by A. Heilig using a Bruker Digital Instruments Dimension 3100 and a NanoWorld silicon SPM-Sensor with a resonance frequency of 285 kHz and a force constant of 42 N $\cdot$ m^{-1} in tapping mode. A droplet of the microgels suspension was air-dried 72 hours on a mica plate at room tempature before measurements. The volume of dry microgels was calculated from AFM images using the software SPIP 5.1.1 (Image Metrology, Denmark). The water content was calculated as the ratio between the volume of water per particle and the volume of swollen particles $V_{swollen}$. The volume of water was determined as the difference between $V_{swollen}$ and V_{dry}. $V_{swollen}$ was calculated from the diameter of PEG microgels measured from optical microscopy images.

Scanning electron microscopy (SEM) images were obtained with a GEMINI LEO 1550 microscope operating at 3 kV. **Cryo-scanning electron microscopy** (cryo-SEM) images were taken with a JEOL JSM-7500F microscope operating at 2 kV. For cryo-SEM measurements, 3-5 µL of the microgels dispersion were plunged in a liquid nitrogen slush, transferred to a Gatan Alto 2500 Cryotransfer system and cooled to -130 °C. The samples were then freeze-fractured, freeze-etched at -95 °C for 2-3 minutes to make the microgels visible with SEM and were finally sputter coated with 2 nm of platinum at -130 °C.

Transmission electron microscopy (TEM) was carried out by R. Pitschke and H. Runge on a Zeiss EM 912 Omega microscope operating at 120 kV. PEG microgels were first embedded in LR white

resin and samples were solidified in gelatin capsules at 60 °C for at least 2 days. Cross-sections with a thickness of ca. 70 nm were then prepared by ultramicrotomy and deposited on TEM grids coated with a thin layer of carbon, for observation with TEM.

The **electrophoretic mobility** of PEG microgels was measured with a Malvern Zetasizer Nano Z instrument at 25 °C, after several washes with deionized water. The ζ-potential was then calculated by the integrated software using the Smoluchowski equation.

Infrared spectroscopy (IR) was performed in water using a Perkin-Elmer Spectrum 100 instrument with ATR sampling. **Nuclear magnetic resonance spectroscopy** (^{1}H and ^{13}C NMR) was conducted in D_2O using a 400 MHz Varian instrument at 25 °C. **UV-visible spectroscopy** (UV-vis) was carried out on a Varian Cary 50 spectrophotometer.

8.1.3. Experimental procedures

Synthesis of porous PEG microgels:

- <u>Synthesis of 17.6 µm porous PEG microgels (Sample 1)</u>: 50 mg of 17.9 µm CaCO$_3$ templates were dispersed in 2 ml of deionized water in a round bottom flask. Subsequently, 100 µL of a 100 mg.ml^{-1} aqueous solution of PEG-dAAm (PEG-dAAm/CaCO$_3$ = 20 wt.%) and 125 µL of a 4 mg.ml^{-1} aqueous solution of Irgacure 2959 (Irgacure 2959/PEG-dAAm = 5 wt.%) were added. The resulting dispersion was allowed to stay at room temperature for 30 minutes and regularly shaken to promote diffusion of the hydrogel precursors into the templates. Water was removed under vacuum, at 60 °C, on a rotary evaporator and the particles were further dried for 90 minutes at 100 °C. The dry particles were scratched from the flask to recover a fine powder. 10 ml of diethyl ether were then added and the mixture was vigorously stirred for 10 min, at least. Afterwards, the dispersion was treated 2 x 90 s with UV-visible light, using a Heraeus HiLite Power curing unit (300-500 nm, Heraeus Kulzer, Germany) to photopolymerize PEG-dAAm. After polymerization, the suspension was vigorously stirred for 5 minutes to prevent aggregation and the composite particles were washed twice with deionized water to remove PEG that did not react or reacted outside of the templates. The composite particles were subsequently dispersed in 1 ml of deionized water and 70 µL of concentrated HCl were added to reach pH 2.0 and dissolve CaCO$_3$ templates. Finally, the microgels were washed by centrifugal filtration on 0.45 µm pore size filters and redispersed in deionized water.

- <u>Synthesis of 9.2 µm porous PEG microgels (Sample 2)</u>: 31.3 µl of a 4 mg.ml^{-1} aqueous solution of Irgacure 2959 containing 2.5 mg of PEG-dAAm were added to 50 mg of 6.9 µm CaCO$_3$ particles (sample 2) in an 1.5 ml Eppendorf tube (PEG-dAAm/CaCO$_3$ = 5 wt.%, Irgacure 2959/PEG-dAAm = 5 wt.%). Water was removed at 100 mbar and 80 °C, for 90 minutes. The remaining steps were similar to the ones presented above.

- <u>Synthesis of 8.3 µm porous PEG microgels (Sample 3)</u>: 125 µl of a 4 mg.ml^{-1} aqueous solution of Irgacure 2959 containing 10 mg of PEG-dAAm were added to 50 mg of 7.3 µm CaCO$_3$ particles (sample 3) in an 1.5 ml Eppendorf tube (PEG-dAAm/CaCO$_3$ = 20 wt.%, Irgacure 2959/PEG-dAAm = 5 wt.%). Water was removed at 100 mbar and 80 °C, for 90 minutes. The remaining steps were similar to the ones presented above.

Synthesis of non-porous PEG microgels: Non-porous PEG microgels (diameter ~ 10 µm) were synthesized with a protocol adapted from Pussak *et al*.[126] PEG-dAAm (M$_n$ = 4600 g.mol^{-1}) was added to 10 mL of a 0.5 M sodium sulfate solution, at a concentration of 0.5 wt.% and vigorously shaken until a homogenous dispersion was formed. The UV photoinitiator Irgacure 2959 was added at

a concentration of 0.01 wt.% and the dispersion was heated at 70 °C for 1 hr. The dispersion was then photopolymerized for 90 s using a Heraeus HiLite Power curing unit (Heraeus Kulzer, Germany). The resulting microparticles were centrifuged at 5000 rpm for 10 minutes and washed 3 times with water to remove salts. Functionalization of these non-porous PEG microgels into PEG-COOH and PEG-Man was done following the same procedure as for the porous PEG microgels.

Functionalization into porous PEG-COOH microgels: The functionalization of PEG microgels was adapted from the procedure reported by Pussak *et al.*[126] Porous PEG microgels obtained from a batch of 50 mg $CaCO_3$ were washed once with ethanol and redispersed in 10 mL of absolute ethanol containing 250 mg of benzophenone (2.5 wt.%) and 0.5 mL of acrylic acid (5 vol.%). The resulting dispersion was allowed to stay at room temperature for 5 minutes to promote the diffusion of acrylic acid into PEG microgels. Afterwards, the dispersion was flushed with argon for 30 seconds and treated 5 x 90 s with UV-visible light, using a Heraeus HiLite Power curing unit (300-500 nm, Heraeus Kulzer, Germany). The dispersion was flushed again with argon for 20 seconds between each irradiation to avoid inhibition of the radical polymerization with O_2. The microgels were then washed with ethanol by centrifugation and redispersed in 1 mL of deionized water. $10\,\mu L$ of a 1 M aqueous solution of NaOH were added to facilitate the redispersion of PEG-COOH microgels. Finally, the microgels were washed with deionized water by centrifugation.

Functionalization into porous PEG-NH$_2$ (from EDA), PEG-Man, PEG-Gal and PEG-Man/NH$_2$ microgels: PEG-COOH microgels were washed once with DMF and redispersed in 10 mL of DMF containing HOBt (76.6 mg, 0.5 mmol), PyBOP (520 mg, 1 mmol) and triethylamine (TEA, $140\,\mu L$, 1 mmol). The microgels were activated for 1 hour on a shaker and the desired amino-terminated compound was finally added. In the case of PEG-NH$_2$ microgels, EDA ($67\,\mu L$, 1 mmol)) was added. For PEG-Man or PEG-Gal, (2-aminoethyl)-2,3,4,6-tetra-O-acetyl-α-D-mannopyranoside hydrochloride or (2-aminoethyl)-2,3,4,6-tetra-O-acetyl-β-D-galactopyranoside hydrochloride (43 mg, 0.1 mmol) was used.[151] For PEG-Man/NH$_2$, 1 mL of DMF containing (2-aminoethyl)-2,3,4,6-tetra-O-acetyl-α-D-mannopyranoside hydrochloride (21.5 mg, 0.05 mmol), EDA ($3.4\,\mu L$, 0.05 mmol) and TEA ($50\,\mu L$, 0.35 mmol) was mixed with the 10 mL solution. In the last case, TEA was added to deprotonate the hydrochloride salt of mannose prior to the addition to PEG-COOH in order to have similar reactivity to EDA and incorporation of mannose and EDA at approximately equal proportions. The reaction was carried out for 4 hours on a shaker and the microgels were finally washed with ethanol by centrifugation. Afterwards, PEG-NH$_2$ microgels were redispersed in 1 mL of deionized water and $10\,\mu L$ of a 1 M aqueous solution of hydrochloric acid (HCl) were added to facilitate the redispersion of the microgels. For PEG-Man and PEG-Gal microgels, the grafted carbohydrates were

deprotected by dispersing the microgels in sodium methoxide (MeONa) solution in methanol (10 mg.mL^{-1}, 1 mL) for 1 hr, and then the microgels were washed again with ethanol by centrifugation. PEG-Man/NH$_2$ were submitted to the same treatments with deprotection first and then the acidic treatment. Finally, all types of microgels were washed with deionized water by centrifugation redispersed in 1 mL deionized water.

Functionalization into PEG-poly(amines) particles: PEG-COOH particles (3.6 x 10^{-4} mmol COOH, obtained from 50 mg CaCO$_3$) were first washed with dimethylformamide (DMF) and dispersed in 10 mL of DMF containing 76.6 mg of HOBt (1400 equivalents), 520 mg of PyBOP (2800 equivalents) and 140 µL of triethylamine (TEA, 2800 equivalents). The particles were then activated for 1 hour on a shaker. Meanwhile a DMF solution containing the desired poly(amine) at high excess ($\geq$ 500 equivalents of NH$_2$) was prepared. The solvent from the initial poly(amine) solution was first removed under vacuum, the dry amine was dissolved in DMF at 60°C for 5 minutes and excess TEA was added to deprotonate the ammonium salts. For example, 500 µL (500 equivalents) of PAMAM dendrimer (B) solution in methanol were dried and dissolved in 1 ml of DMF. This solution was finally added to the solution of activated PEG-COOH particles and the reaction was carried out for 3 hours on a shaker. Afterwards the functionalized particles were washed with ethanol by centrifugation, redispersed in 1 mL of water and mixed on a vortex for 5 minutes after addition of 40 µL of a 1 M aqueous solution of HCl to facilitate their redispersion. Finally, the particles were washed once more with deionized water by centrifugation.

Labeling and quantification of the functional groups on PEG microgels:

- The presence of <u>carboxyl groups</u> on PEG microgels was evidenced by CLSM after labeling with the cationic dye Rhodamine 6G.[144, 145] For this, 10 mg of Rhodamine 6G were dissolved in 10 mL of a phosphate buffer (PBS, pH 11) and extracted twice with 100 mL of toluene. 50 µL of this solution were then added to PEG-COOH particles redispersed in 1 mL of DMF and PEG microgels were incubated 1 hour in the dark. The labeled microgels were then washed with water and CLSM images were taken within one hour after samples preparation.

Carboxyl groups were titrated with the toluidine blue O (TBO) dye adsorption assay.[146] The microgels were dispersed in an aqueous solution of 5x10^{-4} mol.L^{-1} TBO adjusted to pH 10 with NaOH and incubated for 5 hours at room temperature. The microgels were then rinsed five times with NaOH solution (pH 10) to remove the non-complexed TBO molecules and centrifuged. Desorption of the dye was performed in 50 wt % acetic acid solution. The concentration of released TBO was measured from the adsorption at 633 nm and the amount of COOH groups was calculated with the assumption that

1 mol of TBO had complexed with 1 mol of carboxylates. An equivalent sample was dried under vacuum and its dry mass was measured to calculate the mass concentration of COOH groups.

- The presence of <u>amine groups</u> on PEG microgels was evidenced by CLSM after labeling with FITC. For labeling amines on PEG microgels were first deprotonated by addition of 20 µL of a 1 M aqueous solution of NaOH. The microgels were then isolated by centrifugation and redispersed in 1 mL of a 0.1 mg.mL^{-1} solution of FITC in phosphate buffer (Na$_2$HPO$_4$, 10 mM, pH 10). PEG microgels were then incubated for 2 hours in the dark and washed with deionized water by centrifugation before measurements.

The concentration of primary amines on PEG particles was determined by titration with 2,4,6-trinitrobenzenesulfonic acid (TNBS).[48, 176] The amines were first deprotonated by adding 10 µL of a 1 M aqueous solution of NaOH into a 500 µL aqueous suspension of particles. The particles were then washed by centrifugation, redispersed in 1 mL of deionized water and added to 5 mL of 0.2 mM solution of TNBS in borate buffer (0.1 M, pH 9.3). The particles were incubated for 2 hours, in the dark, at 37 °C. After incubation the absorption of the supernatant was measured at 350 nm and compared to the one of a control solution where pure water was incubated instead of particles. The concentration of primary amines on PEG particles was determined from the amount of reacted TNBS, resulting from the difference in absorption between the control and the sample. An equivalent sample was dried under vacuum and its dry mass measured to calculate the mass concentration of NH$_2$ groups.

- The presence of <u>mannose groups</u> on PEG microgels and their ability to bind to mannose-binding protein receptors was evidenced by CLSM with FITC-labeled Concanavalin A (FITC-ConA). For this, a buffer containing 50 mM NaCl, 1 mM MnCl$_2$, 1 mM CaCl$_2$ and 10 mM HEPES (pH 7.4) was first prepared. 20 µL of this buffer were deposited on a glass slide, then 20 µL of a solution of PEG microgels and 5 µL of a 5 mg.mL^{-1} aqueous solution of FITC-ConA were added. CLSM images were taken within one hour after samples preparation. For the experiments on the release of FITC-ConA, PEG-Man microgels were mixed with FITC-ConA as described above and incubated for 15 minutes. Then 20 µL of a solution of methyl α-D-mannopyranoside of 2 M were added. CLSM images were taken within 1 hour after samples preparation.

- The presence of <u>carbamate groups</u> on PEG microgels was evidenced by CLSM after labeling with the cationic dye Rhodamine 6G.[144, 145] An aliquot of particles was redispersed in 100 µL of a 10 mM phosphate buffer at pH 9. 20 µL of this suspension were deposited on a glass slide and 3 µL of a 0.1 mg.mL^{-1} solution of Rhodamine 6G in a 10 mM phosphate buffer at pH 9 were added for measurements.

Loading of citrate-coated iron oxide NPs into PEG-NH$_2$ or PEG-Man/NH$_2$ microgels: PEG microgels were redispersed in 1 mL of deionized water in a 2 mL glass vial. Then 1 mL of either a 0.2 mg.mL^{-1} or a 2 mg.mL^{-1} aqueous solution of citrate-coated iron oxide NPs (8-15 nm) was added. The dispersion was shaken and then incubated for 1 hour at room temperature. Afterwards, the magnetic microgels were collected with a supermagnet (NdFeB, 30x30x10mm, BR Technik Kontor GmbH) over 2 min, the supernatant was removed and the microgels were redispersed in 1 mL of deionized water. The mass concentration of unbound NPs in the supernatant was measured by UV-visible spectroscopy using a calibration curve and compared to the initial concentration to determine the mass of NPs which effectively bound to PEG microgels. By dividing this mass to the total dry mass of PEG microgels, the mass fraction of NPs and therefore the loading could be estimated.

Bacterial growth: The strains of bacteria *E. coli* ORN178 (mannose binding strain) and ORN208 (mutant strain which does not bind mannose) were kindly donated by Prof. Orndorff (College of Veterinary Medicine, Raleigh, NC United States). Cells were grown in the nutritionally rich LB (Luria-Bertani) medium. The inoculated culture was incubated overnight at 37 °C by shaking on an incubator shaker at 220 rpm. Aliquots of bacteria were removed from the batch culture to monitor growth until they reached an optical density at 600 nm of 1.0 (OD600, 8x10^8 cells$^.$mL^{-1}). Aliquots of cultures were then centrifuged for 10 minutes at 1600g. The resulting pellets were then washed twice with PBS buffer and resuspended in PBS. The final concentration of bacteria was measured again via the optical density at 600 nm and the solutions of bacteria were diluted to the desired concentrations.

Binding of bacteria on PEG-Man and PEG-Man/NH$_2$ microgels with and without NPs: 100 µL of PEG microgels functionalized with mannose moieties in PBS buffer were added to 100 µL of solutions of bacteria *E. coli* ORN178 in PBS buffer at the concentration of 8x10^8 cells$^.$mL^{-1} (OD600=1.0). The suspension was incubated for 60 min, at room temperature, with gentle shaking. As a control, pure PEG, PEG-COOH, PEG-NH$_2$, PEG-Gal and non-porous PEG-Man were also incubated with bacteria ORN178, while PEG-Man was incubated with the strain ORN208. After incubation, the suspension was centrifuged and washed three times with PBS buffer. The bacteria were then fixed with 100 µL of a 4% (w/v) solution of paraformaldehyde for 15 minutes. The suspension was then centrifuged and the resulting pellet was resuspended in 100 µL of PBS buffer containing the organic dye 4',6-diamidino-2-phenylindole dihydrochloride (DAPI) at dilution of 1/300 and incubated for 15 minutes. The suspension was then centrifuged, washed twice with PBS and resuspended in 100 µL PBS for observation by confocal microscopy.

For binding in protein-rich media, incubations were performed under the same conditions but in PBS or DMEM (Dulbecco's Modified Eagle Medium) solutions containing 1 wt% of the protein BSA (bovine serum albumin) instead of pure PBS. Subsequent washes were performed in pure PBS buffer, bacteria were fixed with paraformaldehyde and labeled with DAPI following the same procedure as mentioned above.

Binding of PEG-Man in a mixture of *E. coli* bacteria strain ORN178 and ORN208: Bacteria ORN178 were first labeled with the organic dye SYBR® Green I in PBS buffer at dilution of 1/5000, while bacteria ORN208 were labeled with acridine orange in PBS buffer at dilution 1/6500 for 15 minutes. Both bacteria strains were then centrifuged, washed twice with PBS buffer, diluted to the concentration of $8x10^8$ cells$\cdot$mL^{-1} (OD600=1.0) and then mixed in equal proportion. 200 µL of this mixture were then added to 200 µL of PEG-Man microgels in PBS buffer. The suspension was incubated for 60 min, at room temperature, with gentle shaking. After incubation, the suspension was centrifuged and washed three times with PBS buffer. The bacteria were then fixed with 100 µL of a 4% (w/v) solution of paraformaldehyde for 15 minutes. The suspension was then washed twice with PBS and resuspended in 100 µL PBS for observation by confocal microscopy.

As a control pure solutions of labeled ORN178 and ORN208 were also observed by confocal microscopy. We found out that at an excitation wavelength of 488 nm, bacteria ORN 178 labeled with SYBR® were not fluorescent in the emission range of 500 to 520 nm but in the range 500 – 600 nm while bacteria ORN 208 labeled with acridine orange were always fluorescent on both ranges. Therefore fluorescence in the range 500 - 520 nm was used to differentiate both bacteria strains.

Isolation of bacteria with MaPoS particles: 500 µL of PEG microgels were added to 500 µL of solutions of bacteria at the desired concentration and the suspension was incubated for 1 hr, at room temperature, with gentle shaking. For the negative control, 500 µL of PBS buffer instead of PEG microgels were added to the solutions of bacteria. PEG microgels were then isolated with the help of a magnet. After 2 min, the supernatant was removed with a pipette and reduced to 500 µL after centrifugation. The bacteria were then fixed with 500 µL of a 4% (w/v) solution of paraformaldehyde at room temperature for 1 hr, centrifuged and redispersed in 500 µL of PBS buffer. The number of remaining bacteria was then measured by flow cytometry using a FACSCantoTM II flow cytometer (Becton Dickinson, Germany). The obtained data were analyzed with the FlowJo software (Tree Star, Inc.). The difference in the amount of bacteria in the sample and the control gave the amount of bacteria which attached to PEG microgels. The yield of isolation was calculated as the ratio between the amount of attached bacteria and that in the control sample.

Ammonium-carbamate functionalization in solution:

- <u>NMR study</u>: 10 mg of poly(amine) were dissolved in 1 mL of D_2O containing K_2CO_3 at a ratio of at least 2 carbonate ions per amine, and KOH at a ratio of one hydroxide ion per amine. Gaseous CO_2 was then bubbled through a syringe into the solution for 1 min, which decreased pH to 7.4. Afterwards a 2 M K_2CO_3 solution in D_2O was added dropwise until pH 10 was reached, then a 5 M KOH solution in D_2O was added dropwise to reach pH 12, and the same KOH solution was finally added dropwise till pH 14. Before each new addition, the solution was allowed to rest for 5 minutes. ^{1}H and ^{13}C NMR were measured after pH was adjusted to 14 in order to be able to differentiate peaks. The intensities of the signals attributed to **CH₂**-NHCOO⁻ and **CH₂**-NH₂ were integrated and the yield of carbamation was calculated as the ratio between the integration for carbamates and the sum of integrations for carbamates and amines.

- <u>IR study</u>: Similar conditions have been used but at higher concentrations (*e.g.* 50 mg.mL⁻¹ of poly(amine)) and in water instead of D_2O.

Functionalization into PEG-ammonium-carbamate microgels: porous PEG-PAMAM microgels were dispersed in 1 mL of water at pH 12, containing 0.1 M of K_2CO_3 and 0.1 M of KOH. Gaseous CO_2 was then bubbled through a syringe into the solution for 1 minute. Afterwards 150 µL of a 2 M K_2CO_3 aqueous solution, 100 µL of a 5 M KOH aqueous solution and 50 µL of the same KOH solution were dropwise added to reach pH 14. Before each new addition, the solution was allowed to rest for 5 minutes. The obtained particles were eventually washed 3 times in deionized water by centrifugation at low speed. These particles sometimes showed tendency to aggregate when transferred to pure water, most probably due to the ammonium-carbamates moieties making the particles almost neutral. However, it was possible to easily redisperse them in phosphate buffered saline (PBS buffer).

Loading of Toluidine Blue O (cationic dye) into PEG-ammonium-carbamate microgels: PEG-ammonium-carbamate particles were redispersed in 500 µL of a 5 x 10⁻⁴ M aqueous solution of TBO adjusted to pH 10.0 with 1 M NaOH beforehand. The loading was allowed to proceed 2 hours, at room temperature, on a shaker. Afterwards the particles were rinsed 5 times with an aqueous solution of NaOH at pH 10, by centrifugation at low speed, to remove the non-complexed TBO molecules. In the final wash, the particles were kept 30 minutes in the rinsing buffer prior to centrifugation. As a control to prove that loading was due to the carbamate moieties, PEG-PAMAM particles which were not treated with CO_2 were also loaded with TBO. Since it was observed that the initial pH had an influence on the loading, PEG-PAMAM particles were first treated with a 0.1 M aqueous solution of KOH at pH 14 for 10 minutes and washed three times with deionized water. The particles were afterward incubated with TBO under the same conditions as mentioned above.

The concentration of loaded dye was directly measured by UV-visible spectroscopy, from the difference in the absorption of TBO solutions before and after loading. Absorptions were measured at 635 nm after 1/20 dilution in a 50 wt.% acetic acid solution. This value was confirmed by the absorption of the solution obtained by complete desorption of the loaded dye in a 50 wt.% acetic acid solution. An equivalent sample was dried under vacuum and its dry mass measured to calculate the mass concentration of loaded TBO. This concentration could be correlated to the concentration of anionic groups (*e.g.* carboxylates and carbamates) assuming that TBO complexes anionic groups in a 1/1 stoichiometry.[146]

Release of Toluidine Blue O from PEG-ammonium-carbamate microgels: Release was performed at pH 7.4 in PBS buffer, pH 5.0 in a 0.1 M acetate buffer as well as pH 3.0 in a 0.1 M acetate buffer and measured after 2 min, 5 min, 10 min, 30 minutes and 60 minutes. 1 mL of buffer was each time added to the loaded PEG particles and the suspension was shortly shaken. After due time, the particles were centrifuged at low speed, the supernatant was removed, 1/3 diluted in a 50 wt.% acetic acid solution and its absorption was measured at 635 nm by UV-visible spectroscopy. 1 mL of fresh buffer was then immediately added to pursue the release study. It was however observed that each new addition of buffer artificially induced release of the dye, regardless of incubation time. This error was estimated from the release at 62 minutes since release was so slow after 60 minutes that there should be no dye released between 60 minutes and 62 minutes. Therefore the observed release at 62 minutes could be mainly attributed to the addition of buffer. Measured concentrations were consequently corrected by subtracting the concentration measured at 62 minutes (except for the initial one, after 2 minutes release). To quantify release in percentage, concentrations were then added over time and divided by the total concentration of released dye obtained after complete desorption in a 50 wt % acetic acid solution (see above). As a control, loading and release from PEG-COOH particles were performed under the same conditions.

Loading of Methyl Orange (anionic dye) into PEG-ammonium-carbamate microgels: PEG-ammonium-carbamate particles were first washed in 0.1 M acetate buffer at pH 5 for 5 min, then washed with deionized water and redispersed in 500 µL of a 3×10^{-3} M aqueous solution of MO adjusted to pH 5.0 with 1 M HCl beforehand. The loading was allowed to proceed 2 hours, at room temperature, on a shaker. Afterwards the particles were rinsed 5 times with an aqueous solution of HCl at pH 5, by centrifugation at low speed, to remove the non-complexed MO molecules. In the final wash, the particles were kept 30 minutes in the rinsing buffer prior to centrifugation. As a control to prove that loading was due to the ammonium moieties, unfunctionalized PEG and PEG-PAMAM particles were also loaded with MO under the same conditions as mentioned above.

The concentration of loaded dye was directly measured by UV-visible spectroscopy, from the difference in the absorption of MO solutions before and after loading. Absorptions were measured at 450 nm after 1/100 dilution in a 0.1 M phosphate buffer at pH 10. This value was confirmed by the absorption of the solution obtained by complete desorption of the loaded dye in 0.1 M phosphate buffer at pH 10. An equivalent sample was dried under vacuum and its dry mass measured to calculate the mass concentration of loaded dye.

Release of Methyl Orange from PEG-ammonium-carbamate microgels: Release was performed at pH 7.4 in PBS buffer as well as pH 6.0 in a 0.1 M acetate buffer, following the same protocol as for the release of TBO. Absorptions of release solutions were measured at 450 nm after 1/3 dilution in a 0.1 M phosphate buffer at pH 10. As a control, loading and release from PEG-PAMAM particles that were not treated with CO_2 were performed under the same conditions.

8.2. Analysis and Spectra
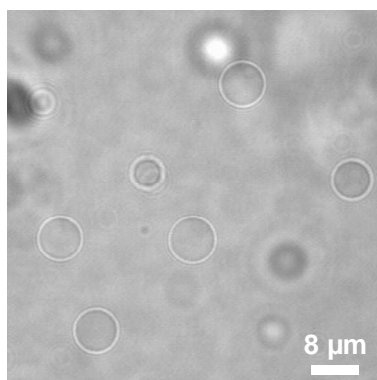
Figure 8.1. *Optical microscopy image of non-porous PEG microgels of ~ 10 µm.*
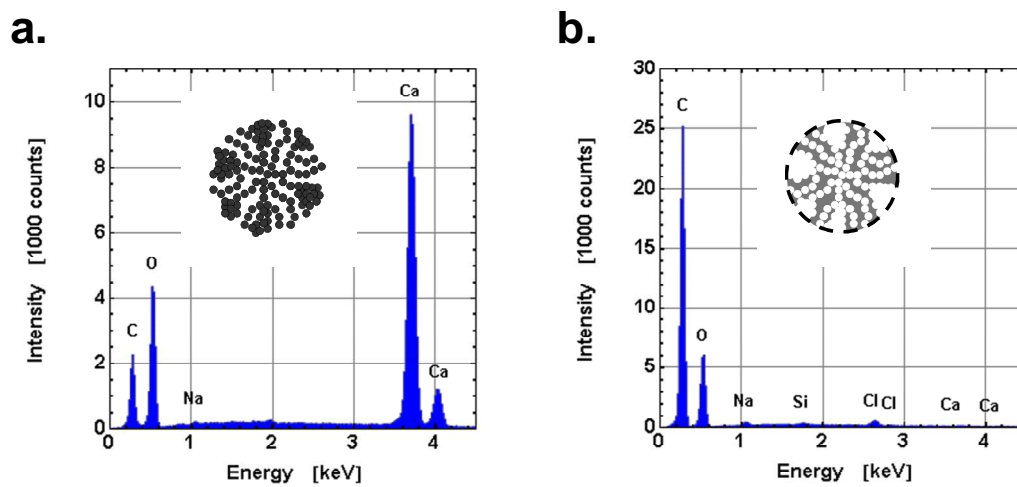
Figure 8.2. *Energy-dispersive X-ray spectra (EDS) of a. pure CaCO₃ microparticles of 17.9 µm (sample 1) and b. resulting pure porous PEG microgels of 17.6 µm after washes (sample 1).*
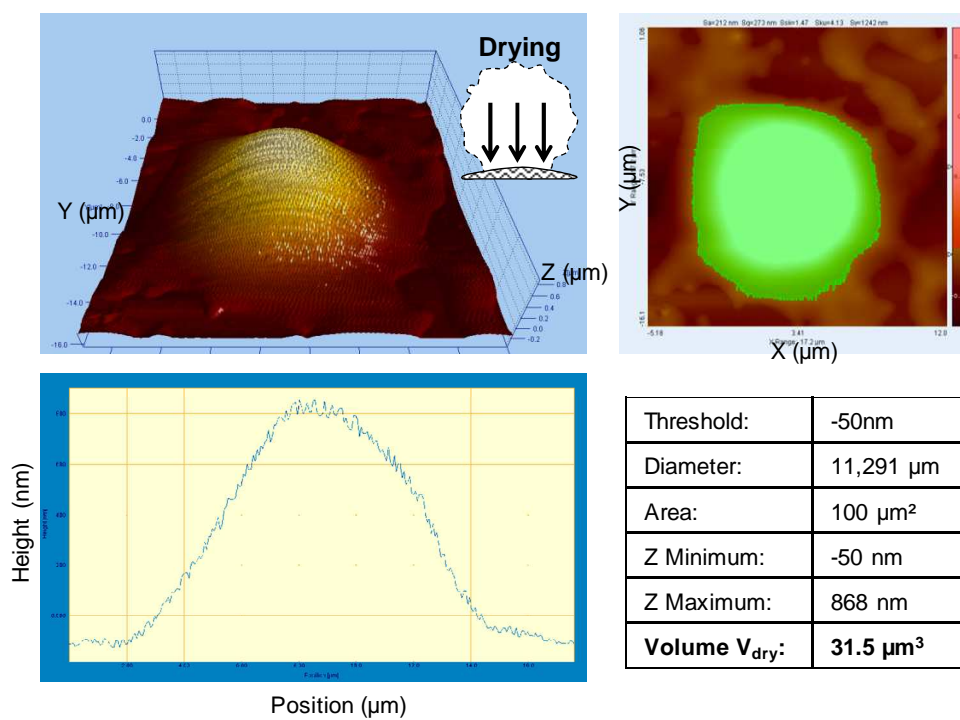
Figure 8.3. AFM images and analysis of a porous PEG microgel of 17.6 µm after drying (sample 1). The volume of the dry particle V_{dry} was determined by using the software SPIP 5.1.1. The average volume V_{dry} was calculated over three particles and estimated to be 27 µm^3.

Figure 8.4. TEM image of the Fe_3O_4@citrate NPs used to prepare magnetic porous PEG microgels.

Figure 8.5. *Calibration curve of the absorbance of the solution of iron oxide NPs in function of its concentration (UV-vis spectroscopy).*

List of Abbreviations

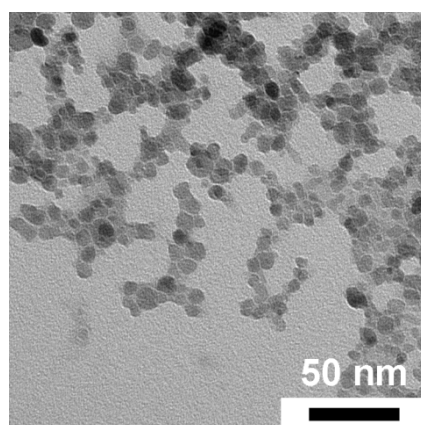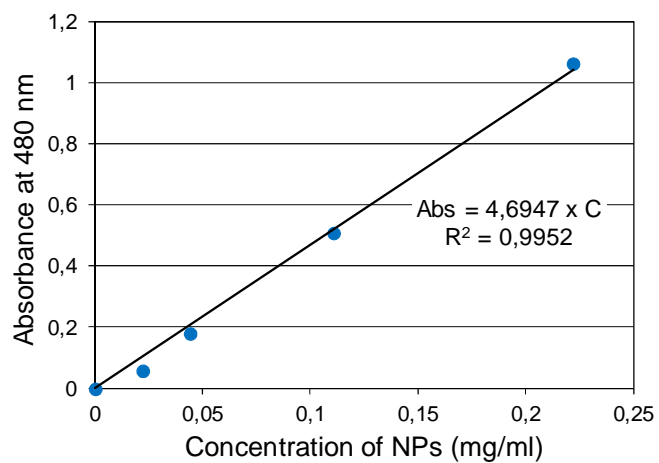|	
AA	Acrylic Acid
AEMA	2-Aminoethyl Methacrylate
AFM	Atomic Force Microscopy
BET	Brunauer-Emmett-Teller (model)
BSA	Bovine Serum Albumin
CLSM	Confocal Laser Scanning Microscopy
ConA	Concanavalin A
Cryo	Cryogenic
DAPI	4',6-Diamidino-2-Phenylindole Dihydrochloride
DMEM	Dulbecco's Modified Eagle Medium
DMF	N,N-Dimethylformamide
DNA	Deoxyribonucleic Acid
E. coli	Escherichia Coli
EDTA	Ethylenediaminetetraacetic Acid
Et_2O	Diethyl Ether
EDA	Ethylenediamine
EDS	Energy-Dispersive X-Ray Spectroscopy
FDA	Food and Drug Administration
FITC	Fluorescein Isothiocyanate
FTIR	Fourier Transform Infrared
Gal	Galactose
HOBt	1-Hydroxybenzotriazole
IPN	Interpenetrated Network
LbL	Layer-by-Layer
Man	Mannose
MaPoS	Magnetic, Porous, Sugar-functionalized
Me-Man	Methyl α-D-mannopyranoside
M_n	Number Average Molecular Weight
M_w	Weight Average Molecular Weight
MO	Methyl Orange
NMR	Nuclear Magnetic Resonance
NPs	Nanoparticles
OAMAM	Oligo(amidoamine)
OD	Optical Density
PAA	Poly(acrylic Acid)
PAH	Poly(allylamine) (Hydrochloride)
PAMAM	Poly(amidoamine)
PBS	Phosphate Buffer Saline
PEG	Poly(ethylene glycol)
PEG-dAA	Poly(ethylene Glycol)-Diacrylate
PEG-dAAm	Poly(ethylene Glycol)-Diacrylamide
PEG-dmAA	Poly(ethylene Glycol)-Dimethacrylate
PEO	Poly(ethylene Oxide)
PLGA	Poly(lactic-co-glycolic Acid)
PLL	Poly(L-lysine)
PNIPAAm	Poly(N-isopropylacrylamide)
PyBOP	Benzotriazole-1-yl-Oxy-tris-Pyrrolidinophosphonium Hexafluorophosphate

RNA	Ribonucleic Acid
SAXS	Small-Angle X-Ray Scattering
SEC	Size Exclusion Chromatography
SEM	Scanning Electron Microscopy
TBO	Toluidine Blue O
TEA	Triethylamine
TEM	Transmission Electron Microscopy
THF	Tetrahydrofuran
TNBS	2,4,6-Trinitrobenzenesulfonic Acid
UV	Ultraviolet
V_{dry}	Volume in the Dry State
$V_{swollen}$	Volume in the Swollen State

References

[1]   T. Sugimoto, "*Monodispersed Particles*", Elsevier Science B.V., Amsterdam, 2001, p. 792.
[2]   B. R. Saunders, B. Vincent, *Adv. Colloid Interface Sci.* **1999**, *80*, 1.
[3]   M. Das, H. Zhang, E. Kumacheva, "Microgels: Old materials with new applications", in *Ann. Rev. Mater. Res.*, Annual Reviews, Palo Alto, 2006, p. 117.
[4]   D. H. Napper, "*Polymeric Stabilization of Colloidal Dispersions*", Academic Press, 1983.
[5]   H. Kawaguchi, *Progress in Polymer Science* **2000**, *25*, 1171.
[6]   C. D. Jones, L. A. Lyon, *Macromolecules* **2000**, *33*, 8301.
[7]   D. Suzuki, S. Tsuji, H. Kawaguchi, *J. Am. Chem. Soc.* **2007**, *129*, 8088.
[8]   P. Bouillot, B. Vincent, *Colloid Polym. Sci.* **2000**, *278*, 74.
[9]   J. B. Thorne, G. J. Vine, M. J. Snowden, *Colloid Polym. Sci.* **2011**, *289*, 625.
[10]   M. J. Murray, M. J. Snowden, *Adv. Colloid Interface Sci.* **1995**, *54*, 73.
[11]   Cuatreca.P, *J. Biol. Chem.* **1970**, *245*, 3059.
[12]   J. S. Fruchtel, G. Jung, *Angew. Chem.-Int. Edit. Engl.* **1996**, *35*, 17.
[13]   S. Nayak, L. A. Lyon, *Angew. Chem.-Int. Edit.* **2005**, *44*, 7686.
[14]   B. R. Saunders, N. Laajam, E. Daly, S. Teow, X. H. Hu, R. Stepto, *Adv. Colloid Interface Sci.* **2009**, *147-48*, 251.
[15]   J. K. Oh, R. Drumright, D. J. Siegwart, K. Matyjaszewski, *Progress in Polymer Science* **2008**, *33*, 448.
[16]   M. Kumar, *J. Pharm. Pharm. Sci.* **2000**, *3*, 234.
[17]   C. Ramkissoon-Ganorkar, F. Liu, M. Baudys, S. W. Kim, *J. Control. Release* **1999**, *59*, 287.
[18]   V. C. Lopez, J. Hadgraft, M. J. Snowden, *Int. J. Pharm.* **2005**, *292*, 137.
[19]   S. Freiberg, X. Zhu, *Int. J. Pharm.* **2004**, *282*, 1.
[20]   H. Staudinger, E. Husemann, *Berichte Der Deutschen Chemischen Gesellschaft* **1935**, *68*, 1618.
[21]   A. Elaissari, "*Colloidal polymers: synthesis and characterization*", CRC, 2003.
[22]   J. M. Asua, "*Polymeric Dispersions: Principles and Applications*", 1997, p. 565.
[23]   E. Kissa, "*Dispersions : characterization, testing, and measurement*", M. Dekker, New York, 1999.
[24]   J. P. Sibilia, "*A Guide to Materials Characterization and Chemical Analysis*", VCH Publishers, Inc, 1996, p. 388.
[25]   M. J. Dykstra, "*Biological Electron Microscopy: Theory, Techniques, and Troubleshooting*", Plenum Press, New York, 1992.
[26]   Y. Cai, Y. Chen, X. Hong, Z. Liu, W. Yuan, *International journal of Nanomedicine* **2013**, *8*, 1111.
[27]   Q. Li, M. Retsch, J. J. Wang, W. G. Knoll, U. Jonas, "Porous Networks Through Colloidal Templates", in *Templates in Chemistry Iii*, P. Broekmann, K.H. Dotz, and C.A. Schalley, Eds., Springer-Verlag Berlin, Berlin, 2009, p. 135.
[28]   M. T. Gokmen, F. E. Du Prez, *Progress in Polymer Science* **2012**, *37*, 365.
[29]   Q.-H. Shi, X. Zhou, Y. Sun, *Biotechnol. Bioeng.* **2005**, *92*, 643.
[30]   P. J. Dowding, B. Vincent, *Colloid Surf. A-Physicochem. Eng. Asp.* **2000**, *161*, 259.
[31]   A. Guyot, M. Bartholin, *Progress in Polymer Science* **1982**, *8*, 277.
[32]   H. P. Hentze, M. Antonietti, *Curr. Opin. Solid State Mat. Sci.* **2001**, *5*, 343.
[33]   A. Thomas, F. Goettmann, M. Antonietti, *Chem. Mat.* **2008**, *20*, 738.
[34]   N. R. Cameron, *Polymer* **2005**, *46*, 1439.
[35]   J. Texter, *Colloid Polym. Sci.* **2009**, *287*, 313.
[36]   H. P. Hentze, E. W. Kaler, *Curr. Opin. Colloid Interface Sci.* **2003**, *8*, 164.
[37]   S. D. Kimmins, N. R. Cameron, *Adv. Funct. Mater.* **2011**, *21*, 211.
[38]   J. M. Harris, "*Poly(ethylene Glycol) Chemistry: Biotechnical and Biomedical Applications*", 1992, p. 412.
[39]   Y. C. Bae, S. M. Lambert, D. S. Soane, J. M. Prausnitz, *Macromolecules* **1991**, *24*, 4403.
[40]   K. Knop, R. Hoogenboom, D. Fischer, U. S. Schubert, *Angew. Chem.-Int. Edit.* **2010**, *49*, 6288.
[41]   U. Wattendorf, H. P. Merkle, *J. Pharm. Sci.* **2008**, *97*, 4655.

[42]   J. M. Harris, R. B. Chess, *Nat. Rev. Drug Discov.* **2003**, *2*, 214.

[43]   R. Haag, F. Kratz, *Angew. Chem.-Int. Edit.* **2006**, *45*, 1198.

[44]   L. Hartmann, K. Watanabe, L. L. Zheng, C. Y. Kim, S. E. Beck, P. Huie, J. Noolandi, J. R. Cochran, C. N. Ta, C. W. Frank, *J. Biomed. Mater. Res. Part B* **2011**, *98B*, 8.

[45]   D. L. Elbert, J. A. Hubbell, *Biomacromolecules* **2001**, *2*, 430.

[46]   M. D. Nichols, E. A. Scott, D. L. Elbert, *Biomaterials* **2009**, *30*, 5283.

[47]   M. M. Flake, P. K. Nguyen, R. A. Scott, L. R. Vandiver, R. K. Willits, D. L. Elbert, *Biomacromolecules* **2011**, *12*, 844.

[48]   D. Pussak, M. Behra, S. Schmidt, L. Hartmann, *Soft Matter* **2012**.

[49]   D. A. Hammer, D. E. Discher, *Ann. Rev. Mater. Res.* **2001**, *31*, 387.

[50]   A. O. Eniola, D. A. Hammer, *J. Control. Release* **2003**, *87*, 15.

[51]   B. I. Haukanes, C. Kvam, *Bio-Technology* **1993**, *11*, 60.

[52]   O. Olsvik, T. Popovic, E. Skjerve, K. S. Cudjoe, E. Hornes, J. Ugelstad, M. Uhlen, *Clin. Microbiol. Rev.* **1994**, *7*, 43.

[53]   I. Safarik, M. Safarikova, S. J. Forsythe, *Journal of Applied Bacteriology* **1995**, *78*, 575.

[54]   A. A. Neurauter, M. Bonyhadi, E. Lien, L. Nokleby, E. Ruud, S. Camacho, T. Aarvak, "Cell isolation and expansion using Dynabeads((R))", in *Cell Separation: Fundamentals, Analytical and Preparative Methods*, A. Kumar, I.Y. Galaev, and B. Mattiasson, Eds., Springer-Verlag Berlin, Berlin, 2007, p. 41.

[55]   T. J. Freemont, B. R. Saunders, *Soft Matter* **2008**, *4*, 919.

[56]   O. Philippova, A. Barabanova, V. Molchanov, A. Khokhlov, *Eur. Polym. J.* **2011**, *47*, 542.

[57]   J. Ugelstad, A. Berge, T. Ellingsen, R. Schmid, T. N. Nilsen, P. C. Mork, P. Stenstad, E. Hornes, O. Olsvik, *Progress in Polymer Science* **1992**, *17*, 87.

[58]   V. Lund, R. Schmid, D. Rickwood, E. Hornes, *Nucleic Acids Res.* **1988**, *16*, 10861.

[59]   G. B. Karlsson, F. M. Platt, *Analytical Biochemistry* **1991**, *199*, 219.

[60]   K. S. Cudjoe, R. Krona, *Int. J. Food Microbiol.* **1997**, *37*, 55.

[61]   J. Krizova, A. Spanova, B. Rittich, D. Horak, *J. Chromatogr. A* **2005**, *1064*, 247.

[62]   D. Horak, N. Benedyk, *J. Polym. Sci. Pol. Chem.* **2004**, *42*, 5827.

[63]   Y. Wu, J. Guo, W. L. Yang, C. C. Wang, S. K. Fu, *Polymer* **2006**, *47*, 5287.

[64]   A. Khan, *Mater. Lett.* **2008**, *62*, 898.

[65]   R. Langer, *Nature* **1998**, *392*, 5.

[66]   R. Langer, *Science* **1990**, *249*, 1527.

[67]   A. V. Kabanov, S. V. Vinogradov, *Angew. Chem.-Int. Edit.* **2009**, *48*, 5418.

[68]   A. S. Huffman, A. Afrassiabi, L. C. Dong, *J. Control. Release* **1986**, *4*, 213.

[69]   H. Tanii, K. Hashimoto, *Toxicol. Lett.* **1991**, *58*, 209.

[70]   I. Vyas, H. E. Lowndes, R. D. Howland, *Neurotoxicology* **1985**, *6*, 123.

[71]   R. C. Mundargi, V. R. Babu, V. Rangaswamy, P. Patel, T. M. Aminabhavi, *J. Control. Release* **2008**, *125*, 193.

[72]   S. Cohen, T. Yoshioka, M. Lucarelli, L. H. Hwang, R. Langer, *Pharm. Res.* **1991**, *8*, 713.

[73]   D. A. Edwards, J. Hanes, G. Caponetti, J. Hrkach, A. BenJebria, M. L. Eskew, J. Mintzes, D. Deaver, N. Lotan, R. Langer, *Science* **1997**, *276*, 1868.

[74]   K. R. West, S. Otto, *Current Drug Discovery Technologies* **2005**, *2*, 123.

[75]   K. Raemdonck, J. Demeester, S. De Smedt, *Soft Matter* **2009**, *5*, 707.

[76]   W. T. Godbey, K. K. Wu, A. G. Mikos, *J. Control. Release* **1999**, *60*, 149.

[77]   "Bacteria", in *Encyclopædia Britannica. Encyclopædia Britannica Online Academic Edition.*, Encyclopædia Britannica Inc., 2013.

[78]   M. Vaara, *Microbiol. Rev.* **1992**, *56*, 395.

[79]   N. Sharon, *FEBS Lett.* **1987**, *217*, 145.

[80]   W. I. Weis, K. Drickamer, *Annu. Rev. Biochem.* **1996**, *65*, 441.

[81]   E. H. Beachey, *J. Infect. Dis.* **1981**, *143*, 325.

[82]   L. L. McKay, K. A. Baldwin, *Fems Microbiol. Rev.* **1990**, *87*, 3.

[83]   M. Schallmey, A. Singh, O. P. Ward, *Can. J. Microbiol.* **2004**, *50*, 1.

[84]   F. Baneyx, *Curr. Opin. Biotechnol.* **1999**, *10*, 411.

[85]   K. E. Jones, N. G. Patel, M. A. Levy, A. Storeygard, D. Balk, J. L. Gittleman, P. Daszak, *Nature* **2008**, *451*, 990.

[86]   P. C. Ray, S. A. Khan, A. K. Singh, D. Senapati, Z. Fan, *Chem. Soc. Rev.* **2012**, *41*, 3193.

[87]   S. B. Levy, B. Marshall, *Nat. Med.* **2004**, *10*, S122.

[88]   H. Nikaido, "Multidrug Resistance in Bacteria", in *Annu. Rev. Biochem.*, Annual Reviews, Palo Alto, 2009, p. 119.

[89]   E. J. Threlfall, L. R. Ward, J. A. Frost, C. A. Willshaw, *Int. J. Food Microbiol.* **2000**, *62*, 1.

[90]   P. S. Stewart, J. W. Costerton, *Lancet* **2001**, *358*, 135.

[91]   Benvenis.R, J. Davies, *Annu. Rev. Biochem.* **1973**, *42*, 471.

[92]   J. E. Hobbie, R. J. Daley, S. Jasper, *Appl. Environ. Microbiol.* **1977**, *33*, 1225.

[93]   P. Jain, T. Pradeep, *Biotechnol. Bioeng.* **2005**, *90*, 59.

[94]   G. Salvatorelli, S. Medici, G. Finzi, S. De Lorenzi, C. Quarti, *J. Hosp. Infect.* **2005**, *61*, 270.

[95]   U. Palmgren, G. Strom, G. Blomquist, P. Malmberg, *Journal of Applied Bacteriology* **1986**, *61*, 401.

[96]   K. A. Krogfelt, *Reviews of Infectious Diseases* **1991**, *13*, 721.

[97]   H. Connell, W. Agace, P. Klemm, M. Schembri, S. Marild, C. Svanborg, *Proc. Natl. Acad. Sci. U. S. A.* **1996**, *93*, 9827.

[98]   E. V. Sokurenko, V. Chesnokova, R. J. Doyle, D. L. Hasty, *J. Biol. Chem.* **1997**, *272*, 17880.

[99]   R. Bentley, R. Meganathan, *Microbiol. Rev.* **1982**, *46*, 241.

[100]   "Escherichia coli", http://en.wikipedia.org/wiki/Escherichia_coli, 2013.

[101]   J. P. Nataro, J. B. Kaper, *Clin. Microbiol. Rev.* **1998**, *11*, 142.

[102]   P. M. Griffin, R. V. Tauxe, *Epidemiol. Rev.* **1991**, *13*, 60.

[103]   D. J. Wright, P. A. Chapman, C. A. Siddons, *Epidemiol. Infect.* **1994**, *113*, 31.

[104]   R. E. W. Hancock, R. Lehrer, *Trends Biotechnol.* **1998**, *16*, 82.

[105]   N. V. Kulagina, K. M. Shaffer, G. P. Anderson, F. S. Ligler, C. R. Taitt, *Anal. Chim. Acta* **2006**, *575*, 9.

[106]   B. Swaminathan, P. Feng, *Annu. Rev. Microbiol.* **1994**, *48*, 401.

[107]   P. P. Banada, A. K. Bhunia, "Antibodies and Immunoassays for Detection of Bacterial Pathogens. Principles of Bacterial Detection: Biosensors, Recognition Receptors and Microsystems", M. Zourob, S. Elwary, and A. Turner, Eds., Springer New York, 2008, p. 567.

[108]   S. S. Iqbal, M. W. Mayo, J. G. Bruno, B. V. Bronk, C. A. Batt, J. P. Chambers, *Biosens. Bioelectron.* **2000**, *15*, 549.

[109]   M. D. Disney, J. Zheng, T. M. Swager, P. H. Seeberger, *J. Am. Chem. Soc.* **2004**, *126*, 13343.

[110]   M. D. Disney, P. H. Seeberger, *Chem. Biol.* **2004**, *11*, 1701.

[111]   R. Kikkeri, B. Lepenies, A. Adibekian, P. Laurino, P. H. Seeberger, *J. Am. Chem. Soc.* **2009**, *131*, 2110.

[112]   P. Laurino, R. Kikkeri, N. Azzouz, P. H. Seeberger, *Nano Lett.* **2011**, *11*, 73.

[113]   I. Papp, J. Dernedde, S. Enders, S. B. Riese, T. C. Shiao, R. Roy, R. Haag, *ChemBioChem* **2011**, *12*, 1075.

[114]   I. Papp, C. Sieben, A. L. Sisson, J. Kostka, C. Bottcher, K. Ludwig, A. Herrmann, R. Haag, *ChemBioChem* **2011**, *12*, 887.

[115]   S. R. Haseley, *Anal. Chim. Acta* **2002**, *457*, 39.

[116]   K. El-Boubbou, C. Gruden, X. Huang, *J. Am. Chem. Soc.* **2007**, *129*, 13392.

[117]   J. Porter, J. Robinson, R. Pickup, C. Edwards, *J. Appl. Microbiol.* **1998**, *84*, 722.

[118]   T. K. Lindhorst, C. Kieburg, U. Krallmann-Wenzel, *Glycoconjugate J.* **1998**, *15*, 605.

[119]   P. J. Vikesland, K. R. Wigginton, *Environ. Sci. Technol.* **2010**, *44*, 3656.

[120]   R. Pelton, *Adv. Colloid Interface Sci.* **2000**, *85*, 1.

[121]   D. M. Hatch, A. A. Weiss, R. R. Kale, S. S. Iyer, *ChemBioChem* **2008**, *9*, 2433.

[122]   M. J. Payne, S. Campbell, R. A. Patchett, R. G. Kroll, *Journal of Applied Bacteriology* **1992**, *73*, 41.

[123]   P. M. Fratamico, F. J. Schultz, R. L. Buchanan, *Food Microbiol.* **1992**, *9*, 105.

[124]   A. Lund, A. L. Hellemann, F. Vartdal, *J. Clin. Microbiol.* **1988**, *26*, 2572.

[125]   W. J. Lee, D. K. Choi, Y. Lee, D. N. Kim, J. W. Park, W. G. Koh, *Sens. Actuator B-Chem.* **2008**, *129*, 841.

[126]   D. Pussak, M. Behra, S. Schmidt, L. Hartmann, *Soft Matter* **2012**, *8*, 1664.

[127]   S. J. Parkin, R. Vogel, M. Persson, M. Funk, V. L. Y. Loke, T. A. Nieminen, N. R. Heckenberg, H. Rubinsztein-Dunlop, *Opt. Express* **2009**, *17*, 21944.

[128] J. P. Andreassen, *J. Cryst. Growth* **2005**, *274*, 256.
[129] G. B. Sukhorukov, D. V. Volodkin, A. M. Gunther, A. I. Petrov, D. B. Shenoy, H. Mohwald, *J. Mater. Chem.* **2004**, *14*, 2073.
[130] D. V. Volodkin, A. I. Petrov, M. Prevot, G. B. Sukhorukov, *Langmuir* **2004**, *20*, 3398.
[131] D. V. Volodkin, N. I. Larionova, G. B. Sukhorukov, *Biomacromolecules* **2004**, *5*, 1962.
[132] T. Borodina, E. Markvicheva, S. Kunizhev, H. Moehwald, G. B. Sukhorukov, O. Kreft, *Macromol. Rapid Commun.* **2007**, *28*, 1894.
[133] C. Y. Wang, C. Y. He, Z. Tong, X. X. Liu, B. Y. Ren, F. Zeng, *Int. J. Pharm.* **2006**, *308*, 160.
[134] I. E. Palama, A. M. L. Coluccia, A. della Torre, V. Vergaro, E. Perrone, R. Cingolani, R. Rinaldi, S. Leporatti, *Sci. Adv. Mater.* **2010**, *2*, 138.
[135] A. B. Joshi, R. Srivastava, *Adv. Sci. Lett.* **2009**, *2*, 329.
[136] D. V. Volodkin, R. von Klitzing, H. Mohwald, *Angew. Chem.-Int. Edit.* **2010**, *49*, 9258.
[137] D. V. Volodkin, S. Schmidt, P. Fernandes, N. I. Larionova, G. B. Sukhorukov, C. Duschl, H. Mohwald, R. von Klitzing, *Advanced Functional Materials* **2012**, *22*, 1914.
[138] M. Behra, S. Schmidt, J. Hartmann, D. V. Volodkin, L. Hartmann, *Macromol. Rapid Commun.* **2012**, *33*, 1049.
[139] L. C. Dong, A. S. Hoffman, Q. Yan, *J. Biomater. Sci.-Polym. Ed.* **1994**, *5*, 473.
[140] S. R. Wickramasinghe, S. E. Bower, Z. Chen, A. Mukherjee, S. M. Husson, *J. Membr. Sci.* **2009**, *340*, 1.
[141] H. M. Ma, R. H. Davis, C. N. Bowman, *Macromolecules* **2000**, *33*, 331.
[142] M. H. Schneider, Y. Tran, P. Tabeling, *Langmuir* **2011**, *27*, 1232.
[143] M. Behra, N. Azzouz, S. Schmidt, D. V. Volodkin, S. Mosca, M. Chanana, P. H. Seeberger, L. Hartmann, *Manuscript submitted* **2013**.
[144] Y. B. Zhu, C. Y. Gao, J. C. Shen, *Biomaterials* **2002**, *23*, 4889.
[145] S. R. Palit, P. Ghosh, *Journal of Polymer Science* **1962**, *58*, 1225.
[146] E. T. Kang, K. L. Tan, K. Kato, Y. Uyama, Y. Ikada, *Macromolecules* **1996**, *29*, 6872.
[147] M. Behra, L. Hartmann, *Manuscript in preparation* **2013**.
[148] L. Hartmann, M. Bedard, H. G. Börner, H. Möhwald, G. B. Sukhorukov, M. Antonietti, *Soft Matter* **2008**, *4*, 534.
[149] D. A. Tomalia, A. M. Naylor, W. A. Goddard, *Angew. Chem.-Int. Edit. Engl.* **1990**, *29*, 138.
[150] D. Choi, W. Lee, J. Park, W. Koh, *Bio-Med. Mater. Eng.* **2008**, *18*, 345.
[151] D. Ponader, F. Wojcik, F. Beceren-Braun, J. Dernedde, L. Hartmann, *Biomacromolecules* **2012**, *13*, 1845.
[152] M. Dubois, K. Gilles, J. K. Hamilton, P. A. Rebers, F. Smith, *Nature* **1951**, *168*, 167.
[153] C. Fasting, C. A. Schalley, M. Weber, O. Seitz, S. Hecht, B. Koksch, J. Dernedde, C. Graf, E. W. Knapp, R. Haag, *Angew. Chem.-Int. Edit.* **2012**, *51*, 10472.
[154] J. D. Badjic, A. Nelson, S. J. Cantrill, W. B. Turnbull, J. F. Stoddart, *Accounts Chem. Res.* **2005**, *38*, 723.
[155] D. A. Mann, M. Kanai, D. J. Maly, L. L. Kiessling, *J. Am. Chem. Soc.* **1998**, *120*, 10575.
[156] S. L. Harris, P. A. Spears, E. A. Havell, T. S. Hamrick, J. R. Horton, P. E. Orndorff, *J. Bacteriol.* **2001**, *183*, 4099.
[157] P. A. Spears, D. Schauer, P. E. Orndorff, *J. Bacteriol.* **1986**, *168*, 179.
[158] D. Walczyk, F. B. Bombelli, M. P. Monopoli, I. Lynch, K. A. Dawson, *J. Am. Chem. Soc.* **2010**, *132*, 5761.
[159] M. P. Monopoli, C. Aberg, A. Salvati, K. A. Dawson, *Nat. Nanotechnol.* **2012**, *7*, 779.
[160] N. McCann, D. Phan, X. G. Wang, W. Conway, R. Burns, M. Attalla, G. Puxty, M. Maeder, *J. Phys. Chem. A* **2009**, *113*, 5022.
[161] X. Wang, L. B. Zhang, L. Wang, J. Q. Sun, J. C. Shen, *Langmuir* **2010**, *26*, 8187.
[162] D. B. Dell'Amico, F. Calderazzo, L. Labella, F. Marchetti, G. Pampaloni, *Chem. Rev.* **2003**, *103*, 3857.
[163] M. Caplow, *J. Am. Chem. Soc.* **1968**, *90*, 6795.
[164] W. H. Schaefer, *Curr. Drug Metab.* **2006**, *7*, 873.
[165] R. K. Khanna, M. H. Moore, *Spectroc. Acta Pt. A-Molec. Biomolec. Spectr.* **1999**, *55*, 961.
[166] K. Masuda, Y. Ito, M. Horiguchi, H. Fujita, *Tetrahedron* **2005**, *61*, 213.

[167]   H. S. Randhawa, K. G. Rao, C. N. R. Rao, *Spectroc. Acta Pt. A-Molec. Biomolec. Spectr.* **1974**, *A 30*, 1915.

[168]   H. Xu, D. M. Rudkevich, *Chem.-Eur. J.* **2004**, *10*, 5432.

[169]   S. R. Bhatia, S. F. Khattak, S. C. Roberts, *Curr. Opin. Colloid Interface Sci.* **2005**, *10*, 45.

[170]   P. Jackson, A. Beste, M. Attalla, *Struct. Chem.* **2011**, *22*, 537.

[171]   S. Ghosh, *J. Chem. Res.-S* **2008**, 419.

[172]   U. Gupta, H. B. Agashe, A. Asthana, N. K. Jain, *Biomacromolecules* **2006**, *7*, 649.

[173]   S. Schmidt, M. Behra, K. Uhlig, N. Madaboosi, L. Hartmann, C. Duschl, D. Volodkin, *Adv. Funct. Mater.* **2012**, DOI: 10.1002/adfm.201201321

[174]   Y. Sahoo, A. Goodarzi, M. T. Swihart, T. Y. Ohulchanskyy, N. Kaur, E. P. Furlani, P. N. Prasad, *J. Phys. Chem. B* **2005**, *109*, 3879.

[175]   M. Racuciu, D. E. Creanga, A. Airinei, *Eur. Phys. J. E* **2006**, *21*, 117.

[176]   C. Weber, C. Coester, J. Kreuter, K. Langer, *Int. J. Pharm.* **2000**, *194*, 91.